1-1-2021

SURFACE AND INTERFACIAL PHENOMENA BETWEEN SOIL AND OIL

Md Firoz Ahmed
University of Mississippi

SURFACE AND INTERFACIAL PHENOMENA BETWEEN SOIL AND OIL

A Thesis

presented in partial fulfillment of requirements for the degree of Master of Science in the

Department of Chemical Engineering

The University of Mississippi

by

MD FIROZ AHMED

August 2021

ABSTRACT

Crude oil and motor oil spills on land have severe environmental consequences that pose threats to both humans and natural resources. It is particularly important to know the flow behavior of oils to protect terrestrial ecosystems from this kind of damage. The spreading kinetics, contact angle (CA), and droplet baseline studies of crude oil and motor oils were investigated over several realistic soil-based matrices composed of topsoil (silt-dominant), sand, clay, and moisture. It was found that with an increase in moisture content (MC), the spreading area decreased, and initial spreading time increased for all given oil. The initial CA generally increased with an increase in MC on all substrates except clay, where the baseline was always high for low viscous oil. The oil drops showed incomplete wetting rather than complete wetting in the vast majority of cases. The CA curve shows a significant deviation from the discussed universal curve cited in literature with increasing MC due to the change of porosity and roughness of the surface, where less deviation was noticed in the baseline curve. Xanthan gum (XG), a bioemulsifier was introduced into soil-based matrices to understand its influence on the spreading kinetics and dynamic contact angle in clay and mixture matrices. There was a significant change of oil flow behavior noticed in both clay and mixture matrix in presence of XG. This study has shed new light on the effect of the MC, the viscosity of oils, different components within the substrates and XG on spreading and penetration rate of oils in a realistic soil-based matrix to help reduce the rate of environmental damage by the land-based oil spill.

DEDICATION

This thesis is dedicated to those persons who helped and guided me in my stress and anxiety period to get the writing out successfully. Especial dedication to my father, Md Azizul Haque; mother, Rahela Bibi & my brothers Md Anwar Hossain, and Md Shariful Islam.

ACKNOWLEDGMENTS

I would like to thank and immense gratitude to my advisor Dr. Brenda Prager for her help and support during the course of my research. I would also like to thank my committee members for their support and valuable time. I would also like to thank the University of Mississippi for its internal funds for making this research possible.

I would like to acknowledge Debbie Frank-briggs, Jasmine Stevens, and Justin Puhnaty for conducting several experiments.

.

TABLE OF CONTENTS

LIST OF FIGURES

LIST OF TABLES

CHAPTER I

INTRODUCTION

1.1 Motivation and background

Oil is an important driving force supporting to build up the world economy. The role of crude oil is one of the reasons behind the continuous development of the modern world. But the demand for oil transportation is increasing day by day due to the unequal distribution of oil resources. In addition, the rate of oil transportation by land has been increasing due to the declining waterways [1]. In the United States, more than 90% of crude oil and refined petroleum products are transported by pipeline at some point [1]. On the other hand, more than 91% of crude oil is transported from Canada to the USA through road-based transportation including truck, mini truck, and rail ways [1]. Additionally, the number of automobile companies is increasing in an upward slope and so is the use of motor oil [1]. Large numbers of car wash shops, and large and small-scale automobile mechanic shops release significant amount of used motor oil on land which is accelerating the rate of environment pollution [2]. When oil spills in a particular area, it immediately starts to spread and penetrate into the land, blocking the pores of the soil. An anaerobic environment is created, and hence the soil microorganisms die due to insufficient air passing into the soil pores [3]. One of the most important processes in the early stages of oil spillage in water is to increase the overall area of flow, thereby increasing mass transfer through evaporation and dissolution processes [4]. However for land based oil spills, the direction of oil

spreading in the early stages is mostly horizontal and then starts penetrate gradually into the soil in a vertical direction [4,5]. The main reasons for these spreading directions are gravity, inertia, viscosity, and surface tension of oils [4,5].

Air pollution is one of the worst consequences of oil spills. The air pollutant from oil spills can affect human health and society [6]. The adverse effects on the ecosystem and the long-term effects of environmental pollution caused by oil spills call for an urgent need to develop comprehensive methods to reduce oil spills and penetration rates in the affected areas. A significant amount of research [4,5,7–12] on oil spill cleanup and studies have focused on the oil spill over water surfaces, with less focus on land-based spills [3,13–16]. Most of the oil cleanup methods for water spills are not applicable to retard oil spreading and penetration for land-based oil spills. However, land-based oil spill controlling techniques and methods are increasing nowadays due to the huge call for the protection of terrestrial ecology [13,16].

The purpose of this study is to firstly characterize the spreading kinetics of oil through soil matrices and study the resulting interfacial characteristics between oil and soil components. Subsequently, Xanthan Gum (XG) - a bioemulsifier will be introduced into the soil matrices to investigate its ability to reduce oil spreading and penetration. Should this be successful, this method may be explored further as a potential method to minimize oil spreading and penetration during a land oil spill and make oil spill cleanup easier. It is outside the scope of this study is to present the best way of applying XG onto the spill area; rather, this research focuses on determining the effect of XG on spreading kinetics and penetration rate of oil in model soil matrices using laboratory-based experiments. Future work will concentrate on developing XG technology for soil remediation efforts.

1.2 Research objectives

The primary purpose of this research is to investigate the surface and interfacial phenomena between model soils and oils, to understand spreading kinetics and drop dynamics of the oil on land to develop a new soil remediation method for reducing environmental damage. Significant research has already been done on oil spills over water surfaces [4,5,7,8,17], but to the best of my knowledge, less studies have been conducted on oil spills on land [13,14,18]. The key objectives of this study are:

i. To determine the surface tension, viscosity, and density of oils, and their potential effects on oil spreading characteristics. Also, to determine the porosity, and roughness of the topsoil, sand, clay and mixture matrices and their effects on oil spreading characteristics.

ii. To understand the spreading kinetics of oils through soil matrices.

iii. To investigate the surface and interfacial energy behavior among three different types of oils: two crude oils (CO-1 and CO-2), and motor oil (MO); and soil mixtures prepared from topsoil, sand, clay, and moisture.

iv. To determine the effects of XG on spreading and penetration rate of oils in model soil matrices which may be used to mitigate spreading rate of oils on land.

v. To identify which variables, such as moisture content, matrix components, oil viscosity, porosity, and roughness of the substrate surface, affect the spreading and penetration of oils in soil matrices as well as the interfacial characteristics between the oils and soils.

CHAPTER II

LITERATURE REVIEW

2.1 Soil ecosystem and notable oil spills

Soil is a vital element of our ecosystem, which is a mixture of organic matter, liquids, gases, and microorganisms. A major threat to the environment from oil spill pollution exists for wetlands, agricultural fields, shoreline, forested areas, mangrove forests and salt marshes. Most plants and animals are prone to the effects of oil spills [9]. Soil can become contaminated from oil spills all across the world, and examples include the Gulf War oil spill, Deepwater Horizon oil spill [16], and Exxon Valdez Tanker leakage [16]. Oil spills have enormous potentials for various degrees of environmental damage [19]. At present, no known method is available to completely contain, control and remove these hazardous spills [19]. Oil spills often occur in and around oil production facilities, and in areas with pipeline or along oil transport routes [16]. Oil spills spread very quickly, which is why a timely response is needed to physically contain the spills.

The largest sea oil spill in world history was recorded in 1991 in the Persian Gulf, Kuwait, where the amount of spilled oil was approximately 380 million gallons [16]. The Mingbulak oil spill in Uzbekistan in 1992 occurred in the city of Fergana, and 88 million gallons of oil released [18]. In the Komi spill, the amount of oil spilled was three times that released in Alaska's Exxon Valdez catastrophe in 1989 [13]. Another notable spill was the northwestern Amazon oil spill,

which polluted many areas including rainforests, streams, and rivers of Ecuador, Peru, and Columbia [14]. These studies showed that the oil spill affected the environment, as well as human health. A study conducted by Beland et al. [17] also revealed that oil spill and cleanup activities are responsible for air pollution due to the increase of specific components in the air, such as particulate matter (PM), nitrogen dioxide (NO_2), sulfur dioxide (SO_2) and carbon monoxide (CO). These pollutants have been linked to low weights of neonatal babies and health risks for pregnant women, such as premature births [17].

Additionally, the physical and chemical properties of the soil are changed because of oil contamination, such as increases in soil temperature that cause damage to seedlings. Spillage of crude oils create an anaerobic environment inside the soil by inhibiting the diffusion of air particles inside the soil pores, which has a detrimental effect on microorganisms inside the soil. Furthermore, the pH, total organic carbon, and other chemical properties of the soil are also drastically changed due to oil spilling into the soil pores [20,21].

2.2 Oil spill cleanup methods

Several studies have been conducted on the oil spill cleanup on the ground and water surface [7,10–12], but those are time-consuming and costly. Different methods can be used separately or together [7] and can be classified into three major groups. In the first group, mechanical methods such as adsorbents are employed; the second group consists of biological processes such as bioremediation, and the third one considers chemical methods such as dispersion, in-situ burning, and solidifiers [7,10]. The main limitations of mechanical and chemical treatments are their high cost and low adsorption capacity. Mechanical treatments are not efficient

in the shallow marine area due to rough sea waves and high wind velocity. Chemical treatments are effective if immediately applied after an oil spill, but due to high toxicity, chemical treatment is not environmentally friendly. In-situ burning is efficient in land-based oil spills, but this method is limited by wind conditions and by the proximity of the spill to the human locality [7,8]. In a review by Adebajo et al. [12], they revealed that synthetic sorbents such as polypropylene and polyurethane were used in land-based oil spill cleanups. Still, the detrimental effect of these adsorbents is environmentally undesirable in landfill disposal due to non-biodegradability [12]. The bio-emulsifier (XG) used in this study for investigating its response towards oil spreading in land. This bio-emulsifier is soluble in water, biodegradable [22] and cheap in price. Also, XG could increase the viscosity of aqueous solution significantly and the solution exhibits highly pseudoplastic flow [22]. An effective way to apply this bio-emulsifier in a spiling area could be a new method to clean up the oil spill area.

2.3 Surface and interfacial interaction models and equations

The dynamic contact angle (CA) plays a vital role in understanding interfacial interactions as well as the wettability of oils in soils. Wettability varies with the moisture content (MC) present in matrices, which also affects the spreading kinetics of the oil. The precondition of wetting is a CA less than 90° [23]. Darband et al. [24] conducted a study demonstrating that wettability significantly changed with roughness and porosity of the surface. CA increases with the roughness of a surface and also increases the interfacial curvature of the oil droplet, causing it to bead up on the surface rather than spread. Li et al.[25] conducted another study on super-hydrophobicity, a

phenomenon commonly compared with the lotus leaf and known as the 'lotus effect.' A liquid with CA >150° will not wet a substrate surface, whereas one with CA<90° will spread across a surface, and one with CA=0° will completely wet the surface [25]. The first case is called anti-wetting, and the last case is called super wetting [24]. CA is an essential factor in determining the spreading behavior and the wettability of oils when they come into contact with a soil matrix. For controlling the wettability of oil, surface roughness, surface porosity, and surface energy are three important parameters [23]. The soil matrix contains air and water inside the matrix pore. In an uneven surface like soil matrix, air bubbles are caught in the ups and downs of the surface [24]. When oil is spilled on the land, it comes in contact with various soil components as well as air. Due to the presence of air, oil could not easily penetrate into the soil matrix pore which may reduce the spreading area [24]. The rougher surface also makes it more difficult for oils to spread and if the surface energy of the liquid is higher than the solid, the liquid will bead up on the solid surface.

2.3.1 Young's and Wenzel equation

Surface energy considerations are considered with wetting theory, where wetting is possible when the surface energy of the substrate (σ), is equal to or larger than the surface tension (γ) of the liquid [26]. Typically the surface energy of almost all types of oils between 25 to 32 mN/m [27]. Usually, Young's equation **(Equation (1)**) explains the solid-liquid interactions in wetting using overall surface energy of solid and liquid in the case of a smooth and flat surface where the Wenzel equation introduces an additional roughness factor. According to the Wenzel equation **(Equation (2)**), surface roughness will further increase a CA already greater than 90° on a perfectly smooth surface. Alternatively, a CA <90° will be further reduced with the addition of

roughness [24]. The Equation (1) and Equation (2) represent the Young's equation and Wenzel equation, respectively.

$$\gamma_{SL} = \gamma_{SA} - \gamma_{LA} cos\theta_0 \quad (1)$$

$$\cos\theta = r\ \cos\theta_0 \quad (2)$$

Where γ_{SL}, $\gamma_{SA,}$ and γ_{LA} are the surface energies of the solid in contact with liquid, solid in contact with air and liquid in contact with air, respectively, r is the roughness factor, θ is observed CA and θ_0 is equivalent CA on a flat surface.

A study conducted by Song et.al [26] revealed that a particular liquid wets a surface completely only if the spreading parameter (S) is greater than or equal to zero ($S \geq 0$). The possible reason is the surface energy of the solid surface is generally higher than the particular liquid at $S \geq 0$. S increases when the surface energy of the solid, γ_s , increases, which indicates the general tendency of favorable wetting of solids that have a higher surface energy than the liquid, and vice versa. The spreading parameter defined as in **Equation (3)**:

$$S = \gamma_s - (\gamma_{SL} + \gamma_L) \quad (3)$$

Here, γ_L is the surface tension of the liquid, and γ_{SL} is the interfacial energy between the solid and liquid.

Another study conducted by Leelamanie [28] revealed that the surface free energy also has a relationship with CA in wetting a surface. A solid with high γ_s (mNm^{-1}), is readily wetted by any liquid such as oils if the surface tension of the liquid less than the solid. The surface free energy of solids is determining by the **Equation (4)**:

$$\gamma_s = \left(\frac{\cos\theta+1}{2\phi}\right)^2 + \gamma_L \quad (4)$$

Where θ is CA, ϕ is the Goods – Girifalco interaction parameter, where considering ϕ = 1-0.011,

and γ_L is the surface tension of the liquid [29].

2.3.2 Cassie and Baxter model

In the case of a heterogeneous surface, both roughness and porosity are responsible for increasing the CA in both hydrophilic and hydrophobic regions [30]. In this regard, Cassie and Baxter established a model for heterogeneous surfaces (porous solid) composed of two fractions [31]**,** defined as in **Equation (5)**:

$$cos\theta_b = rcos\theta_0 - f_{LA}\,(rcos\theta_0 + 1) \qquad (5)$$

Where θ_b is observed CA, r is roughness, θ_0 is the equivalent CA on a flat surface, and f_{LA} is the fractional area of liquid-air contact between water particle and air pockets [32]**.**

According to the Cassie-Baxter model, it is assumed that the observed CA increases with increasing roughness and porosity of the soil matrix, dictating the spreading or repelling of oils. The θ_b increases with increasing roughness and porosity of the soil matrix, dictating the spreading or repelling of oils. In the case of the oil and soil interface, the high roughness of the soil matrix has minimized the spreading of the oil. Hence, CA increases with increasing roughness of the land surface [24]. In this way, the amount of oils spread across the land depend on the roughness of the land surface. Porosity in the soil texture is another factor that allows oils to penetrate the matrix. Land with less porosity can retain the oil drops on the surface more so than a porous land. A study conducted by Kettler et. [33] revealed that the pores between the particles in sands are quite large in well sorted sand, which allows the water to drain quickly into the pore. On the other hand, the pores in clay are less than those in sand due to a smaller particle size [34].

Generally, the nearshore region contains more sand than clay and soil. Oil can spread more quickly over coastal areas compared with inland. As the particle size of clay is small, the oil

spreading across the land is slower due to less porosity. The CA might increase due to higher porosity and low roughness in the hydrophilic region, but it is possible to make the surface more hydrophilic (up to the CA 60°) by increasing surface roughness and reducing porosity. Conversely, the porosity and roughness dominate in different CA range in the hydrophobic region. Within the CA ranges 90°-120°, the porosity of the surface dominates more strongly than the roughness of the surface, whereas roughness dominates strongly than porosity between the CA range of 120-150° [30].

2.4 Properties of oils, different matrices, and bio-emulsifiers

2.4.1 Crude oil

Crude oils are commonly found in oil spills during crude oil extraction, transportation, and refinement [35]. Also, crude oil is a liquid petroleum which is found accumulated in different porous rock formations in Earth's crust and is extracted to produce a wide range of chemical products. Crude oil is composed of different kinds of hydrocarbons with the carbon number ranging from C_5 – $C_{15,}$ including resins, asphaltenes, saturates, and aromatics [36]. Another common component of crude oil is naphthene compounds, which is almost 10% of the total composition [37]. Along with those compounds, crude oil may contain a wide variety of heteroatomic chemical constituents including sulfur, oxygen, nitrogen, carbon dioxide and trace metals. One of the most dangerous components for environmental disruption in crude oil is trace metals [37].

2.4.2 Motor oil

Motor oil may also be used in research to model oils in soil remediation work [38]. Motor oil in the form of lubricants is used in the automobile industry to enhance the internal combustion of engines as well as complete protection of all moving parts. It is sticky and frequently used as a lubricant because of its viscoelastic properties. In addition, motor oil contains some long-chain polymers such as polyalphaolefins (PAOs), polyolesters (POE), and polyalkylene glycols (PAG) with additives. The chemical structure of some polymer compounds used in motor oil production is shown in **Figure 2.1**. Usually, motor oil is composed of two basic components: 90% petroleum fraction and 10% chemical additives. The additives used in motor oil also contain hazardous materials, including magnesium, silicon, zinc, and other organic compounds that increase the concentration of chlorine, sulfur, and nitrogen in lube oil. These compounds increase the viscoelastic properties of motor oil and prevent them from penetrating the soil due to the complex polymer network system [39].

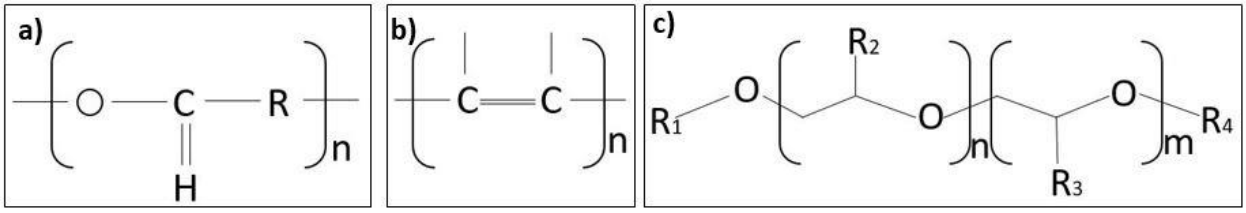

Figure 2.1: The chemical structure of polymer compounds using in the motor oil production-a) monomer of esters, b) monomer of olefins, c) typical chemical structure of Polyaklylene glycols (PAG).

2.4.3 Topsoil

Soil is a complex mixture of organic matters, mineral particles, air, water and living organisms [40]. A typical soil contains 50% solids, 6% minerals, and 44% of void spaces (vol%) of which half is occupied by water and the other half filled with air or gas [41]. The main character of the pore space of soil is influenced by the critical aspects of almost everything that happens on the ground: the movement of water, air and other liquids [34]. Topsoil such as that used in this study, contains peat moss, rice hulls, native soil, and food waste.

2.4.4 Sand

Sand is a granular material that comprises of different mineral particles and finely divided rock. Sand is defined by its grain size (0.05-2.00 mm) [33] which is smaller than gravel and coarser than silt. The basic composition of sands varies, depending on the sources of rocks and conditions. but the most common constituent of sand is silica in the form of quartz which is chemically known as silicon dioxide [42].

2.4.5 Clay

The clay fraction of a soil includes all particles less than 0.002 mm in diameter. Clay can swell up when absorbing water and retain its shape when dry depends on the minerals present in the clay [43]. Also, due to a molecular film of water surrounding the clay particles, it gains plasticity at a certain extent when wet but becomes hard and rigid upon drying or firing [44]. There

are different shapes but most of them have sheetlike geometry such as phyllosilicates [43].

2.4.6 Bio-emulsifiers

Xanthan Gum (XG) a common bio-emulsifier, an extracellular polysaccharide naturally secreted by the *Xanthomonas campestris* micro-organism [22,45,46]. Due to the huge demand of XG across the world, commercial production is needed to meet the world requirement. Commercially, XG is produced by an aerobic, immersed fermentation process from a pure culture of bacteria in a well-aerated medium [45]. The complex chemical structure of the XG consists of

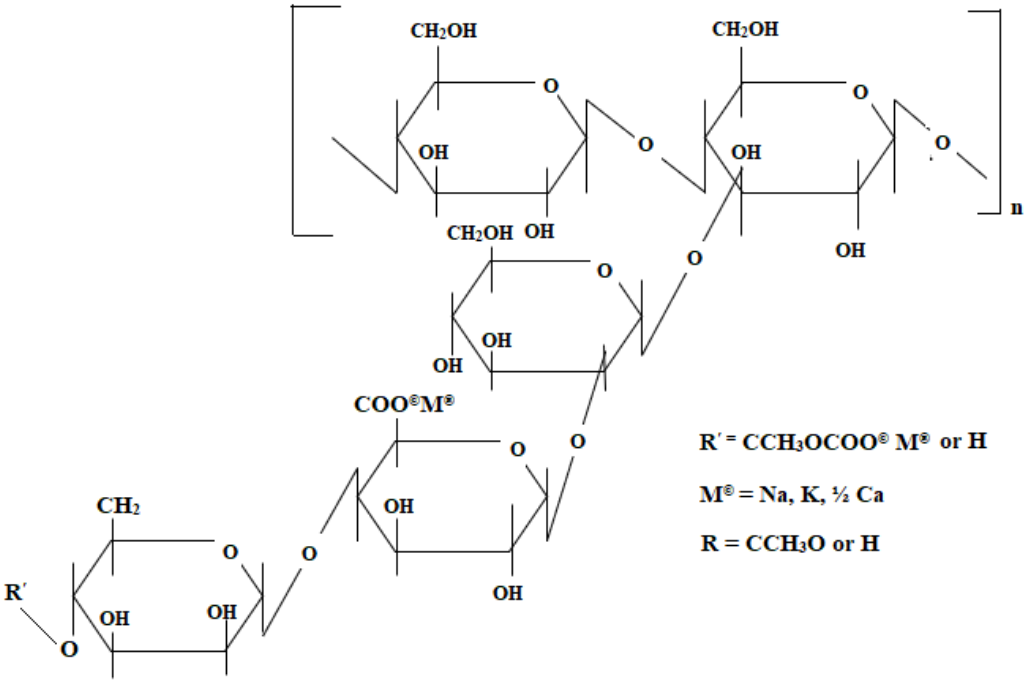

Figure 2.2: A typical chemical structure of xanthan gum [22].

β-D-glucose, d-mannose, and d-glucuronic acid as a building block. A typical chemical structure of XG is shown in **Figure 2.2** [22]. XG has an excellent capacity to increase the viscosity of the aqueous solutions and demonstrates pseudoplastic behavior [22,46]. Also, XG solutions exhibits

high zero-shear viscosity and shear thinning behavior, so are widely used to stabilize dispersions and emulsions due to their ability to resist particle sedimentation and droplet creaming [46]. In addition, using XG to mitigate oil spreading would be cost-effective in comparison to the other oil spill cleaning methods [7,17]. To the best of my knowledge XG did not use before to reduce oil spreading and penetration rate in a spilling region, however, several studies revealed that the XG could significantly increase the viscosity of liquids, as for example water [22]. Also, XG could form a polymer network into the solid porous matrix in contact with water which could slow down the fluid flow into the soil matrix [22,46]. Therefore, an effective way of apply XG in a spilling region could be a new method to mitigate the spreading of oil.

2.4.7 Other physical properties of oils and matrices

Oil spreading depends upon the viscosity of the oil along with the other factors, such as the surface energy, and CA of the oils. The higher the viscosity of the oil, the higher the surface energy, which tends to cause the oil to bead up on the surface [47]. Hence, the oils with low viscosity spread and penetrate more quickly than those with high viscosity [16,47]. The density and surface energy of oils also plays a vital role on spreading and penetration rate in different matrices. The surface roughness and porosity of the matrices also influence the oil spreading rate to a certain extent which is modeled by the Cassie-Baxter equation (see in section 2.3.2).

2.5 Focus of the study

In this work, spreading kinetics and dynamic CA analysis of three oils (two crude oils and

motor oil) on different realistic soil-based matrices will be investigated. The method developed for conducting all experimental trials is simplistic, but is able to provide a variety of unique information to adequately investigate this topic. Several studies [48–52] were performed on the spreading of liquid over porous surfaces including cellulose, sponge, papers, and other solid surfaces but not on a realistic soil-based matrix. Therefore, the method used in this study could be a new approach to developing additional knowledge on inhibiting oil spreading on land.

To overcome the ecological and environmental damage by the spilled oil, a more convenient, economic, and comparatively quicker method is urgently needed to minimize the oil spreading and penetration rate. In this work, the effect of the bioemulsifier XG, on the spreading and penetration rate of oil in different matrices was studied to determine the likelihood of employing a bioemulsifier in future responses to oil spills. The physical properties of oil, and soil-based matrix properties including viscosity, surface tension, porosity, roughness, and density were also measured, as these properties have a significant effect on oil flow behavior on matrix surfaces and through the matrix.

CHAPTER III

EXPERIMENTAL MATERIALS AND METHODS

3.1 Materials used

MO (SupetechTM SAE 5W -20) was purchased from Walmart superstores, Oxford, MS. CO-1 was generously donated by Ram Petroleum, LLC, located in Tylertown, MS; and CO-2 by Coastal Chemical Co., L.L.C., LA 70518. Xanthan Gum (XG) was purchased from Fisher scientific^{TM}. Quikrette premium play sand and Scotts Premium Topsoil were also purchased from Walmart superstores, Oxford, MS. The topsoil was considered to be silt loam, according to the USDA procedure done to test the texture of the soil [53]. Clay was supplied by the University of Mississippi field station, Abbeville, MS. Petri dishes (87 mm) and petri dish lid (90mm) were provided by Fisher brand. Leur lock BD syringes (3 mL) were used with the CA studies.

3.2 Equipment and methods

3.2.1 Basic properties of the oils

The viscosity of CO-1, CO-2, and MO was measured using a controlled stress/strain, Discover HR-2 hybrid rheometer at the Chemical Engineering Laboratory, Mississippi State

University (MSU). It was equipped with parallel-plate geometry (set gap: 570 μm, torque: 3.09094 x 10^{-3} mNm, solvent trap: 500 μm). The temperature of the laboratory was fixed by using a Peltier plate steel – 105471 system at 22°C. Each sample was placed in the plate by a 1 mL plastic dropper at the edge of the plate and cleaned with a cotton bud if the oil spilled. All rheological tests were performed at least twice for repeatability purposes. Oil density was measured according to ASTM D 1475-98(2003) at a constant temperature of 24°C. The method was first calibrated and confirmed with water as per the test procedure. Measurements were performed in triplicate. Surface tension of the oils was measured using the pendant drop method on a Biolin Scientific OneAttension CA analyzer, with NAVITAR camera and OneAttension software. Again, all measurements were done in triplicate.

3.2.2 Preparing the matrices

The matrix preparation was performed in two ways: the first way was without XG; and the second way was with XG. After adding XG in different amounts to determine the workable amount of XG in the mixture matrix, it was found that 1g XG into the matrices was optimal. For the purposes of discussion and identification, from hereon in, a mixture matrix will comprise of topsoil, sand, and clay (and water where applicable) with and without XG; while individual substrates will be referred to as a topsoil matrix, a sand matrix, and a clay matrix. Mixture matrices prepared for spreading kinetics experiments required five main steps. Topsoil, sand, and clay were initially placed in Pyrex dishes and dried in a Precision oven at 105°C for 48 h. Topsoil and clay were then sieved using a 5 mm opening sieve supplied by Fisher Scientific to remove oversized particles. In the third step, each component was weighed according to the amounts given in **Table**

3.1 using an Adventurer^{TM} brand electronic scale. In step four, components were mixed for 5 minutes with a stainless-steel spatula. Finally, the mixture was transferred into an 87 mm petri dish base (Fisher brand) and prepared as either loosely or densely packed matrices. To prepare matrices with 5 or 10% MC, the amount of water was calculated on a wet basis and added at step four. The formulae used for this calculation are given by **Equation (6)** and **(7)**:

$$MC = \frac{M_w - M_d}{M_w} \times 100 \quad \text{..... (6)}$$

$$H_2O = M_w - M_d \quad \text{..... (7)}$$

where MC is the moisture content (%) of the material; M_w is the wet mass of the mixture, M_d is the mass of the mixture after drying, and H_2O is the mass of water added to prepare the targeted mixture.

Matrices prepared for surface interactions included individual component matrices as well as mixture matrices with the same composition as shown in Table 3.1. Clay and topsoil were ground – rather than sieved – using a mortar and pestle to create uniform particle size. Matrices were prepared dry and with 5 and 10% MC to assess the effect of moisture on CA. The dry basis mass for all preparations (individual and mixture matrices) was 63.69 g to completely fill a 90 mm petri dish lid (Fisher brand) and generate a flat surface at constant packing. However, when the XG was used for measuring the CA on the matrix surface, the mass was 64.69g due to the addition of 1g XG.

Table 3.1: Composition of loosely and densely packed mixture matrices without XG and mixtures with XG. Water was added to the dry mixture for MC studies. The combined composition of the three soil components resulted in a clay-based soil overall, based on the USDA soil texture triangle [53] and mimicking clay-based soils in MS [54].

Components	Without Xanthan gum (XG)		Composition with Xanthan gum (XG) (63g mixture + 1g XG)	
	Loosely packed composition (63 g total as dry basis)	Densely packed composition (70 g total as dry basis)		
Clay	50% (31.50g)	50% (35.00g)	50% (31.50g)	1 g XG
Sand	35% (22.05g)	35% (24.50g)	35% (22.05g)	
Topsoil	15% (9.45g)	15% (10.50g)	15% (9.45g)	
Water – 5% MC	3.32 g	3.68 g	3.32 g	
Water – 10% MC	7.00 g	7.78 g	7.00 g	

3.2.3 Porosity and Density of the matrices

Porosities were estimated according to Matko [55], where known amounts of water were poured over dry prepared matrices in the petri dishes (or lids) until it reached the top. The volume of water, divided by the volume of the petri dish (or lid), provided an indication of each substrate's porosity. While it is acknowledged that some of this water may have become bound to one or more of the components within the matrix, this estimation was performed for relative comparison across the matrices prepared. The method followed appears widely used in such estimations. Densities of each matrix were determined by dividing the mass of contents added to the petri dish (or lid) by its volume3.2.4 Spreading kinetics experiments

For densely packed trials, the mixture matrix was pressed by hand into the petri dish until it was the same height as the petri dish walls (1.3 cm). For loosely packed trials, no pressure was

needed to spread the contents into the dish. The experimental setup is shown in **Figure 3.1**. The filled petri dish containing the mixture was mounted by two clamps attached to two ring stands. The distance from the benchtop to the clamp was measured on each side and adjusted if needed, to ensure the petri dish was horizontal. A graduated measuring cylinder was used to measure 10 mL of oil, which was then poured onto the mixture matrix surface from above, at a vertical distance of 7.0 cm and a rate of approximately 20 mL/min. Oil quantity was large enough to represent a puddle, but small enough to not spread to the edges of the petri dish container. A video of the oil spreading process was recorded from beneath the petri dish using smartphone imaging capabilities (Huawei KII-L21, 13 MP) for 20 min. Still images were extracted from the resulting video every 30s and exported into ImagePro Premier (v9.2 software), where the oil spreading area was quantified. All spreading experiments were done in triplicate, and one standard deviation in the area determinations was not more than ± 0.9 cm^2.

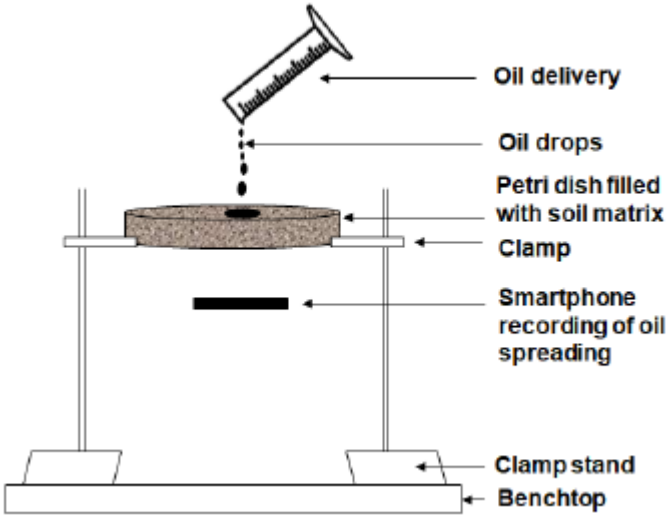

Figure 3.1: Schematic diagram of the experimental set-up for spreading kinetics experiments.

3.2.5 Measuring dynamic contact angle (CA) and droplet baseline

A Biolin Scientific OneAttension CA analyzer, with NAVITAR camera and OneAttension software, was used to perform dynamic CA measurements of sessile oil droplets placed on topsoil, sand, clay, and mixture matrices (and XG where applicable), with and without MC. Oil droplets were delivered manually using the disposable syringes to prevent contamination between each oil, and the average droplet size delivered for each oil was 27.7 ± 1.3 μL. All measurement trials were at least done in triplicate, and the experimental error was routinely no more than ± 5° for the CA, and ± 1.6 cm for the baseline, defined as the droplet diameter in contact with the matrix surface at any given time.

3.2.6 Roughness measurement

A NextEngine^{TM} (model 2020i) Multistripe Laser Triangulation (MLT) scanner and a ScanStudio^{TM} 3D software was used to measure the surface area of matrix surfaces. This software allows the objects to be scanned in two modes: macro and wide. The instrument can capture a photo of an object with a wavelength of 650 nm and twin 5.0-megapixel metal-oxide-semiconductor image sensor, and ensure a ± 100-micron dimensional accuracy in macro mode. During the scanning operation, the scanner first captures a digital photograph of the matrix surfaces. Then multiple, projected, vertical light stripes sweep across the targeted matrix surface. The scanner was connected to the AutoPositioner^{TM}, a base that automatically rotates an object to obtain a 360° scan. This instrument has three available scan types including single (digitizes one view of an object), bracket (digitizes three view of an object) and 360° (allows multiple scans during the complete rotation of an object). The mixture and individual matrices were placed on the

AutoPositioner™ and scanned with the laser scanner using the highest possible resolution settings. The scan type was 360°; 16 divisions and macro mode. After the scanning process was completed, the scanned model was trimmed, fused and filled, and the total surface area of the scanned surface was calculated by the ScanStudio™ 3D software. Finally, the total surface area data of the scanned surface was used to calculate surface roughness of the scanned surface by using **Equation (8):**

$$\text{Surface roughness} = \frac{\text{total surface area}}{\text{Projected surface area}} \quad \text{..... (8)}$$

All surface scanning trials were measured, at least, in triplicate.

3.3 Statistics analysis

3-way ANOVA was applied to both sets of results (spreading kinetics and surface energy data) with and without XG using Minitab ®, 19.2020.1, © 2020. Individual influences (matrix, MC, oil type) and dual influences of these parameters were investigated. The null hypothesis was that the means of all populations compared were equal, while the alternate hypothesis was that one or more of the populations means compared were not equal. A significance level of $\alpha = 0.05$ was used for all analyses, and the inverse cumulative distribution function (ICDF) of the Chi-Square distribution was used to calculate critical F values (F_{crit}). Hypotheses were accepted or rejected by comparing the calculated F values (F_{calc}) in the statistics analyses with F_{crit}. The R^2 of all statistics models created for each condition ranged between 91.76 and 98.76% except for one condition without XG and one condition for with XG, which was 87.86% and 85.40%, respectively (refer to appendix A). Hence all models were considered excellent fits of the experimental data.

CHAPTER IV

RESULTS AND DISCUSSION

[Section 4.1 was published in the Journal of Environmental Challenges. Mr. Firoz Ahmed performed all the experimental work and generated graphs of the raw data and was responsible for writing early drafts of the introduction and methodology sections of the paper.]

The results and discussion chapter are divided into four different sections to facilitate a better understanding of this thesis. In the first section, the different physical properties of oils and soil-based substrates used in this study are discussed. In the second section, the spreading kinetics of oils on different matrices has been investigated. The third section discusses surface and interfacial phenomena between different soil-based matrices and oils. In section four, the effects of XG on spreading behavior and interfacial phenomena of various oils in matrices have been investigated.

Statistical analyses of these results are discussed in chapter five to investigate the effect of different variables on oil spreading behavior and interfacial phenomena in matrices. Also, a comparison of flow models of oils with the other flow models of liquid droplets [49,50,52] is studied to verify authenticity of the data presented in this current research.

4.1 Physical properties of oils and substrates

Several physical properties of different oils and substrates were measured such as viscosity,

surface tension, density, porosity, and roughness. The average steady-state viscosity of the oils chosen for this investigation was observed after 10 s^{-1} at a temperature of 22°C, and the constant viscosity values are reported in **Table 4.1**. A linear viscoelastic behavior was noticed in the case of all oils within the shear rate range under which they were tested. The other properties including surface tension and density of the oil were measured at 24°C and the values are reported in Table 4.1.

Table 4.1: Viscosity, density, and surface tension of selected oils with standard deviation no more than 1.

Name of the oil	**Measured viscosity (Pa.s)**	**Measured density (kg/m^3)**	**Surface Tension (mN/m)**
CO-1	0.5299 ± 0.0058	926 ± 2	40.44 ± 2.20
MO	0.0949 ± 0.0225	850 ± 1	37.75 ± 0.25
CO-2	0.0089 ± 0.0004	840 ± 1	33.18 ± 0.24

Crude oil consists of petroleum and different hydrocarbon compounds that are collected in the liquid state after several different extraction process. Generally, the carbon range of hydrocarbons such as alkylparaffins, naphthenes, alkylbenzenes present in crude oil is in between C_5-C_{15} [37]. Motor oils commonly contains different additives, long chain polymeric compounds, viscosity modifiers and some hazardous components including zinc, magnesium, calcium sulphonates which may interact with the soil matrix components and affect the flow behavior of oils [56].

Table 4.2 reports the measured value of porosities, roughness, and densities of each matrix.

Porosities were measured only for the dry matrices (i.e. 0% MC), and may be influenced by water becoming bound to some of the soil components [57]. However, they serve as a useful relative comparison amongst the different matrices prepared. The porosity of several marine sands off the coast of Florida, measured using imaging techniques, was reported as low as 37.7% [58], a little higher but reasonably close to the value reported in Table 4.2. Ghanbarian et. al [41] has sand porosity at 35.4%. Likewise, the mass ratio for total porosity of clays (defined as mass of water / mass of water plus clay) was reported as approximately 0.3 by Savage and Liu [57], for a density of 1250 kg/m^3 (the same density used in the present study). When converting the reported volume-based porosity for clay in Table 4.2 into a mass-based porosity, this value comes to 0.35, which is again quite close. The propensity of clay to adsorb water results in a higher-than-expected porosity (vol%), regardless of particle size (coarse or ground). Silt loam was quoted as low as 44.2% [41], which is similar in composition to the top soil used. Although impossible to discern whether or not the samples referenced by literature were identical to those used in the present study, both sets of values notionally confirm that the porosity measurements reported in Table 4.2 correlate well with other data.

Table 4.2: Densities, porosity, and roughness of dry matrices. Densities were measured from the matrix masses divided by the calculated volume. One standard deviation is shown for the porosity measurements. Roughness was measured from the total surface area divided by the projected area of the petri dish containing matrices. The experimental error in mass measurement can be assumed ± 0.02g.

Matrix	Density (g/cm^3)	Porosity (vol%)	Roughness
Loosely packed	0.76	66 ± 2	5.82

Densely Packed	0.84	59 ± 1	5.23
Topsoil	1.25	41 ± 2	3.84
Sand	1.25	33 ± 1	3.22
Clay	1.25	68 ± 3	6.53
Mixture	1.25	67 ± 2	4.00

Polydisperse mixtures of different components have higher porosity and often a larger pore size distribution than monodisperse mixtures, and those with irregular-shaped particles also tend to increase the porosity [34]. The loosely and densely packed matrices have larger particles sizes (up to 5 mm) compared with matrices where the components were ground down, and hence resulted in larger porosity values. However, this trend was not observed with the clay or mixture matrices. Clay is known to readily adsorb water depend on the minerology due to its plentiful –OH groups [57], and likely explains the breakdown in trend for this matrix. Clay particles, however, are also the smallest of the three components [33,53], and are prone to aggregate, forming larger pore sizes between aggregates [34]. It is possible that the ground mixture matrix may have formed powdered aggregates, causing much larger pores than might otherwise have been expected with a more uniform particle-size matrix. The resulting mixture matrix for surface studies therefore had a similar porosity to the loosely packed matrix used for kinetics studies.

A 3D laser scanner was used to measure the roughness of the different matrices shown in Table 4.2. The clay matrix has the highest roughness value among the roughness data reported in Table 4.2. The reason for the highest roughness value of clay particle compared with other matrix is not clear enough, however, the different shapes of clay particles and minerals present in the clay

could be a reason for high roughness [43]. Among the other matrices, the loosely packed mixture was the second roughest matrix, followed by the densely packed matrix. The densely packed matrix was pressed by hand into the petri dish, and this may have reduced the overall roughness of the surface. The individual matrices were grounded by a mortar and pestle to make them powder form. Therefore, individual matrices show less roughness, though the clay did not follow the expected trend due to its particle shapes as mentioned earlier. The mixture matrix was comprised of individual matrices and shows less roughness compared with loosely packed matrix as expected due to the less roughness of individual matrices.

4.2 Spreading kinetics study

4.2.1 Effect of MC on spreading kinetics

Mixture matrices were prepared with topsoil, sand and clay with different MC to investigate the oil spreading kinetics through the matrices. MC is one of the crucial factors that affects oil spreading on a soil matrix [59]. **Figure 4.1** illustrates the spreading kinetics of the three oils (low, medium and high viscosity) into the soil matrix at three different MC (0, 5 and 10%) for the densely packed trials.

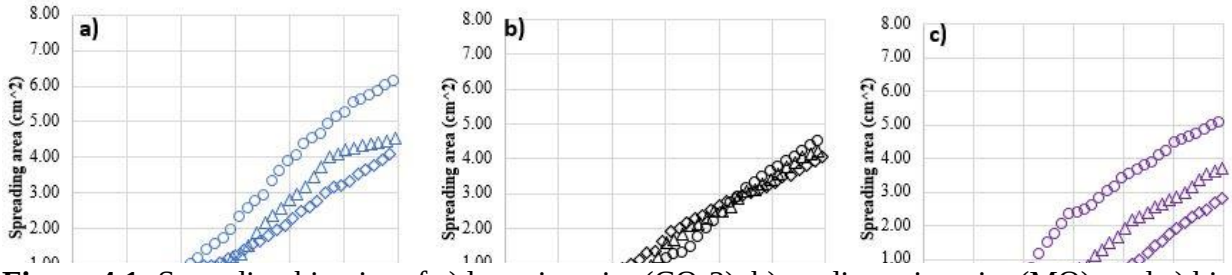

Figure 4.1: Spreading kinetics of a) low viscosity (CO-2); b) medium viscosity (MO); and c) high viscosity (CO-1) oils at different MC for densely pack soil mixture matrices. The spreading area (Y-axis) is the area of oil spread through the matrix at any given time measured from the base of the matrix sample.

As seen from the traces, fastest spreading is observed in the case of low and high viscosity oil at 0% MC, slower spreading at 5% MC, and slowest spreading at 10% MC. In contrast, there is no significant changes in spreading rate observed in the case of medium viscosity oil (MO) in different MC. The reason might be the different additivies frequently present in MO which comprises up to 10% of the total compositon [60] depending on the MO brand. In additon, antioxidants, corrosion inhibiitors, viscosity modifiers and detergents are also often used in MO production [60].

Generally, the spreading kinetics and consequently the spreading area were decreased with an increase in MC regardless of matrix density (loosely packed matrix data not shown). This may be attributed to the additional moisture that has filled the pores of the matrices which allows the oil to more easily slip on the matrix surface at the interface of oil-water. Accordingly, the oil tends to bead up on the surface, which decreases the rate of spreading. This result is supported by other investigations on liquid drop spreading on solid porous surface [47,51,52,59]**.**

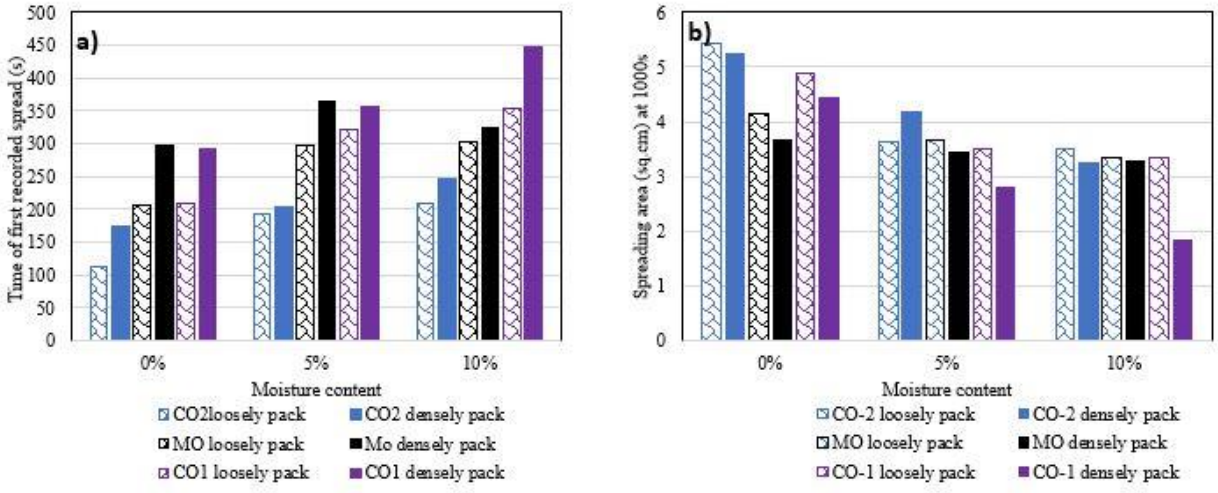

Figure 4.2: Key summary of the effect of MC on loosely and densely packed matrices in the case of three different oils, showing a) time of first recorded spread, b) spreading area at 1000s. The spreading kinetics trials was repeated triplicate, and the calculated error was no more than ± 0.9 cm^2.

To simultaneously investigate the effects of different variables, **Figure 4.2** plots the two main points obtained from all the raw data graphs: the time of first spread (Figure 4.2a)) and the spreading area at 1000s (Figure 4.2b)). The 1000s is chosen as an arbitrary number for quantitative comparison of spreading kinetics over different conditions. Key results from Figure 4.2 show that in most cases, initial spreading times were faster; and spreading areas at 1000s were larger; in loosely packed matrices, lower viscosity oils, and lower MC. The effect of all variables were more significant and dominant on the time of first recorded spread. However, less influence of variables on spreading area at 1000s was observed, especially in 5 and 10%MC. It is noted that the all experimental trials were done in triplicate with an experimental error no more than ± 30s and ± 0.9 cm^2.

4.2.2 Effects of matrix packing density on spreading kinetics

Matrix density is a factor that influences the spreading kinetics of oil through the soil matrix, according to Williams [59]. To further understand the effects of soil matrix densities on spreading kinetics of oil, loosely and densely packed soil matrices were investigated. **Figure 4.3** shows a predominant trend of spreading kinetics of different oils over soil matrices, prepared at 10% MC for loosely and densely packed trials. Key features of these graphs and others (not shown) are reported in **Table 4.3**, where initial spreading time, and spreading area at 1000s are collated. The oils in densely packed trials were less likely to spread than the oils in loosely packed trials (Figure 4.3). There is an exception noticed in the case of medium viscosity oil (MO), which showed a decrease of initial spreading time rather than an increase at 10% MC. When the water

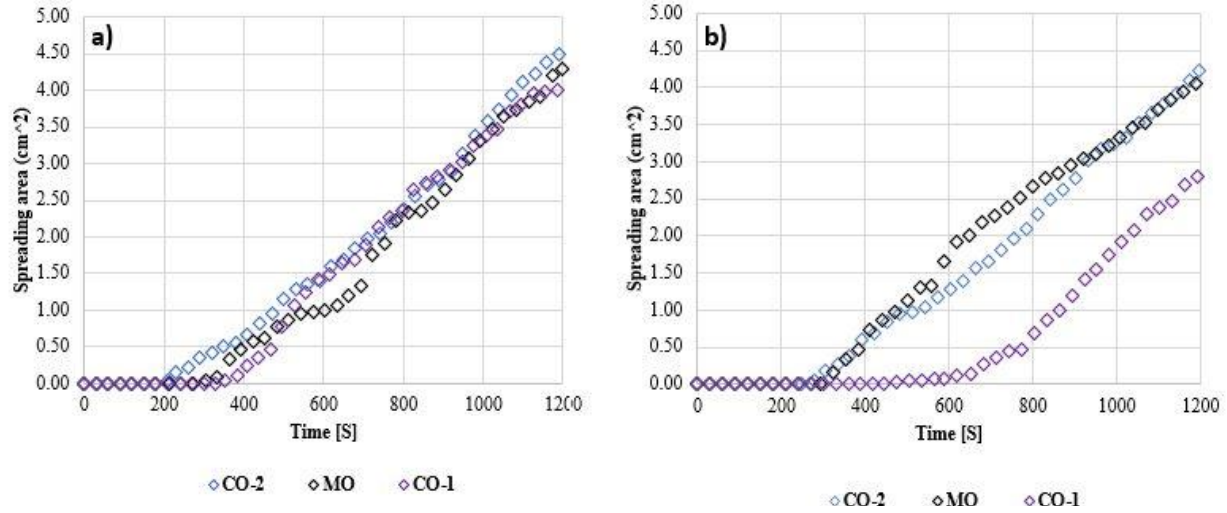

Figure 4.3: Effect of packing density of mixture matrix on spreading kinetics of three oils at 10%MC for a) spreading kinetics in loosely packed trial, b) spreading kinetics in densely packed trial. The spreading area data is plotted as a function of spreading time.

molecules occupy the matrix pores, this causes the oils to slip on the surface. This indicates that a densely packed matrix surface was less porous than the loosely packed surface, and inhibited the oil spreading across the matrix.

Several studies [48–50] revealed that the spreading rate decreases inside the porous substrate with an increase in MC into the matrix to a specific extent. These results are consistent with Williams [59], who described that the CA of oils increased with an increase of MC into the soil matrix which can affect the oil spreading at the spilling region. Also, the kinetics of oil spreading on the porous surface have been thoroughly investigated elsewhere [52]. In their critical review study, Johnson, Trybala, and Starov [52], revealed that the major factors that influence the spreading kinetics of oil over a porous surface are porosity of the surface and the viscosity of the liquid – oil spreads faster on a more porous surface than a less porous surface.

The high oil spreading rate in loosely packed trials indicated that the oil spill spot with high porosity and low MC might face more ecological damage than the oil spill spot with less porosity

and high MC [17,61]. This is likely due to the fact that more oil flowed through loosely packed trials than densely packed trials.

Table 4.3: Initial spreading time and the spreading area at 1000s of three oils at different MC for loosely packed, densely packed, and loosely packed with 1gm XG matrix.

Mixture matrix	MC	CO-2 (low viscosity)		MO (medium viscosity)		CO-1 (high viscosity)	
		Time (s) of first recorded spread	Spreading area (cm^2) at 1000 s	Time (s) of first recorded spread	Spreading area (cm^2) at 1000 s	Time (s) of first recorded spread	Spreading area (cm^2) at 1000 s
Loosely packed	0%	113	5.44	207	4.14	210	4.88
	5%	193	3.63	297	3.67	320	3.51
	10%	210	3.51	303	3.35	353	3.35
Densely packed	0%	173	5.25	297	3.67	293	4.44
	5%	203	4.17	363	3.44	357	2.81
	10%	247	3.25	323	3.29	447	1.84
Loosely packed+1gm XG	0%	150	4.97	235	4.39		
	5%	300	4.53	323	2.16		
	10%	338	6.26	390	3.08		

The viscosity of the oils became an influencing factor on the rate of spreading through the mixture matrices in both loosely and densely packed trials. The medium viscosity oil, MO (Figure 4.3) tended to show less influence in loosely packed matrix at 10% MC on spreading rates compared with the two crude oils. This may be attributed to the long-chain polymeric components, additives, antioxidants present within the MO, which are responsible for the stickiness of such lubricating oils. The stickiness with the high lubricating properties of MO helps it to remain on the mixture surface rather than spread into the mixture [38,60,62]. The spreading kinetics of CO-1 was drastically reduced in densely packed trials due to the high packing density of the soil matrices

and high viscosity of the CO-1. This result shows that there is a direct link on the surface and interfacial tension between oil and soil matrices based on the viscosity of the oils because varying the viscosity of the oil often changes its surface tension, as confirmed in a recent study conducted by Shlegel et. al [47]. Computational viscosity studies [63–65] confirmed the inverse relationship between viscosity and spreading kinetics of oil. This study also revealed that the high viscosity of the oil limits its spreading because of the small velocity gradient, which limits its interfacial interaction of oils with soil matrix.

Other studies performed at 0% and 5% MC, revealed that the spreading rate was faster compared with the 10% MC trials, which was valid for all the oils in both types of soil mixture matrix density. This indicates that the spreading kinetics of oils decreased when MC percentage and viscosity of the oil increased. Furthermore, the spreading rate was always higher in the low-density soil mixture matrix.

4.3 Surface and interfacial studies

4.3.1 Effect of MC on CA in different matrices

CA is the most common and classical index of quantitative measurements of wettability for a liquid on a solid surface [51,52,66]. Topsoil, sand, and clay were finely ground with mortar and pestle to better measure the effects of MC on CA in the mixture matrix and individual matrices for the three selected oils. The contact angle of oils with time on different substrates with three

different MC is investigated, and an example is shown in **Figure 4.4** for the mixture matrix.

As seen from these traces, a high initial CA was recorded in the case of high viscosity CO-1 compared with the other two oils, especially in 5 and 10% MC. The time delay in oil penetration in matrices differs with MC and oil viscosity. The presence of water in the mixture matrices raised the initial CA of the immiscible oil at the gas-solid-liquid interface, and typically increased the penetration time.

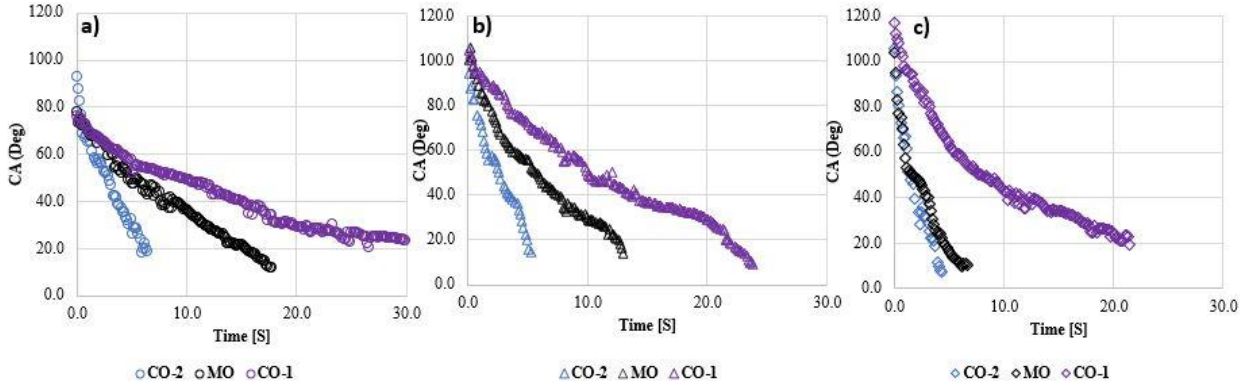

Figure 4.4: Graphical representation of oil CA on the Mixture matrix at three different MC – a) effect of 0%MC; b) effect of 5%MC and c) effect of 10% MC.

The time required to reach a CA of 20° for the oil droplets was selected randomly but works as a parameter to determine the penetration capabilities of the three oils at different MC. The penetration of oil in the solid porous matrix takes place when the surface tension of the matrix is appreciably higher than the surface tension of the oil [23]. Seo et al. [67] conducted a study on the effect of surface wettability on the dew moisture and fog of a tubular surface. This study [67] revealed that the recorded CA was low in samples without water, but high in the samples containing water. As shown in Figure 4.4, high viscosity oils generated high initial CA with the matrix surface, with the exception of the low viscosity oil (CO-2) and 0% MC, which also generated a high initial CA with the surface.

The change of CA over time was also recorded for better understanding of oils penetration through the matrices. The viscosity is the most dominant factor to decrease the penetration rate and the CA of oils in the matrices. Also, the penetration time of oils increased linearly with the viscosity of the oils [64,68], and the initial CA increased linearly with MC [52,59].

As already mentioned, the penetration rate increased with an increase in MC in the matrices [69]. However, there was an abrupt fall of initial CA identified in the case of CO-2 and MO at 10%MC (Figure 4.4c)). This sudden drop of CA could be a result of the lower viscosity of oils (CO-2 and MO) and an increase in the porosity of the mixture matrix (to a certain extent) with an increase in the amount of MC as confirmed by others [69]. In the case of CO-1, a slower penetration curve was observed – at 20 seconds the CA recorded was 20°.

4.3.2 Effect of individual matrix components on CA in matrices

This section investigates how the CA of each oil changes with MC on individual components. Each component was ground to powder with a mortar and pestle for uniform particle distribution so that accurate contact angles could be measured. CA vs time graphs at 10% MC are

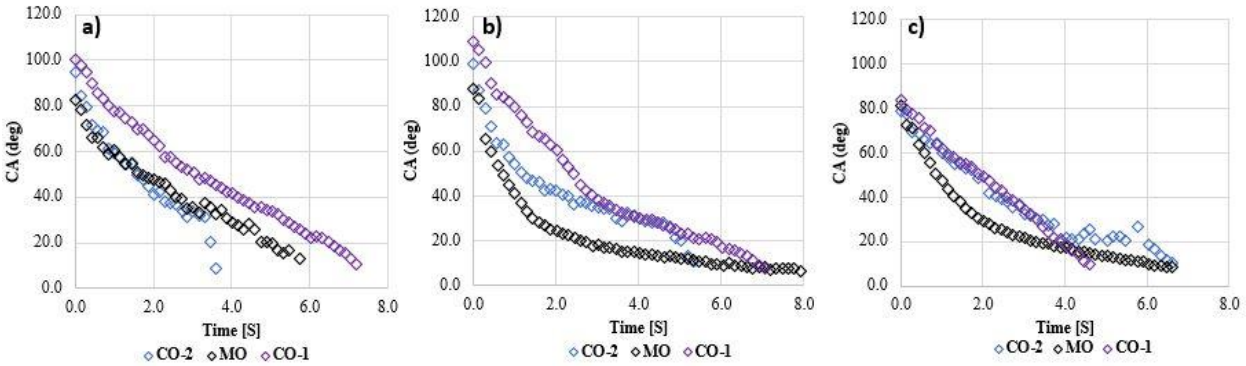

Figure 4.5: CA of oils plotted as function of time on individual components of the mixture matrices at 10% MC: a) Topsoil; b) Sand; and c) Clay. Each trial was repeated in triplicate to ensure repeatability of results, with an experimental error no more than ±5°.

shown in **Figure 4.5,** while initial CA and time taken to reach a CA of 20° are recorded in **Table 4.4** for all conditions tested.

Referring to Figure 4.5, CO-1 shows the highest initial CA among the three oils in all three individual matrices, but the highest CA is recorded in the sand matrix and the lowest CA is recorded in the clay matrix. One of the main reasons for this may be the particle size distribution of the matrix and its water absorption capacity. Generally, sand has the lowest water absorption capacity among the matrices [34]. Unabsorbed water molecules in the sand matrix block the pores and inhibit increased porosity. No cracks were observed on the surface which helped increase the CA on the sand matrix. Additional moisture, on the other hand, allows the clay matrix to absorb more water, which creates clumps, and increases porosity. As a result, oils penetrate rather than bead up on the clay matrix surface, resulting in smaller initial CA on the clay matrix compared with the sand matrix.

Table 4.4: Initial CA, and the time required to reach a CA of 20° of droplets from the three oils applied on topsoil, sand, and clay at different MC. Time taken to reach CA = 20° was arbitrarily selected to form a quantitative comparison of spreading rates between matrices.

MC	Matrix	CO-2 (low viscosity)		MO (medium viscosity)		CO-1 (high viscosity)	
		CA (°) at t=0 (s)	Time (s) taken to reach at CA = 20°	CA (°) at t=0 (s)	Time (s) taken to reach at CA = 20°	CA (°) at t=0 (s)	Time (s) taken to reach at CA = 20°
0%	Topsoil	83.9	3	64.5	3	75.8	7
	Sand	91.7	2	74.1	3.6	71.7	4
	Clay	61.8	3	75.3	6.6	74.6	4
	Mixture	92.8	6	77.7	15	76.1	26
5%	Topsoil	93.0	2.5	72.7	3.6	91.3	6
	Sand	85.0	3	75.4	3	96.4	2.5
	Clay	71.5	2.8	90.7	5.2	66.3	3
	Mixture	94.7	5	101.0	12	104.8	21

10%	Topsoil	94.9	3.5	82.5	4.5	100.5	6.5
	Sand	98.8	3.5	87.9	2.5	109.2	5.5
	Clay	78.9	4	81.5	3.2	84.0	7
	Mixture	105.8	4	103.9	5	117.3	20

Slower penetration rates were observed in MO compared to CO-1 in clay matrix at 0%MC and 5%MC. This may be attributed to the low porosity of the clay matrix at low MC, and the stickiness nature of the MO. Another important point reported in Table 4.4 is that, although the initial CA was high in the sand matrix, the recorded time to reach CA at 20° was lower than other matrices.

In order to investigate the influence of several variables simultaneously, **Figure 4.6** plots two key points obtained from all raw data graphs: the CA at t=0 s (Figure 4.6a)) and the time taken to reach at CA = 20° (Figure 4.6b)). This data is taken from the results shown in Table 4.4. With the exception of the high viscosity oil (CO-1) at 0%MC in clay matrix, all moisture conditions and droplets prepared with low and high viscosity oils (CO-2 and CO-1) showed an experimentally significant reduction in initial CA when in contact with clay matrices (experimental error no more than ± 5^{o}). The reason may be the high porosity (Table 4.2) of clay particles which

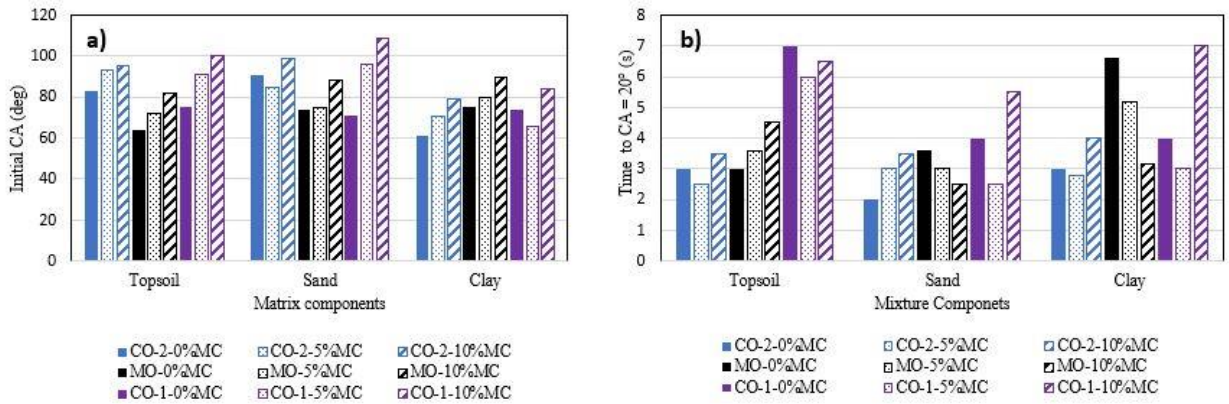

Figure 4.6: Behavior of CO-2, MO, and CO-1 oil droplets applied to topsoil, sand, and clay matrices at different MC (0, 5, and 10%MC) - a) CA at t = 0 sec; b) time taken to reach at CA of 20°.

allow oils to more quickly penetrate inside the matrix. Also, the different shapes of clay particles [43] and the many -OH groups in the clay matrix [57] could enhance the oil absorption capacity, and hence be responsible for the reduction in initial CA.

There was an increasing trend of initial CA for the medium viscosity oil (MO), found for a given matrix across the different matrices, reported on Table 4.4. However, only a small variation in penetration times was observed when comparing individual component matrices at a given MC, as well as a given matrix with increasing MC. This was also true across each viscosity oil – the small variations observed are likely to be within experimental error. Penetration times were however considerably slower for sand matrices, with the exception of the medium viscosity oil (MO). For these cases, there was also a clear trend of more rapid penetration times found with increasing MC.

4.4 Effects of bioemulsifier to assist remediation efforts

In this section, the effects of bio-emulsifier XG on oil spreading and interfacial behavior are investigated in order to get an idea of the effect of XG in preventing oil spills. Based on statistical analysis of first set of data, it can be seen that oil spreading and flow behavior was the most statistically significant in the clay and mixture matrix compared to other matrices with different variables. Therefore, this investigation has only been conducted on clay and mixture matrices at different MC for two of the oils (CO-2 and MO). The statistical analysis of all data is discussed in chapter V and all other raw data is attached in appendix A.

4.4.1 Effects of XG on spreading kinetics of oils

The spreading kinetics of two different oils on the mixture matrix was investigated in the presence of XG. With XG, a significant change in both initial spreading time and spreading area at 1000s was noticed in the case of both oils (CO-2 and MO), as shown in **Figure 4.7**. Key results from Figure 4.7 show that the initial spreading times were slower with the higher viscosity oil, higher MC and XG.

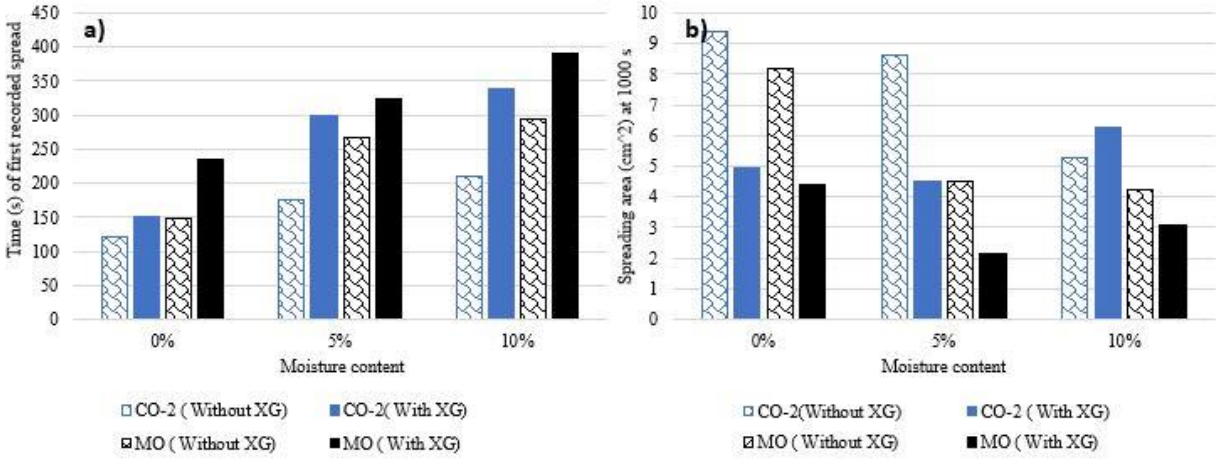

Figure 4.7: The effect of XG on clay and mixture matrix for two oils (CO-2 and MO) at three MC. Summary results of key points with the spreading kinetics trials, showing a) the time of first recorded spread; and b) the spreading area at 1000s. The typical experimental error was no more than ±0.87 cm^2.

The spreading area of oils at 1000s at three different MC was also investigated. The spreading area decreased significantly with XG for both oils at 0 and 5%MC which indicates the lower penetration rate of oils. This effect is not so noticeable at 10% MC for the low viscosity oil (CO-2). The probable cause of these results may be the polymer network forming character of the XG into the matrix. The XG is a bio-emulsifier that could form a polymer network within the matrix upon contact with liquids to a certain extent. This polymer network may block the pores of the mixture matrix [22] and reduce oil spreading. The increasing MC could increase the porosity of the matrices [69], and solubility of XG [22,45], which may increase the spreading area at

10%MC compared with 0 and 5%MC. Due to these reasons, the rate of oil spreading in the matrix decreases (especially at 0 and 5%MC) which allows the oil to remain on the matrix surface for longer time and inhibit the oil spreading rate.

4.4.2 Effect of XG on CA over different matrices

The key results of CA analysis on clay and mixture matrices with and without XG were investigated at two different MC (0 and 5%MC) as shown in **Figure 4.8.** The trends of initial CA and time taken to reach a CA of 20° were identical to the spreading kinetics trend discussed in section 4.3.2. There is no significant change of initial CA noticed in presence of XG either in clay or in the mixture matrix. However, a strong influence of XG was observed in the time taken to reach a CA of 20°. Figure 4.8 shows that there is a significant time delay to reach a CA of 20° for both oils when XG was added with the matrices in clay matrix at both 0 and 5% MC, which means the XG could slow down the penetration rate (Figure 4.8b)) of oils into the clay matrices. A slower

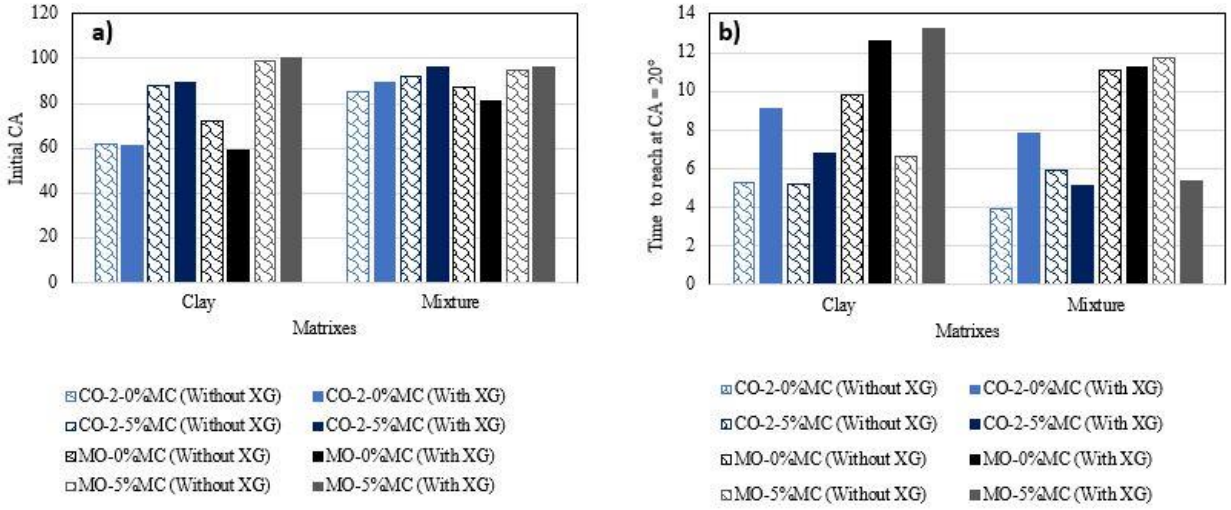

Figure 4.8: Behavior of CO-2, and MO oil droplets applied to clay and mixture matrix with and without XG at different moisture contents (0, 5% MC). a) Initial CA; b) time taken to reach a CA of 20°.

penetration rate was also found in mixture matrices at 0%MC with XG for both low and medium viscosity oil (barely for the medium oil). However, a quicker penetration rate was found at 5%MC in mixture matrix for both oils. The reason may be the increasing porosity with an increase in MC inside the mixture matrix which enhance the oil penetration rate inside the matrix [69].

It is worth noting that, the medium viscosity (MO) oil shows a slower penetration rate than the low viscosity oil (CO-2) in clay matrix with XG as well. This result may be attributed to the polymer network forming nature of XG inside the matrices, which could reduce the penetration rate in matrices [22,45].

CHAPTER V

ANALYSES OF RESULTS

[Sections 5.1.1, 5.1.3, and 5.2.1 were published in the Journal of Environmental Challenges. Mr. Firoz Ahmed performed all the experimental work and generated graphs of the raw data and was responsible for writing early drafts of the introduction and methodology sections of the paper.]

In this section, a statistical analysis has been done on all raw data from the response to spreading kinetics (time of first recorded spread; spreading area at 1000s) and CA and baseline measurement (initial CA; time at CA = 20°; maximum baseline). This analysis has been performed to determine the most dominant variables on oil spreading and penetration behavior in different matrices. Also, a comparison study has been conducted with other flow model data to check the validity of this research data. All statistically analyzed (ANOVA analyses by using Minitab software) raw data of spreading kinetics, surface and interfacial study of this research is attached in Appendix A.

5.1 Statistical analysis of spreading kinetics and interfacial studies data

5.1.1 Statistical analysis of spreading kinetics data without XG

Statistical analyses investigating the individual and combined effects of matrix packing, MC, and oil type, showed that the time of first recorded spread was strongly influenced by all three

variables when considered individually (irrespective of the other two variables). The strongest influence of these was the oil type, with F comparisons: $F_{calc} > F_{crit}$ (32.59 > 5.99); followed by MC (20.25 > 5.99); and finally, matrix packing (12.98 > 3. 84). This indicates that oil properties such as viscosity and surface tension played a dominant role in influencing its movement through the matrix. Packing, and hence porosity, of the matrices, had the least influence in this response variable, although was still deemed statistically significant. The spreading area at 1000s was arbitrarily chosen as a constant data point to quantitatively compare spreading kinetics over different conditions. Statistical analysis of this data showed that only the influence of MC was dominant in affecting the spreading area. The main effects data for both these responses is shown in **Figure 5.1**. Referring to section A2 in appendix A for interaction plot and main effects of different variables on spreading kinetics of oils.

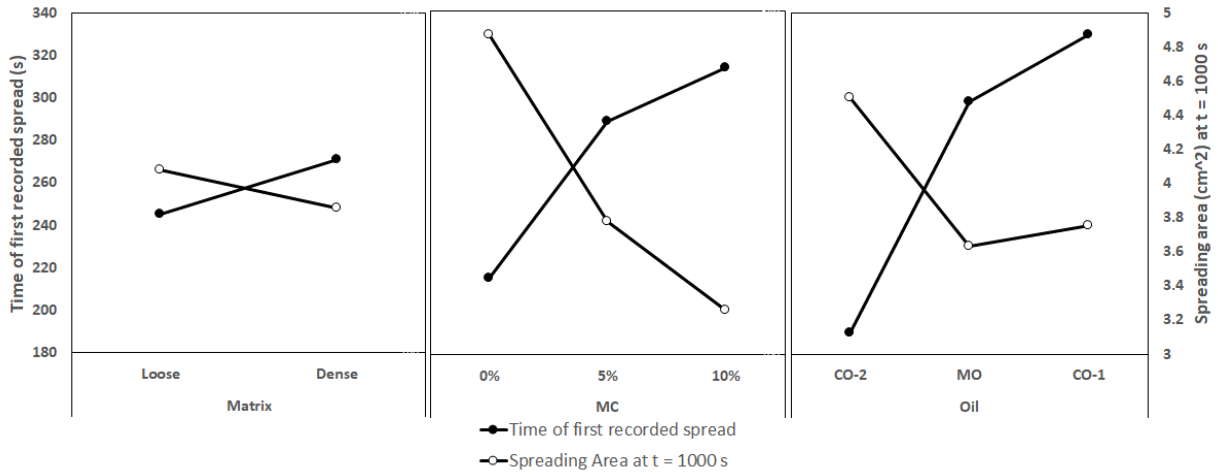

Figure 5.1: Graphical representation of statistical analysis result of spreading kinetics data, showing the influences of matrix type, MC, and oil type on the time of first recorded spread (primary y-axis) and spreading area at 1000s (secondary y-axis). All variables are statistically significant for the time of first recorded spread, while only the MC is significant for the spreading area.

While many of these observations are intuitive, they also serve to validate the experimental

methods chosen for this work. The data provided a snapshot of various influences on spreading kinetics and spreading area through the matrices, at a cross-section positioned 1.3 cm from the surface. The viscosity of an oil reflects its ability to flow, and hence low viscosity oils more

Table 5.1: Overall summary identifying the relative influence (weak, medium, strong) of considered variables on the responses measured in the spreading kinetics study; the surface interactions study; and existing theoretical models of fluid flow behavior cited in the literature. *Also, a combined effect that was statistically significant.

Spreading Kinetics Study		
Variables Investigated	**Time of first Recorded Spread**	**Spreading Area**
Moisture Content (MC)	Medium	Strong
Matrix Packing Density	Weak	None
Oil Type (viscosity)	Strong	None

Surface Interactions Study					
Variables Investigated	**Initial CA**	**Time at CA = 20º**	**Initial Baseline**	**Maximum Baseline**	**Time at Maximum Baseline**
MC	Strong	Weak	None	None	Weak
Substrate Type (chemistry)	Medium	Strongest*	None	None	Strong
Oil Type (viscosity)	None	Strong*	Strong	Strong	Medium

Theoretical Models of Fluid Flow Behavior	
Variables Considered	**Universality of Flow Behavior**
MC	Increased MC reduced universality
Substrate Type (chemistry)	Increased heterogeneity reduced universality
Oil Type (viscosity)	More complex components within oil reduced universality

quickly flowed through a given matrix than high viscosity oils. Additionally, oils with higher surface tensions were less likely to wet a surface if these values surpassed the surface energy of the matrix. The surface tensions of the three oils were reasonably similar in value, and therefore, it is likely that viscosity was the dominating factor affecting kinetics of flow.

As MC increases within the matrix, an oil-water immiscibility develops, and has the effect of slowing down the spreading kinetics as well as minimizing the area of the spread. Finally, loosely packed matrices were more porous and less dense, and therefore allowed fluids to flow more quickly through their depth, hence explaining quicker times for the first observance of spread. **Table 5.1** summarizes the influences of the main variables under consideration on the responses measured, for all studies discussed in this study without XG.

5.1.2 Statistics analysis of spreading kinetics data with XG

Two different kinds of loosely packed matrix packing (one with and one without XG) were prepared for investigating the effect of the XG in matrices for two oils at three different MC, as shown in **Figure 5.2**. The compositions of the matrix with and without XG is reported in the Table 3.1, chapter III. The experimental data showed that the time of first recorded spread was influenced by all three variables (XG, MC, and oil type) when considered individually, as seen in Figure 5.2. The two strongest influences were XG and MC, with F comparisons: ($F_{calc} > F_{crit}$) 21.48 > 3.84; and 21.14 > 5.99; respectively. The oil type (10.54 > 3.84) showed the least dominating effect on oil spreading kinetics within these comparisons. This result indicates that XG played a dominant role in influencing the oil flow through the matrix. The viscosity of oils showed the least influence

in these response variables, though the viscosity of oils does play a significant role on oil spreading in matrices, as observed in the previous section (5.1.1).

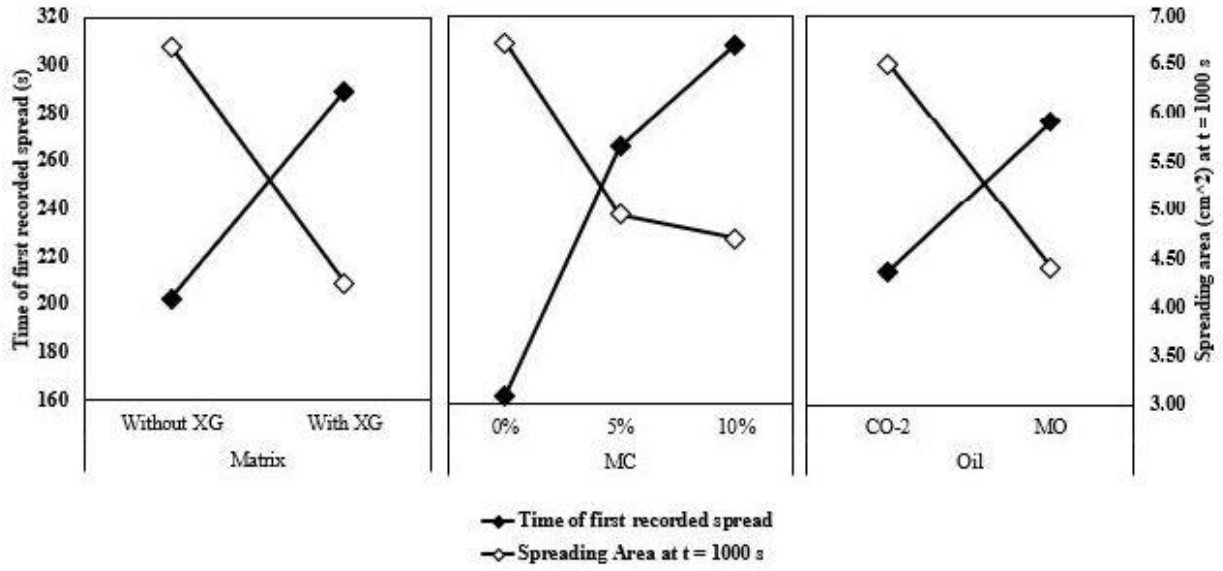

Figure 5.2: Statistical analysis of the spreading kinetics data with XG on two different conditions - the time of first recorded spread (primary y-axis) and spreading area at 1000s (secondary y-axis), showing the effect of different variable over different variables.

The influence of these same variables was also investigated on spreading area response at 1000s. A significant change of the influence of variables was noticed in the matrix with XG on spreading area at 1000s. The XG reduces the spreading area, irrespective of MC amount or oil type. The effect of XG on spreading area at 1000s was the most statistically dominant variable among the three variables. The F value comparisons of the effect of XG matrix, and oils are: $F_{calc} > F_{crit}$ (18.54 > 3.84); and (13.31 > 3.84) respectively (Section A3, appendix A). It is worth noting that the MC was not statistically significant on oil flow behavior within this set of comparisons. Figure 5.2 also highlights that the MO shows a smaller spreading area than CO-2. Finally, the 5%

and 10%MC show the lower spreading areas compared with 0%MC. These results indicate that the bioemulsifier XG played an important role in making the matrix less porous, hence the spreading rate of oils slow down into the matrix. Also, the polymer network of XG could reduce

Table 5.2: The key summary of statistical analysis with XG categorizing the relative influence (weak, medium, strong) of different variables on the spreading kinetics study; the surface interactions study; and existing theoretical models of fluid flow behavior cited in the literature. *Also, a combined effect that was statistically significant.

Spreading Kinetics Study		
Variables Investigated	**Time of first Recorded Spread**	**Spreading Area**
Moisture Content (MC)	Medium	None
Matrix Type	Strong	Strong
Oil Type (viscosity)	Weak	Weak

Surface Interactions Study					
Variables Investigated	**Initial CA**	**Time at CA = 20º**	**Initial Baseline**	**Maximum Baseline**	**Time at Maximum Baseline**
MC	Strong*	None	None	Strong	None
Substrate Type (chemistry)	Medium*	None	None	Weak	None
Oil Type (viscosity)	Weak	Strong	None	None	Weak

Theoretical Models of Fluid Flow Behavior	
Variables Considered	**Universality of Flow Behavior**
MC	Increased MC reduced universality
Substrate Type (chemistry)	Increased heterogeneity reduced universality
Oil Type (viscosity)	Decreased oil viscosity reduced universality

the spreading rate of oils into the matrix. An overall summary of statistical analysis with XG

including the effect of different variables on spreading and penetration of oils in different matrices is reported on the **Table 5.2**.

5.1.3 Statistics analysis of CA and baseline over different variables without XG

The initial CA was strongly influenced by the matrix components and MC, with MC being more dominant than the components themselves, as shown in **Figure 5.3a)**. Higher MC resulted in an increase in surface energy of the matrix, reducing wetting capabilities and hence leading to a higher CA value [26]. Figure 5.3a) also highlights a considerably lower initial CA for clay matrices (irrespective of oil type and MC) and MO oil (irrespective of matrix and MC); and the considerably higher initial CA for mixture matrices. The sheet-like geometry of clay and its abundance of –OH groups [43] enables adsorption of several components that can H-bond [70], and cationic exchange with organic-cations also improves sorption capacity of organic molecules [71]. These properties have prompted investigations into the capabilities of clay to help contain land oil spills [71], and may also explain the obvious reduction in initial CA of the oils when in contact with clay substrates. The reduction in initial CA for the medium viscosity oil (MO) could be due to the contribution of several additives within this oil, as outlined earlier. Finally, the much higher initial CA for mixture matrices is due to the additional effects of chemical heterogeneity and high porosity, as confirmed via Cassie-Baxter theory [72] (equation (5)). For a situation where beading of a liquid is already occurring on a given surface, this beading is further promoted due to the presence of roughness and heterogeneity, created either by multiple chemicals at the surface or increased surface porosity [30].

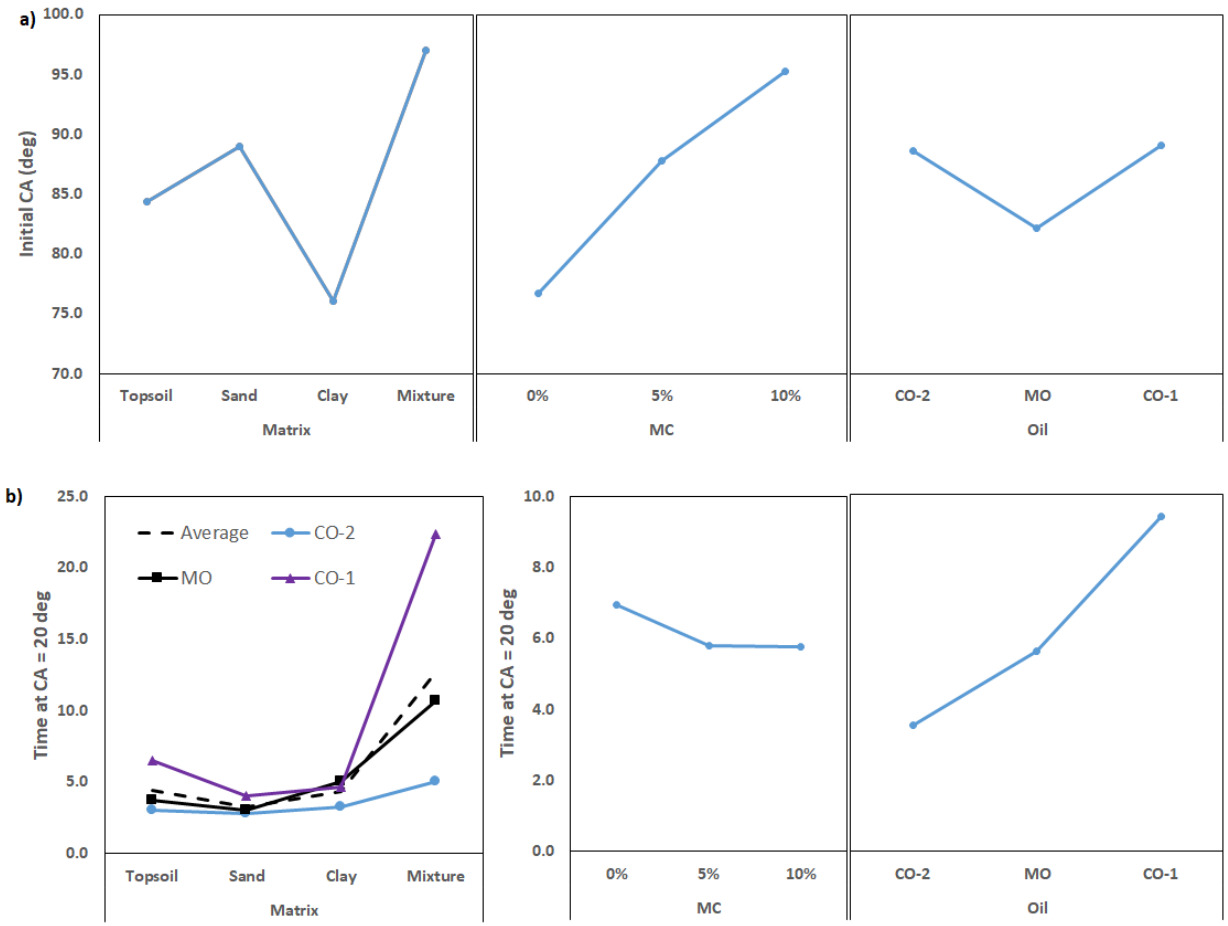

Figure 5.3: a) Main effects of matrix type, MC, and oil type on the initial CA of oil droplets contacting the matrix surface. Initial CA are averaged across two variables and plotted against the third. These plots show statistically significant effects of matrix type and MC on the initial CA. **b)** Main effects of matrix type, MC, and oil type on the time taken for the CA of the oil droplets to reach 20°. All three individual variables were shown to be statistically significant in the response time, with MC being the least significant of the three. Combined influences of matrix and oil types were also found to be statistically significant in influencing the response time.

The time taken for the CA to reach 20° was strongly influenced by the matrix components, with F comparisons: $F_{calc} >> F_{crit}$ (120.43 >> 7.81); followed by oil type (66.35 >> 5.99); combined influence of matrix components and oil type (29.32 > 12.59); and finally, the MC (11.01 > 5.99). These effects are summarized in **Figure 5.3b)**, clearly showing that the mixture matrix had the most effect on the resulting penetration time for a given oil, further accentuated by higher viscosity

oils with reduced flow capabilities. The analysis showed that while the initial CA is essentially affected by the contact first made with the surface (matrix component, with or without moisture), travel of the droplets through the matrix clearly depended on the matrix as well as the flow characteristics of the oil. While MC affected the initial CA made with the surface, this was less important than the flow properties of the oil when penetrating through the matrix. The interaction plot, model summary, and main effects of different variables without XG on different responses including initial CA, time to reach a CA of 20°, and baselines are attached in appendix A (section A4).

Statistical analysis of the baseline data showed that the initial baseline was strongly affected only by the oil type, where trends were more pronounced with clay and mixture matrices. Higher viscosity (less ability to flow) and higher surface tension (more likely to bead up on a surface) oils consistently generated lower initial baselines, as expected. The lower values frequently observed with the medium viscosity oils (MO) were likely affected by the additives present, as described earlier (Figure 4.1b)). The maximum baseline data was the only set of data where the R^2 value was just below 90%, and this value was also strongly affected by the oil type.

The time taken to reach the maximum baseline was individually influenced by matrix type, oil type, and MC, in that order, as shown in Figure 5.4. This mimics the ANOVA results for time taken to reach a CA of 20^o, with the exception that the CA was additionally influenced by the combined influence of the matrix and oil types. A more complex or chemically heterogeneous mixture matrix accounts for an increase in tortuosity of penetrating fluids, hence influencing surface observations by longer times to reach a CA of 20^o and maximum baseline of the droplet. Additionally, higher viscosity oils also are less able to flow freely through a matrix and take longer

time.

The main effects influencing time to maximum baseline are plotted in **Figure 5.4**, and it is again seen that the mixture data is significantly different from the remaining matrix components, leading to the rejection of the null hypothesis. The differing porosities of each matrix did not appear to influence times required to reach the maximum baseline, with topsoil and sand having relatively low porosities, and clay and mixture matrices having much higher porosities. The difference between maximum and initial baseline values was determined to be experimentally significant for all conditions tested with low viscosity oils. This was significant only half the time for medium viscosity oils, and not significant for any high viscosity oils, suggesting that the oil viscosity impacts its spreading capabilities in the lateral direction (data not shown).

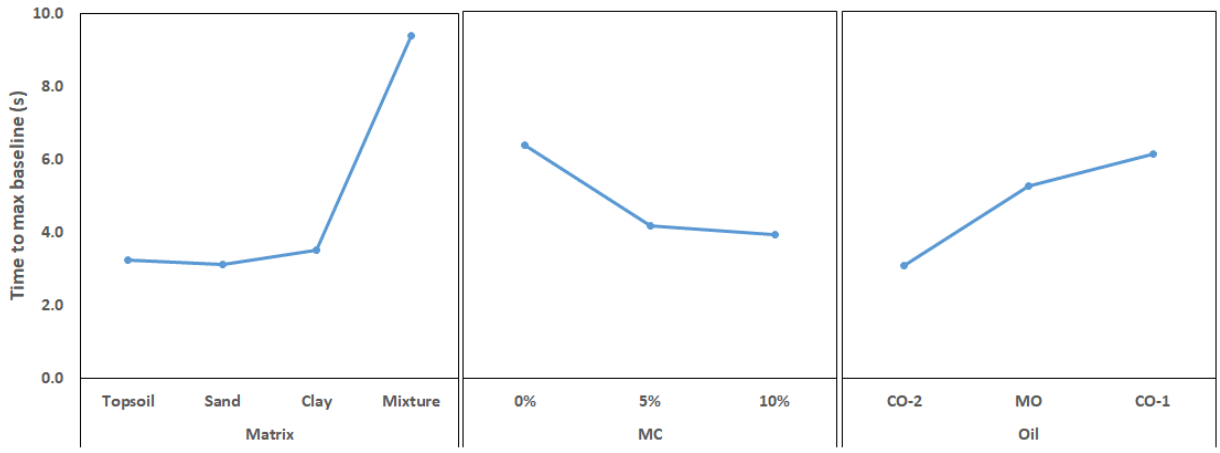

Figure 5.4: Main effects of matrix type, MC, and oil type on the time to reach maximum baseline of oil droplets contacting the matrix surface. These times are averaged across two variables and plotted against the third. Plots show statistically significant effects of matrix type, oil type, and finally MC on the recorded time of the maximum baseline.

The least dominant influence of MC – but one that was still recorded as statistically significant – was opposite to expected trends. Both analyses of penetration time responses showed that for any matrix or oil type, higher MC corresponded to quicker times to reach a pre-defined

penetration level (low CA or maximum baseline). This is in direct contradiction to the results obtained from the spreading kinetic studies, where it was clear that higher MC resulted in longer times being recorded for first recorded spread, and smaller spreading areas. The kinetics studies essentially represent a snapshot of oil penetration at a certain cross-section depth into the matrix, while the latter study investigates surface influence on the ability of the oil to penetrate into the depths of the matrix. Although the particle sizes were necessarily different between the two studies, their resulting porosities were similar (for multicomponent matrices), enabling qualitative comparisons of surface and bulk influence on oil spreading behavior. These results provide important insights in developing time-sensitive responses to oil spills, where both surface and bulk influences may need to be considered when developing suitable materials to hinder progress of the spill. The key summary of the influence of different variables on CA and baseline data without XG is reported in Table 5.1, which is broadly discussed in this section.

5.1.4 Statistics analysis of CA and baseline data over different variables with XG

Matrices were prepared both as mixtures and as individual components with and without XG to better understand the chemical influence of matrix components including XG at the interface. The specific matrices investigated were clay with XG; clay without XG; mixture with XG; and mixture without XG. From the experimental data of first set of work, it is found that the MC, oil type and matrix type were statistically significant in influencing the penetration rate of oil in matrices. Therefore, the main effect of all three variables (MC, oil type, and XG) were investigated again on the initial CA, time at CA reached 20°, and maximum baseline with XG.

The initial CA was most strongly influenced by MC among the three variables as shown

Figure 5.5a). The F values comparisons are follows: matrix component, $F_{calc} > F_{crit}$ (20.89 > 7.81); MC (184.53 >> 3.84); and oil types (5.32 > 3.84). There is no significant change noticed on initial CA in the case of matrix type regardless of with or without XG. However, the initial CA was increased significantly with an increase in MC, irrespective of whether the matrices contained XG (Figure 5.5a, second graph)). The oil type had the least influence affecting the initial CA, although

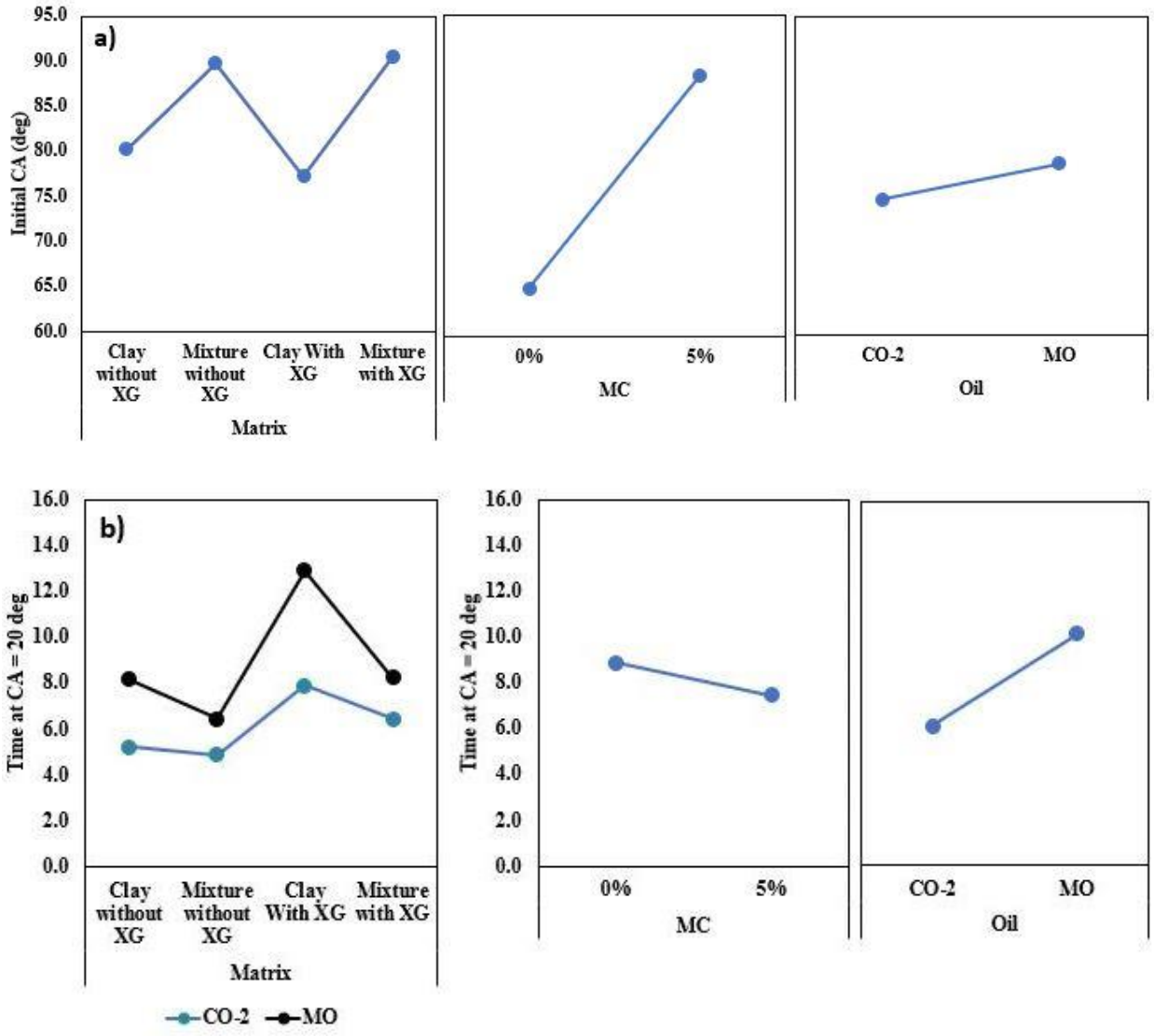

Figure 5.5: a) Main effects of matrix type (with and without XG), MC (0 and 5%), and oil type (CO-2 and MO) on the initial CA of oil droplets contacting the matrix surface. b) Main effects of matrix type, MC, and oil type on the time taken for the CA of the oil droplets to reach 20°.

it was still statistically significant. The high viscosity oil (MO) generates a higher initial CA than the low viscosity oil (CO-2). The reason may be the stickiness, and different additives present in the MO as outlined earlier. Referring to appendix A (section A5) to explore more about the interaction plot, model summary, and main effects of different variables without XG on different responses including initial CA, time to reach a CA of 20°, and baselines.

Statistical analysis was also performed on the data for time taken to reach a CA of 20° for CO-1 and MO, as shown in **Figure 5.5b)**. Longer times are observed for both oils to reach a CA of 20° in the clay and mixture matrix with XG. It is clearly noticed that the higher viscosity oil took more time to reach a CA of 20° which indicated reduced penetration rate. These two responses showed that the XG and viscosity played a dominant role in delaying the oil penetration into the matrix. Figure 5.5b) also highlights the effect that MC is not statistically significant to inhibit the penetration rate of oil.

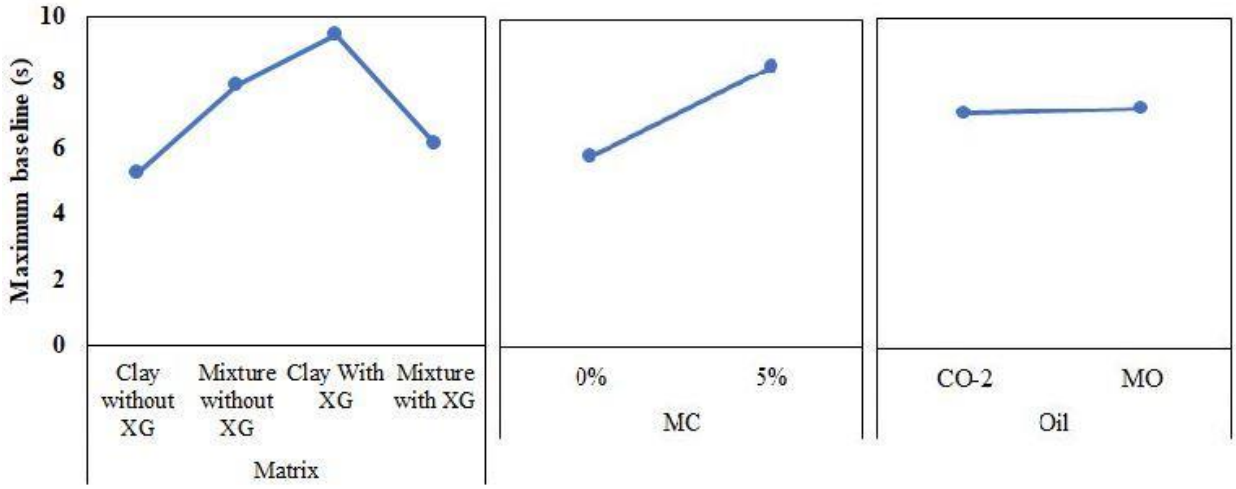

Figure 5.6: Main effects of matrix type, MC, and oil type on maximum baseline of oil droplets contacting the matrix surface. These are averaged across two variables and plotted against the third. Plots show statistically significant effects of matrix type, oil type, and MC on maximum baseline.

For more in-depth analysis, the data of maximum baseline was also statistically analyzed to investigate which factor was more dominant for the two oils. The key summary of these effects is displayed in **Figure 5.6**.

As shown, the maximum baseline was affected by the MC, with F comparisons: $F_{calc} > F_{crit}$ (23.73 > 3.84); and matrix components (10.94 > 7.81). It is seen that maximum baseline was strongly influenced by the clay matrix with XG compared with no XG. The water absorption propensity of clay matrix due to abundance of -OH enhances the solubility of the XG (XG is soluble in water) [22], which helps to form the XG polymer network into the pores of the clay matrix and minimize penetration of the oil, hence maximizing lateral spread instead. Although, MC strongly influenced the maximum baseline according to Figure 5.6 (second graph), MC was more dominant in cases with XG compared to those without XG. In the case of with XG, the matrix with 5% MC affected the maximum baseline more than the matrix containing 0%MC. This result indicates that increasing MC could affect the maximum baseline significantly with XG, though MC was not statistically significant to affect maximum baseline without XG (data not shown). The oil type was not a significant factor affecting the maximum baseline with XG, suggesting that the viscosity of oils does not play a dominant role influencing the maximum baseline. These results indicate that the penetration rate of oils would be reduced in the presence of XG with an increase in MC. Overall, a summary of the results of the effect of different variables on CA and baseline data of oils on the different matrices with XG is reported in Table 5.2.

5.2 Comparison of findings with other flow models

5.2.1 Comparison of findings without XG with other flow models

CA and baseline data vs time are measurements commonly utilized to develop empirical or numerical models of fluid flow behavior over porous substrates. Several studies [49,52,73–77] describe such systems based on the behavior profiles of these measured variables, and the ability to identify either two or three stages which denote complete or incomplete wetting, respectively. Here, I focus on exploring the profiles obtained to help explain the fluid flow behavior observed in our first set of experimental work. **Figure 5.7** shows examples of overlaid baseline and CA data with time for four of 36 different conditions investigated. These examples cover the array of variables tested (matrix components, MC, oil viscosity) and demonstrate the complete and incomplete wetting profiles as described by others [49,52,73,78].

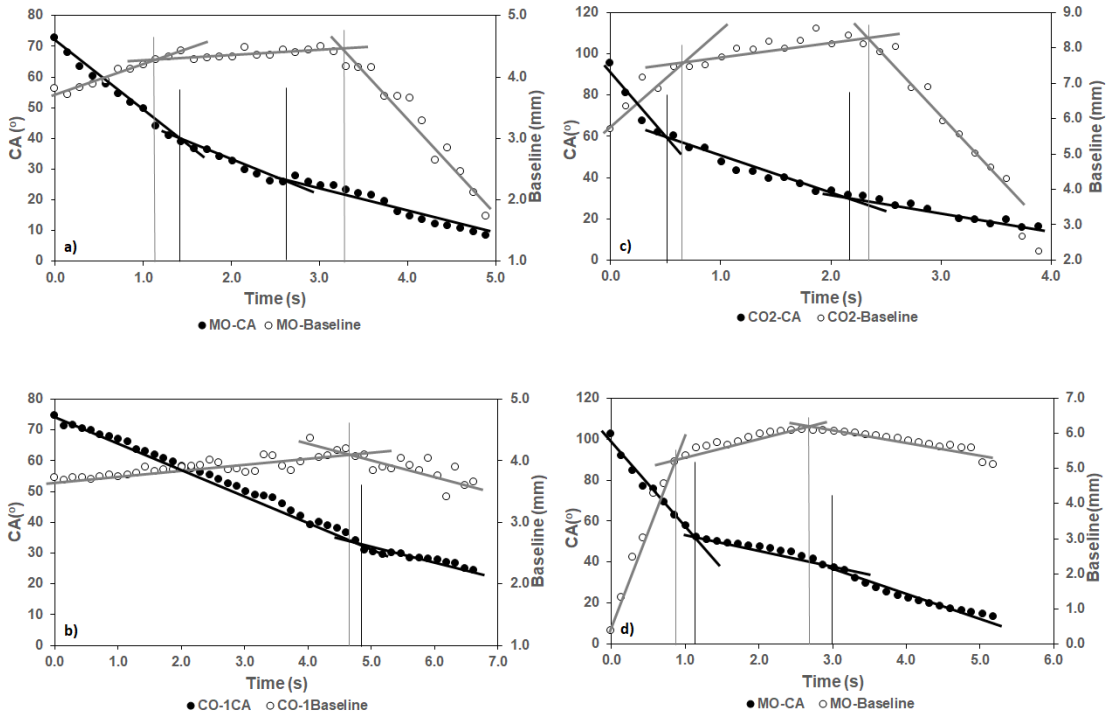

Figure 5.7: CA and baseline profiles for various conditions of oil droplets spreading over porous matrices. a) MO oil on topsoil matrix, 5% MC; b) CO-1 oil on clay matrix, 0% MC; c) CO-2 oil on sand matrix, 5% MC; d) MO oil on mixture matrix, 10% MC.

In all 36 conditions considered, only five were 'not classifiable', meaning that there were different numbers of sections between the CA and baseline profiles, or the change to a new section did not correspond with both profiles. Sections within CA and baseline profiles 'corresponded' if they both began or ended within 1s of each other. Of the remaining 31 conditions, 16% demonstrated complete wetting profiles while 84% conformed to incomplete wetting profiles. Of the complete wetting cases, all but one case was observed at 0% MC. Of the five 'not classifiable' cases, three of these occurred with mixture matrices, substrates that were the most chemically complex and heterogeneous as they contained multiple components.

While the majority of cases such as those shown in Figure 5.7 were identified as complete (two sections) or incomplete (three sections) wetting, their profile shapes frequently did not follow those described by others [49,52]. For example, with the incomplete wetting cases, the middle stage should conform to an approximately constant baseline value, and the third stage should demonstrate an approximately constant CA value. The first stage should also be quite rapid. This behavior was evident in some, but certainly not all, cases investigated, and it is possible that chemically complex and thick porous matrices may not in fact conform as closely to the models proposed. In those studies cited [49,52], the thick porous substrates were glass or metal filters, and sponges, all of which were prepared from chemically homogeneous materials. In the current study, each matrix was chemically heterogeneous even with the individual component matrices (though dominant in the named component), let alone when combined as the mixture matrix. Additionally, these substrates were physically present in compact particulate form, whereas the

filters and sponge were a single, continuous material.

Raw data was converted to dimensionless parameters and further explored to test the claims of universality of baseline and CA with time [49,52,73]. Time was divided by the maximum spreading time; baseline by the maximum baseline recorded; and CA by that recorded at the maximum baseline, in keeping with that described by Starov et al. [49]. Sand was likely to be the most chemically homogeneous of the component matrices, since topsoil and clay were still mixtures of soil, though dominant in their respective components of silt and clay. Consequently, the dimensionless CA and baseline curves for sand were the most likely to follow universal behavior, as shown in **Figure 5.8**, for 0, 5 and 10% MC. The CA universality became increasingly worse as more water was added, due to increasing heterogeneity of the matrix and changes to porosity [69]. Additionally, the baseline universality was observed more closely for low and high viscosity oils (CO-2 and CO-1) compared with medium viscosity oil (MO). As explained earlier, the various additives introduced in MO were found to account for different flow behavior for this oil. Data for the clay matrix at 0% MC and the mixture matrix at 5% MC also somewhat demonstrated universality of data, but all other conditions showed obvious deviations from this behavior.

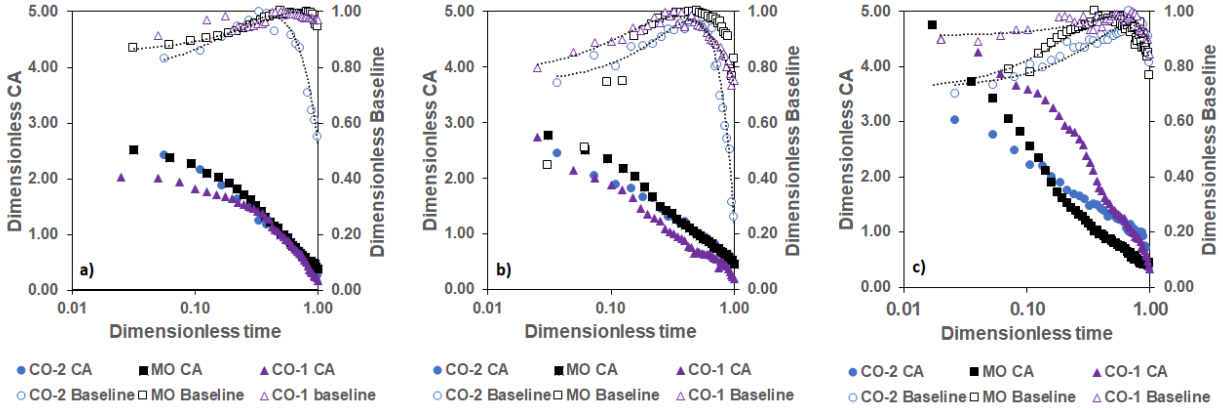

Figure 5.8: Dimensionless profiles of CA and baseline data for sand matrices at a) 0% MC; b) 5% MC and c) 10% MC, for each of the three oils under investigation. Baseline was made dimensionless by dividing the values by the maximum baseline for each trial; CA was made dimensionless by dividing the values by the CA recorded at the maximum baseline. Dotted lines represent lines of best fit through some of the baseline curves.

It is worth noting that much of the experimental data presented by Starov et al [49] demonstrated complete wetting of silicone oils over thick substrates, and the only incomplete wetting cases were again on thin porous substrates. In a study by Johnson et al. [52], additional work was presented for surfactant solutions over thick porous substrates – sponges. While this work followed universal behavior, the behavior profiles again conformed to complete wetting, potentially due to the surface-tension altering properties of the surfactant in the solutions investigated. Alleborn and Raszillier [74] presented a numerical model of liquid droplets spreading over thick, porous substrates. Their model was governed by Navier-Stokes equations for incompressible Newtonian fluids, as well as Darcy's law to describe the imbibition process. There were several key differences in this model compared with that presented by Starov et al [49]. One key difference was that using the lubrication theory approximation, fluid motion was restricted to the vertical dimension only, however the position of the wetting front with time was represented laterally. During the sorption of the droplet into the porous substrate, the wetting front

advancement was delayed, but increased later on to reach a local maximum before decreasing rapidly when the droplet was completely absorbed [74]. In the work by Starov et al [49], there was a rapid increase in baseline (and corresponding rapid decrease in CA) in the first stage of wetting governed by hydrodynamics, prior to the imbibition process taking place for incomplete wetting cases. Much of Starov et al's [49] theory was governed by the complete wetting process, developed on two baseline velocity equations representing the increase, and then decrease, of this front. Consequently, the latter described theory tended to predict a maximum baseline much sooner into the wetting process than the former, due to the incorporation of lateral spreading, prior to imbibition, taking place. This may well be applicable for thin porous substrates where lateral spreading is more expected, but for thick porous substrates, one would expect the imbibition or sorption process to be more dominant.

The descriptive results from the numerical simulations by Alleborn and Raszillier [74] tended to match the profiles observed in Figure 5.8, where a relatively constant baseline is predicted at early times, followed by a later maximum. More than 70% of cases investigated in the current study confirmed that the maximum baseline was not reached until at least half-way into the total penetration time of the droplet, with 30% of cases not reaching the maximum until 75% of the penetration time. Additionally, the lateral spreading as confirmed by differences between maximum and initial baseline showed that there was much less lateral movement of oils as the viscosity increased.

Experimental findings from the present work tended to reveal a difference in oil spreading and penetration behavior at the surface compared with the bulk, and was linked to properties such as porosity that differ substantially at these two positions. A numerical development discussed by

Markicevic et al. [76] identified a primary spreading of a sessile drop composed of two parts: the droplet on the surface of the medium and the liquid imbibing into the porous medium; and a secondary spreading of the liquid when there was no longer a sessile droplet remaining on the surface. All three situations were modeled using a dynamic capillary network model, and backed by experiment using sand medium and a nerve chemical warfare agent, with similar viscosity and surface tension to CO-2. Using the case of a constant droplet baseline being depleted into the porous material, Markicevic et al. [76] confirmed experimental data with the model by the introduction of a remnant liquid layer remaining on the surface. This was first suggested by Denesuk et al. [77], where a very thin film remained while the CA of the droplet reduced. It is plausible that this remnant film, if present, may also contribute to observed differences in spreading behavior of liquids on the surface compared with through the bulk.

Finally, the times taken to reach a maximum baseline and a CA of 20^{o} in the present study were influenced by the matrix type, oil type, and MC. The various models reviewed here that directly rely on baseline and CA data did not consider these influences except the work of Starov and others [49,52,73], where universality of conditions was concluded. The variables investigated (matrix type, oil type, and MC) were found to be statistically significant in many cases regarding their influence on CA and baseline observations, and therefore future modeling work of fluid flow over porous media should consider incorporating these additional influences. The effect of different variables (matrix type, oil type, and MC) on universality of flow behavior in the matrix with XG is summarized in Table 5.1.

5.2.2 Comparison of findings with XG with other flow models

Similar to the data without XG, the raw CA and baseline data of clay and mixture matrix with XG was converted to dimensionless parameters first, and then investigated to test the claims of universality of baseline and CA with time [49,52,73]. The universality of clay and mixture matrix data was tested under two variables (MC and two oil types) due to statistically significant results as mentioned in earlier sections. The raw data of time, baseline, and CA were divided by the maximum spreading time, maximum baseline and CA recorded at the maximum baseline respectively to get the dimensionless data of the corresponding raw data as described by Starov et al [49].

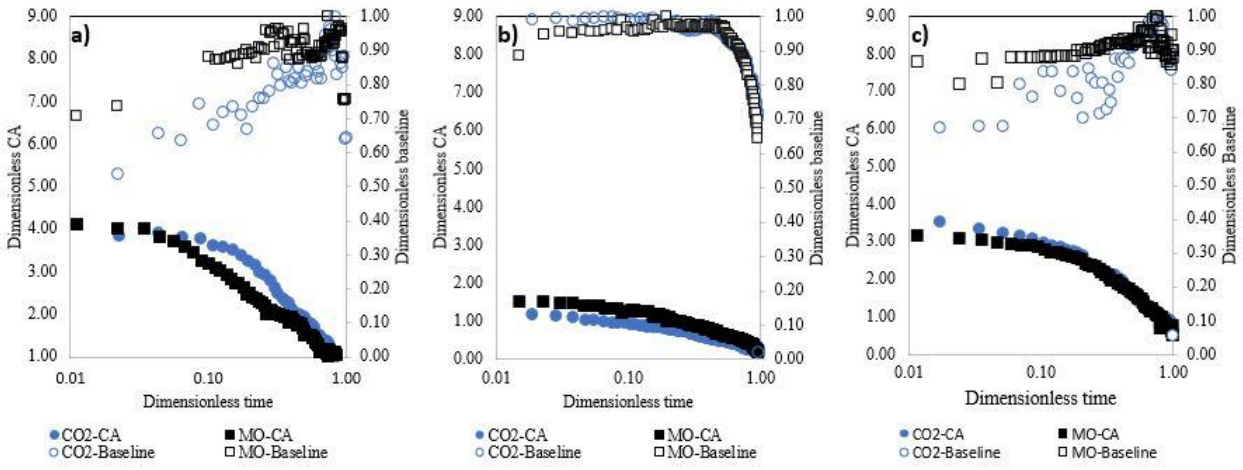

Figure 5.9: Dimensionless profiles of CA and baseline data for clay and mixture matrix with and without XG at 0% and 5% MC for each of the two oils under investigation- a) Mixture without XG at 5%MC; b) Clay with XG at 0%MC; and c) Clay without XG at 0%MC.

The dimensionless data of CA and baseline in clay and mixture matrices is plotted with time at 0 and 5% MC for testing the universal behavior of two oils, as shown in **Figure 5.9**. The mixture matrix was likely to be chemically more heterogeneous compared with the individual clay matrix due to being comprised of topsoil, clay, and sand. This statement is valid for both 0 and 5%

MC. As a result, the CA and baseline curves of the mixture matrix were mostly not following the universal behavior, as shown in **Figure 5.9a)** at 5%MC.

In contrast, the CA and baseline universality profile of clay matrix with and without XG more accurately followed the universal behavior compared with the mixture matrix due to increasing homogeneity of the matrix [69], as shown in **Figure 5.9b)** and **Figure 5.9c)** at 0%MC. Both CA and baseline curve began to deviate from universal behavior with increasing percentage of MC (data of 5%MC for clay matrix is not shown). In contrast with the mixture matrix data in Figure 5.9a), the baseline universality profile was observed quite closely for clay matrix with XG at 0% MC. The reason may be attributed to the uniform particle size and platy shape of clay particles, which helps to generate a more uniform trend of baseline. The viscosity of the oil played a dominant role again in following the universal behavior of flow models proposed by others [49, 52,74]. The MO (more viscous than CO-2) conformed quite accurately with the universality profiles, although both oils conformed to this behavior in the clay sample with XG. These results indicate that the XG played a dominant role in minimizing oil penetration into the soil matrix if the soil is more clay dominated. Further investigation is needed to explore more about the effect of XG in penetration of oils in land.

Similar to the clay matrix without XG, the sand matrix also follows the universal behavior as highlighted in Figure 5.8 due to chemical homogeneity. However, the universality was more pronounced in the clay matrix with XG at 0%MC compared with the sand matrix without XG at 0%MC. The reason may be that XG helps to reduce the oil spreading rate and increase the spreading time inside the clay matrix. The influence of several variables on universality of flow behavior is briefly reported in Table 5.2.

CHAPTER VI

CONCLUSION

This study sought to investigate fluid flow behavior of oils over soil-based matrices, in an effort to better understand the spreading phenomena on realistic, porous, chemically heterogeneous, thick, and rough surfaces. Fluid flow behavior through porous media is a well-studied area, but many studies frequently rely on model systems that do not necessarily represent the actual application – in this case, oil spills on land.

There were some important new learnings from this work. **Firstly**, spreading kinetics studies of oils flowing through soil substrates revealed quicker spreading times and larger areas of oil spread through the matrix depth for low viscosity oils, dry, and loosely packed matrices. All three variables were deemed statistically significant in influencing the time of first recorded spread, while only the MC was significant for the spreading area, suggesting oil-water immiscibility phenomena at play. The oil viscosity was the strongest influential factor on the time of first recorded spread when comparing matrix packing (loosely and densely packed matrix); XG played a dominant role in the time of first recorded spread when added to loosely packed matrices. Also, the spreading area at 1000s in the loosely and densely packed matrices was influenced by only MC. On the other hand, oil viscosity and XG significantly influenced the spreading area at 1000s when XG was added to loosely packed matrices. Therefore, the bio-emulsifier XG could be

a good option to apply in a spilling region to reduce the oil spreading rate.

Secondly, higher viscosity oil droplets took longer to flow through the matrix (with and without XG), and baseline measurements confirmed a reduction in lateral spread as well. The smaller particle sizes of ground components used in the matrices surface energy studies appeared to form aggregates, particularly with moisture, resulting in larger porosities and/or pore sizes, which influenced penetration rates of the different oils. Also, the polymer network of XG could inhibit the penetration rate of oils into the matrices to a certain extent. Therefore, using XG in a spilling region could be a good option to reduce the spreading and penetration of oils.

Thirdly, it has been previously assumed that droplets spreading over thin or thick porous substrates demonstrated a rapid lateral spread to a maximum baseline value, whether demonstrating complete or incomplete wetting of the substrate [49,52]. However, more than 70% of cases investigated in the first set of experimental data showed this maximum being reached at least half-way into the total penetration time, with 30% of these not occurring until 75% of the total penetration time. Also, most of the baseline responses (initial and maximum baseline, time at maximum baseline) was strongly influenced by either oil viscosity or MC both with and without XG. The maximum baseline was strongly influenced by the matrix type, especially the clay matrix with XG. It is clearly noticed that XG could play a dominant role to reduce the oil penetration rate when the soil is clay-dominated.

Fourthly, dimensionless CA and baseline profiles frequently were dependent on the substrate material, thickness of substrate, or viscosity of the fluid, as previously suggested by others [49,52]. Chemical heterogeneity of both component and mixture matrices greatly contributed to profiles deviating from universal behavior, and the different viscosity fluids, often

with complex chemical makeup as well, also contributed to these observed changes.

Finally, the spreading rate of the oil in both clay and mixture matrices was slower due to the addition of XG, which may be helpful in designing a new soil remediation method. In the presence of XG, the matrix type and oil type were the most dominant, although all three variables (matrix type, MC, and oil type) were statistically significant. It was also found from the CA and baseline studies that the penetration rate of oils (CO-2 and MO) was significantly slower in the matrix with XG compared with no XG. The MC and oil were the most dominant variables on oil penetration rate, although the matrix type was also statistically significant with the two variables (MC and oil type).

This study shed new light on understanding and identifying several surface factors that influence the spread of oils over soil-based matrices that were previously thought not to influence fluid flow behavior. These important findings will help shape the development of future materials or spill containment methods to minimize spread and long-term damage to the soil habitat.

CHAPTER VII

FUTURE WORK

A number of recommendations for future research are given. A Quartz Crystal Microbalance with Dissipation (QCM-D) instrument could be used to measure interfacial spreading kinetics of oils at the molecular level to determine the influence of viscoelasticity on oil spreading behavior. Also, the QCM-D could be utilized to determine viscoelastic changes in the oil upon contact with the soil. These QCMD measurement results will represent the oil molecules that initially come into contact with the matrices and spread over the matrices. At any given point on a soil matrix at the molecular scale, individual molecules of oil will experience a homogeneous surface. This important information would provide a new insight to determine the influence of viscous properties on the spreading and penetration of oils at the nanoscale.

X-ray diffraction (XR-D) measurements of the model soil system could be investigated to understand how the minerals and other chemical compounds affect the oil flow behavior present in the soil sample. Having this information would help to understand the chemical interaction between oils, and soils, possibly leading to new knowledge regarding the spreading and penetration of oils. Also, XR-D analysis could help explain the interaction of XG with the model soils. This may provide information on how best to introduce XG into the soils for future remediation efforts.

Prior to finding a suitable method of XG application, it is important to perform a similar

investigation on the actual soil rather than laboratory soil samples. This actual soil could be collected from different places in Mississippi, and then, the response of XG on the flow behavior of oils in the actual soil matrix could be investigated.

The next and final part of this research would be to find the most appropriate method to apply XG on the actual oil spilling region. Therefore, this research will also be focused on the appropriate way of XG application on a particular land-based oil spill area to inhibit the oil spreading. The main goal of this study would be to mitigate oil spreading and penetration into the soil to protect our land-based ecosystem as well as the environment. Finally, this in-depth study of surface and interfacial energies, and their influence on oil spreading and penetration in land could lead to a rapid-response soil remediation strategy in the future.

LIST OF REFERENCES

[1] E. Allison and B. Mandler, “Transportation of Oil, Gas, and Refined Products,” American Geosciences Institute, Jun. 18, 2019. https://www.americangeosciences.org/geoscience-currents/transportation-oil-gas-and-refined-products (accessed Feb. 14, 2021).

[2] R. Vazquez-Duhalt, “Environmental impact of used motor oil,” Sci. Total Environ., vol. 79, no. 1, pp. 1–23, Feb. 1989, doi: 10.1016/0048-9697(89)90049-1.

[3] Y. Wang, J. Feng, Q. Lin, X. Lyu, X. Wang, and G. Wang, “Effects of crude oil contamination on soil physical and chemical properties in Momoge wetland of China,” Chin. Geogr. Sci., vol. 23, no. 6, pp. 708–715, Dec. 2013, doi: 10.1007/s11769-013-0641-6.

[4] D. O. Njobuenwu and M. F. N. Abowei, “Spreading of Oil Spill on Placid Aquatic Medium,” Leonardo J. Sci., no. 12, pp. 11–14, 2008.

[5] H. G. Schwartzberg, “Spreading and movement of oil spills,” 15080, Mar. 1970.

[6] S. Jafarinejad, “Environmental Impacts of the Petroleum Industry, Protection Options, and Regulations,” in Petroleum Waste Treatment and Pollution Control, Elsevier, 2017, pp. 85–116. doi: 10.1016/B978-0-12-809243-9.00003-1.

[7] G. Alaa El-Din, A. A. Amer, G. Malsh, and M. Hussein, “Study on the use of banana peels for oil spill removal,” Alex. Eng. J., vol. 57, no. 3, pp. 2061–2068, Sep. 2018, doi: 10.1016/j.aej.2017.05.020.

[8] E. O. Obi, F. A. Kamgba, and D. A. Obi, “Techniques of Oil Spill Response in the sea,” *IOSR J. Appl. Phys.*, vol. 6, no. 1, pp. 36–41, 2014, doi: 10.9790/4861-06113641.

[9] O. US EPA, “Understanding Oil Spills and Oil Spill Response,” Overviews and Factsheets, Jan. 2018. https://www.epa.gov/emergency-response/understanding-oil-spills-and-oil-spill-response. (Accessed: Feb. 21, 2021).

[10] A. Bayat, S. F. Aghamiri, A. Moheb, and G. R. Vakili-Nezhaad, “Oil Spill Cleanup from Sea Water by Sorbent Materials,” Chem. Eng. Technol., vol. 28, no. 12, pp. 1525–1528, Dec. 2005, doi: 10.1002/ceat.200407083.

[11] L. Peng, H. Li, Y. Zhang, J. Su, P. Yu, and Y. Luo, “A superhydrophobic 3D porous material for oil spill cleanup,” RSC Adv, vol. 4, no. 87, pp. 46470–46475, 2014, doi: 10.1039/C4RA06337F.

[12] M. O. Adebajo, R. L. Frost, J. T. Kloprogge, O. Carmody, and S. Kokot, “Porous materials for oil spill cleanup: A review of synthesis and absorbing properties,” J. Porous Mater., vol. 10, no. 3, pp. 159–170, 2003, doi: 10.1023/A:1027484117065.

[13] R. Stone, “Russian Arctic Battles Pipeline Leak,” Science, vol. 268, no. 5212, pp. 796–797, May 1995, doi: 10.1126/science.268.5212.796.

[14] A. Jernelöv, “The Threats from Oil Spills: Now, Then, and in the Future,” AMBIO, vol. 39, no. 5–6, pp. 353–366, Jul. 2010, doi: 10.1007/s13280-010-0085-5.

[15] J. L. Ramseur, “Oil Spills: Background and Governance,” Congressional Research Service, p.33, Sep. 2017.

[16] J. Chen, W. Zhang, Z. Wan, S. Li, T. Huang, and Y. Fei, “Oil spills from global tankers: Status review and future governance,” J. Clean. Prod., vol. 227, pp. 20–32, Aug. 2019, doi: 10.1016/j.jclepro.2019.04.020.

[17] L.-P. Beland and S. Oloomi, “Environmental disaster, pollution and infant health: Evidence from the Deepwater Horizon oil spill,” J. Environ. Econ. Manag., vol. 98, p. 102265, Nov.

2019, doi: 10.1016/j.jeem.2019.102265.

[18] USDOE Energy Information Administration, “Oil and gas resources of the Fergana Basin (Uzbekistan, Tadzhikistan, and Kyrgyzstan),” USDOE Energy Information Administration, Washington, DC (United States). Office of Oil and Gas, DOE/EIA-TR/0575, Jan. 1995. doi: 10.2172/10103777.

[19] S. Yavari, A. Malakahmad, and N. B. Sapari, “A Review on Phytoremediation of Crude Oil Spills,” Water. Air. Soil Pollut., vol. 226, no. 8, p. 279, Aug. 2015, doi: 10.1007/s11270-015-2550-z.

[20] Z. Yang, S. Fang, M. Duan, Y. Xiong, and X. Wang, “Chemisorption mechanism of crude oil on soil surface,” J. Hazard. Mater., vol. 386, p. 121991, Mar. 2020, doi: 10.1016/j.jhazmat.2019.121991.

[21] C. W. Barney, “Effects of soil temperature and light intensity on root growth of loblolly pine seedlings,” *Plant Physiol.*, vol. 26, no. 1, pp. 146–163, Jan. 1951, Accessed: Apr. 23, 2020.

[22] G. Sworn, “Xanthan gum.,” in Handbook of hydrocolloids, Woodhead Publishing Ltd, 2000, pp. 103–115. Accessed: Feb. 14, 2021.

[23] M. A. Butt, A. Chughtai, J. Ahmad, R. Ahmad, U. Majeed, and I. H. Khan, “Theory of Adhesion and its Practical Implications,” J. Fac. Eng. Technol., pp. 21–45, 2008.

[24] Gh. Barati Darband, M. Aliofkhazraei, S. Khorsand, S. Sokhanvar, and A. Kaboli, “Science and Engineering of Superhydrophobic Surfaces: Review of Corrosion Resistance, Chemical and Mechanical Stability,” Arab. J. Chem., vol. 13, no. 1, pp. 1763–1802, Jan. 2020, doi: 10.1016/j.arabjc.2018.01.013.

[25] S. Li, J. Huang, Z. Chen, G. Chen, and Y. Lai, “A review on special wettability textiles: theoretical models, fabrication technologies and multifunctional applications,” J. Mater.

Chem. A, vol. 5, no. 1, pp. 31–55, Dec. 2016, doi: 10.1039/C6TA07984A.

[26] K. Song, J. Lee, S.-O. Choi, and J. Kim, "Interaction of Surface Energy Components between Solid and Liquid on Wettability, and Its Application to Textile Anti-Wetting Finish," Polymers, vol. 11, no. 3, p. 498, Mar. 2019, doi: 10.3390/polym11030498.

[27] B. Hollebone, "Oil Physical Properties," in Oil Spill Science and Technology, Elsevier, 2017, pp. 185–207. doi: 10.1016/B978-0-12-809413-6.00003-5.

[28] D. A. L. Leelamanie, J. Karube, and A. Yoshida, "Clay effects on the contact angle and water drop penetration time of model soils," Soil Sci. Plant Nutr., vol. 56, no. 3, pp. 371–375, Jun. 2010, doi: 10.1111/j.1747-0765.2010.00471. x.

[29] D. A. L. Leelamanie and J. Karube, "Time dependence of contact angle and its relation to repellency persistence in hydrophobized sand," Soil Sci. Plant Nutr., vol. 55, no. 4, pp. 457–461, Aug. 2009, doi: 10.1111/j.1747-0765.2009.00387. x.

[30] T. Rutter and B. Hutton-Prager, "Investigation of hydrophobic coatings on cellulose-fiber substrates with in-situ polymerization of silane/siloxane mixtures," Int. J. Adhes. Adhes., vol. 86, pp. 13–21, Nov. 2018, doi: 10.1016/j.ijadhadh.2018.07.008.

[31] A. B. D. Cassie and S. Baxter, "Wettability of porous surfaces," Trans. Faraday Soc., vol. 40, no. 0, pp. 546–551, Jan. 1944, doi: 10.1039/TF9444000546.

[32] Y. Xu, S. Vincent, Q.-C. He, and H. Le-Quang, "Spread and recoil of liquid droplets impacting on solid surfaces with various wetting properties," Surf. Coat. Technol., vol. 357, pp. 140–152, Jan. 2019, doi: 10.1016/j.surfcoat.2018.09.079.

[33] T. A. Kettler, J. W. Doran, and T. L. Gilbert, "Simplified Method for Soil Particle-Size Determination to Accompany Soil-Quality Analyses," Soil Sci. Soc. Am. J., vol. 65, no. 3, pp. 849–852, May 2001, doi: 10.2136/sssaj2001.653849x.

[34] J. R. Nimmo and M. Park, “Porosity and Pore Size Distribution,” Earth Syst. Envi Sci Elsevier, vol. 3, p. 11, 2013, doi: 10.1016/B978-0-12-409548-9.05265-9.

[35] H. Huang, J. Tang, Z. Niu, and J. P. Giesy, “Interactions between electrokinetics and rhizoremediation on the remediation of crude oil-contaminated soil,” Chemosphere, vol. 229, pp. 418–425, Aug. 2019, doi: 10.1016/j.chemosphere.2019.04.150.

[36] S.-S. Sheng et al., “Structure-activity relationship of anionic-nonionic surfactant for reducing interfacial tension of crude oil,” J. Mol. Liq., p. 112772, Feb. 2020, doi: 10.1016/j.molliq.2020.112772.

[37] M. A. J. Chinenyeze and U. R. Ekene, “Physical and Chemical Properties of Crude Oils and Their Geologic Significances,” Int. J. Sci. Res., vol. 6, no. 6, p. 8, 2015.

[38] D. Bu and O. Bc, “Remediation of Used Motor Engine Oil Contaminated Soil: A Soil Washing Treatment Approach,” J. Civ. Environ. Eng., vol. 03, no. 02, 2013, doi: 10.4172/2165-784X.1000129.

[39] A. Hamad, E. Al-Zubaidy, and M. E. Fayed, “Assessment of Used Motor Oil Recycling Opportunities in the United Arab Emirates,” J. King Saud Univ. - Eng. Sci., vol. 16, no. 2, pp. 215–227, 2004, doi: 10.1016/S1018-3639(18)30788-8.

[40] B. C. M. Guimarães, J. B. A. Arends, D. van der Ha, T. Van de Wiele, N. Boon, and W. Verstraete, “Microbial services and their management: Recent progresses in soil bioremediation technology,” Appl. Soil Ecol., vol. 46, no. 2, pp. 157–167, Oct. 2010, doi: 10.1016/j.apsoil.2010.06.018.

[41] B. Ghanbarian, A. Hunt, and H. Daigle, “Fluid flow in porous media with rough pore-solid interface,” Water Resour. Res., vol. 52, p. n/a-n/a, Feb. 2016, doi: 10.1002/2015WR017857.

[42] A. Verma, Evaluation of sea sand and river sand properties and their comparison. 2015. doi:

10.13140/RG.2.1.4906.6327.

[43] F. Uddin, “Clays, Nanoclays, and Montmorillonite Minerals,” Metall. Mater. Trans. A, vol. 39, no. 12, pp. 2804–2814, Dec. 2008, doi: 10.1007/s11661-008-9603-5.

[44] S. Guggenheim, “Definition of Clay and Clay Mineral: Joint Report of the AIPEA Nomenclature and CMS Nomenclature Committees,” Clays Clay Miner., vol. 43, no. 2, pp. 255–256, 1995, doi: 10.1346/CCMN.1995.0430213.

[45] S. Y. Khan, M. Yusuf, and N. Sardar, “Studies on Rheological Behavior of Xanthan Gum Solutions in Presence of Additives.,” Pet. Petrochem. Eng. J., vol. 2, no. 5, p. 7, 2018.

[46] A. Alghooneh, S. M. A. Razavi, and F. Behrouzian, “Rheological characterization of hydrocolloids interaction: A case study on sage seed gum-xanthan blends,” Food Hydrocoll., vol. 66, pp. 206–215, May 2017, doi: 10.1016/j.foodhyd.2016.11.022.

[47] N. E. Shlegel, P. P. Tkachenko, and P. A. Strizhak, “Influence of viscosity, surface and interfacial tensions on the liquid droplet collisions,” Chem. Eng. Sci., vol. 220, p. 115639, Jul. 2020, doi: 10.1016/j.ces.2020.115639.

[48] J. B. Rosenholm, “Liquid spreading on solid surfaces and penetration into porous matrices: Coated and uncoated papers,” Adv. Colloid Interface Sci., vol. 220, pp. 8–53, Jun. 2015, doi: 10.1016/j.cis.2015.01.009.

[49] V. M. Starov, S. A. Zhdanov, S. R. Kosvintsev, V. D. Sobolev, and M. G. Velarde, “Spreading of liquid drops over porous substrates,” Adv. Colloid Interface Sci., vol. 104, no. 1–3, pp. 123–158, Jul. 2003, doi: 10.1016/S0001-8686(03)00039-3.

[50] V. M. Starov, S. A. Zhdanov, and M. G. Velarde, “Spreading of Liquid Drops over Thick Porous Layers: Complete Wetting Case,” Langmuir, vol. 18, no. 25, pp. 9744–9750, Dec. 2002, doi: 10.1021/la025759y.

[51] K. S. Lee, N. Ivanova, V. M. Starov, N. Hilal, and V. Dutschk, “Kinetics of wetting and spreading by aqueous surfactant solutions,” Adv. Colloid Interface Sci., vol. 144, no. 1–2, pp. 54–65, Dec. 2008, doi: 10.1016/j.cis.2008.08.005.

[52] P. Johnson, A. Trybala, and V. Starov, “Kinetics of Spreading over Porous Substrates,” Colloids Interfaces, vol. 3, no. 1, p. 38, Mar. 2019, doi: 10.3390/colloids3010038.

[53] Thien S. J, “A flow diagram for teaching texture by feel analysis. Journal of Agronomic Education,”. 8:54-55, 1979.

[54] S. M. Schraer, D. R. Shaw, M. Boyette, W. L. Kingery, and C. H. Koger, “Sorption–desorption of cyanazine in three Mississippi delta soils,” Weed Sci., vol. 51, no. 4, pp. 635–639, Jul. 2003, doi: 10.1614/0043-1745(2003)051[0635: SOCITM]2.0.CO;2.

[55] V. Matko, “Određivanje poroznosti primjenom stohastičke metode,” Autom. J. Control Meas. Electron. Comput. Commun. Koremaferhr Vol44 No3-4, Jan. 2003.

[56] J. M. Herdan, “Lubricating oil additives and the environment — an overview,” Lubr. Sci., vol. 9, no. 2, pp. 161–172, Feb. 1997, doi: 10.1002/ls.3010090205.

[57] D. Savage and J. Liu, “Water/clay ratio, clay porosity models and impacts upon clay transformations,” Appl. Clay Sci., vol. 116–117, pp. 16–22, Aug. 2015, doi: 10.1016/j.clay.2015.08.011.

[58] C. W. Curry, R. H. Bennett, M. H. Hulbert, K. J. Curry, and R. W. Faas, “Comparative Study of Sand Porosity and a Technique for Determining Porosity of Undisturbed Marine Sediment,” Mar. Georesources Geotechnol., vol. 22, no. 4, pp. 231–252, Oct. 2004, doi: 10.1080/10641190490900844.

[59] S. N. Williams, “How Moisture Content Levels and Packing Density in Soil Affect Crude Oil Spreads,” p. 6, 2019.

[60] K. Ramadass, M. Megharaj, K. Venkateswarlu, and R. Naidu, “Ecological implications of motor oil pollution: Earthworm survival and soil health,” Soil Biol. Biochem., vol. 85, pp. 72–81, Jun. 2015, doi: 10.1016/j.soilbio.2015.02.026.

[61] N. Koursari, O. Arjmandi-Tash, P. Johnson, A. Trybala, and V. M. Starov, “Foam drainage placed on a thin porous layer,” Soft Matter, vol. 15, no. 26, pp. 5331–5344, 2019, doi: 10.1039/C8SM02559B.

[62] H. Özbay, “The effects of motor oil on the growth of three aquatic macrophytes,” Acta Ecol. Sin., vol. 36, no. 6, pp. 504–508, Dec. 2016, doi: 10.1016/j.chnaes.2016.08.005.

[63] Q. Chen, M. Wang, N. Pan, and Z.-Y. Guo, “Optimization Principle for Variable Viscosity Fluid Flow and Its Application to Heavy Oil Flow Drag Reduction,” Energy Fuels, vol. 23, no. 9, pp. 4470–4478, Sep. 2009, doi: 10.1021/ef900107b.

[64] J. Jing, R. Yin, G. Zhu, J. Xue, S. Wang, and S. Wang, “Viscosity and contact angle prediction of low water-containing heavy crude oil diluted with light oil,” J. Pet. Sci. Eng., vol. 176, pp. 1121–1134, May 2019, doi: 10.1016/j.petrol.2019.02.012.

[65] D. S. Kolotova, Y. A. Kuchina, L. A. Petrova, N. G. Voron’ko, and S. R. Derkach, “Rheology of Water-in-Crude Oil Emulsions: Influence of Concentration and Temperature,” Colloids Interfaces, vol. 2, no. 4, p. 64, Nov. 2018, doi: 10.3390/colloids2040064.

[66] X. Li, X. Fan, A. Askounis, K. Wu, K. Sefiane, and V. Koutsos, “An experimental study on dynamic pore wettability,” Chem. Eng. Sci., vol. 104, pp. 988–997, Dec. 2013, doi: 10.1016/j.ces.2013.10.026.

[67] D. Seo, J. Lee, C. Lee, and Y. Nam, “The effects of surface wettability on the fog and dew moisture harvesting performance on tubular surfaces,” Sci. Rep., vol. 6, no. 1, p. 24276, Apr. 2016, doi: 10.1038/srep24276.

[68] K. A. Narayana Iyer, R. Pantina, and A. P. Deshpande, “Modelling and simulation of drop spreading on fibrous porous media,” J. Text. Inst., vol. 105, no. 3, pp. 294–303, Mar. 2014, doi: 10.1080/00405000.2013.837605.

[69] A. Abed Gatea Al-Shammary, A. Kouzani, Y. Gyasi-Agyei, W. Gates, and J. Rodrigo-Comino, “Effects of solarisation on soil thermal-physical properties under different soil treatments: A review,” Geoderma, vol. 363, p. 114137, Apr. 2020, doi: 10.1016/j.geoderma.2019.114137.

[70] P. Djomgoue and D. Njopwouo, “FT-IR Spectroscopy Applied for Surface Clays Characterization,” J. Surf. Eng. Mater. Adv. Technol., vol. 03, no. 04, pp. 275–282, 2013, doi: 10.4236/jsemat.2013.34037.

[71] O. Katusich et al., “Evaluation of Sorptive Capacity of Natural Clay, Pillared Clay, and Alga-modified Clay to Contain Oil Spills in Soil,” vol. 2, no. 1, p. 11, 2016.

[72] A. M. A. Mohamed, A. M. Abdullah, and N. A. Younan, “Corrosion behavior of superhydrophobic surfaces: A review,” Arab. J. Chem., vol. 8, no. 6, pp. 749–765, Nov. 2015, doi: 10.1016/j.arabjc.2014.03.006.

[73] V. M. Starov, “Surfactant solutions and porous substrates: spreading and imbibition,” Adv. Colloid Interface Sci., vol. 111, no. 1–2, pp. 3–27, Nov. 2004, doi: 10.1016/j.cis.2004.07.007.

[74] N. Alleborn and H. Raszillier, “Spreading and sorption of a droplet on a porous substrate,” Chem. Eng. Sci., vol. 59, no. 10, pp. 2071–2088, May 2004, doi: 10.1016/j.ces.2004.02.006.

[75] X. Frank and P. Perré, “Droplet spreading on a porous surface: A lattice Boltzmann study,” Phys. Fluids, vol. 24, no. 4, p. 042101, Apr. 2012, doi: 10.1063/1.3701996.

[76] B. Markicevic, T. D’Onofrio, and H. Navaz, “On spread extent of sessile droplet into porous medium: Numerical solution and comparisons with experiments,” Phys. Fluids, vol. 22, Jan.

2010, doi: 10.1063/1.3284782.

[77] M. Denesuk, G. L. Smith, B. J. J. Zelinski, N. J. Kreidl, and D. R. Uhlmann, “Capillary Penetration of Liquid Droplets into Porous Materials,” J. Colloid Interface Sci., vol. 158, no. 1, pp. 114–120, Jun. 1993, doi: 10.1006/jcis.1993.1235.

[78] O. Arjmandi-Tash, N. M. Kovalchuk, A. Trybala, I. V. Kuchin, and V. Starov, “Kinetics of Wetting and Spreading of Droplets over Various Substrates,” Langmuir, vol. 33, no. 18, pp. 4367–4385, May 2017, doi: 10.1021/acs.langmuir.6b04094.

APPENDIX

A1 Statistical analyses of all raw data

In this section, ANOVA analysis of all raw data is presented including the model summary, interaction plot, main effect plot of different variables on different matrices, analysis of variance of different variables and matrices, and the factor information of models. Also, a conclusion is attached at the end of each model for both set of data including spreading kinetics and interfacial data with and without XG.

Table A1: Different symbols and explanations used in a 'model summary' of the various statistical models used to investigate the effect of different variables on oil spreading and penetration rate on several matrices.

Symbol	Remarks
S	Measured in units of the response variable; represents how far the data values differ from the fitted values. The lower the S; the better the fitted model.
R-sq	% Of variation in the response that is explained by the model. The higher the R-sq, the better the model fits the data. R-sq > 90% is excellent.

R-sq (adj)	Adjusted R-sq is the % of variation in the response that is explained by the model, adjusted for the number of predictors in the model relative to the no. of objectives. If adding more predictors (e.g., other factors, e.g., substrate AND MC AND oil), R-sq(adj) will go down, thus reducing the model's predictions.

A1.1 Null and alternate hypothesis

A null hypothesis is a type of conjecture used in statistics that proposes that there is no difference between the mean of variables. On the other hand, the alternative hypothesis proposes that there is a difference exist between the mean of the variables.

P-value ≤ α: The differences between some of the means are statistically significant.

P-value > α: The differences between the means are not statistically significant.

F ≤ F(crit): The null hypothesis is true, i.e., no statistical difference between the means.

F ≥ F(crit): The differences between some of the means is statistically significant.

α (alpha): The significance level of statistical data is denoted by α (alpha). The significance level (α) is the probability of rejecting the null hypothesis when it is true. A significance level of 0.05 indicates a 5% risk of concluding that a difference exists when there is no actual difference between the mean of variables.

F_{crit}: F_{crit} value determines the significance of the groups of variables. F_{crit} value is also used make decisions in support of or against the null hypothesis. If the calculated F-value (F_{calc}) is

greater than F_{crit} value, the null hypothesis is rejected; otherwise, the null hypothesis is not rejected.

Table A2: Experimental approach/Design of experiment for both spreading kinetics and the surface and interfacial study including the different variables and responses with levels.

<table>
<tr><th colspan="3">Spreading Kinetics</th><th colspan="4">Surface and Interfacial study</th></tr>
<tr><th>Responses</th><th colspan="2">Variables</th><th>Responses</th><th colspan="3">Variables</th></tr>
<tr><td rowspan="10">i) Time at first recorded spread(s)

ii) Spreading area at 1000s (cm^2)</td><td rowspan="3">MC</td><td>0%MC</td><td rowspan="10">i) Initial CA

ii) Time taken to reach a CA of 20°

iii) Initial baseline

iv) Maximum baseline

v) Time to maximum baseline</td><td rowspan="4">MC</td><td>Without XG</td><td>With XG</td></tr>
<tr><td rowspan="2">5%MC</td><td>0%</td><td>0%</td></tr>
<tr><td rowspan="2">10%MC</td><td>5%</td><td>5%</td></tr>
<tr><td>10%</td><td></td></tr>
<tr><td rowspan="3">Oil type</td><td>CO-2 (low viscosity)</td><td rowspan="4">Oil type</td><td>CO-2</td><td>CO-2</td></tr>
<tr><td>MO (medium viscosity)</td><td>MO</td><td>MO</td></tr>
<tr><td>CO-1 (high viscosity)</td><td rowspan="2">CO-1</td><td rowspan="2"></td></tr>
<tr><td rowspan="2">Matrix packing (without XG)</td><td>Loosely packed</td></tr>
<tr><td>Densely packed</td><td rowspan="3">Substrate type</td><td rowspan="3">Topsoil, sand, clay, and mixture matrix.</td><td rowspan="3">Clay and mixture matrix.</td></tr>
<tr><td rowspan="2">Matrix type (with XG)</td><td>Loosely packed</td></tr>
<tr><td>Loosely packed +1g XG</td></tr>
</table>

Table A3: Critical F values for different degrees of freedom (from Minitab software). A chi-square distribution was used to determine these values.

Degrees of Freedom (DF)	1-alpha	F_{crit}
1	0.95	3.84146
2	0.95	5.99146
3	0.95	7.81473
4	0.95	9.48773
6	0.95	12.59160

Table A4: Legend for different matrices for statistical analyses.

Legend name	Spreading kinetics data analyses		CA and Baseline data analyses	
	Without XG	With XG	Without XG	With XG
A1	Loosely packed matrix	Loosely packed matrix	Soil	Clay without XG
A2	Densely packed matrix	Loosely packed mixture + 1g XG	Sand	Mixture without XG
A3			Clay	Clay with XG
A4			Mixture	Mixture with XG
B1	0%MC	0%MC	0%MC	0%MC
B2	5%MC	5%MC	5%MC	5%MC
B3	10%MC		10%MC	
C1	CO-2	CO-2	CO-2	CO-2
C2	MO	MO	MO	MO
C3	CO-1		CO-1	

A2 Spreading kinetics data without XG

A2.1 Time of first recorded spread

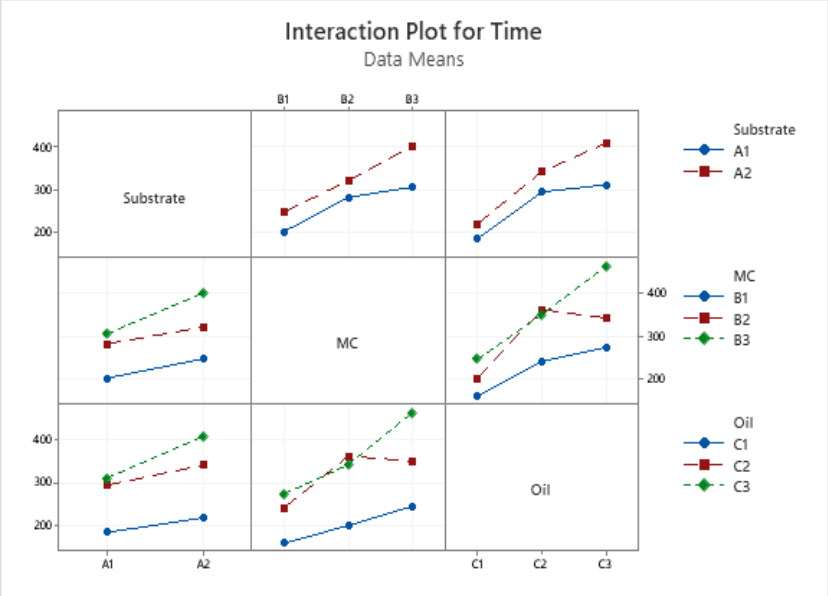

Factor Information

Factor	Type	Levels	Values
Substrate	Fixed	2	A1, A2
MC	Fixed	3	B1, B2, B3
Oil	Fixed	3	C1, C2, C3

Model Summary

S	R-sq	R-sq(adj)
35.1943	97.09%	87.63%

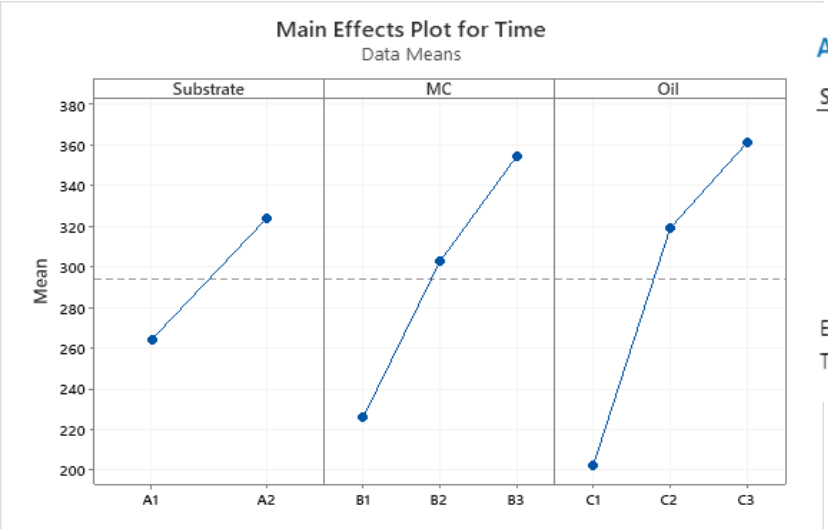

Analysis of Variance for Time

Source	DF	SS	MS	F	P
Substrate	1	16080	16080	12.98	0.023
MC	2	50153	25077	20.25	0.008
Oil	2	80734	40367	32.59	0.003
Substrate*MC	2	2871	1436	1.16	0.401
Substrate*Oil	2	3294	1647	1.33	0.361
MC*Oil	4	12094	3023	2.44	0.204
Error	4	4955	1239		
Total	17	170181			

Conclusions: Substrate, MC, and oil type were statistically significant when considered individually to influence the time of first recorded spread. The reason was the F and P values of these variables satisfied the conditions mentioned in section A1.1 for being statistically significant. Error in time was ±30s. S was good for the model. Also, R^2 and R^2-adj were also good. Refer to

Table A1 to get the explanations of S, R^2, and R^2-adj.

A2.2 Spreading area at t = 1000s

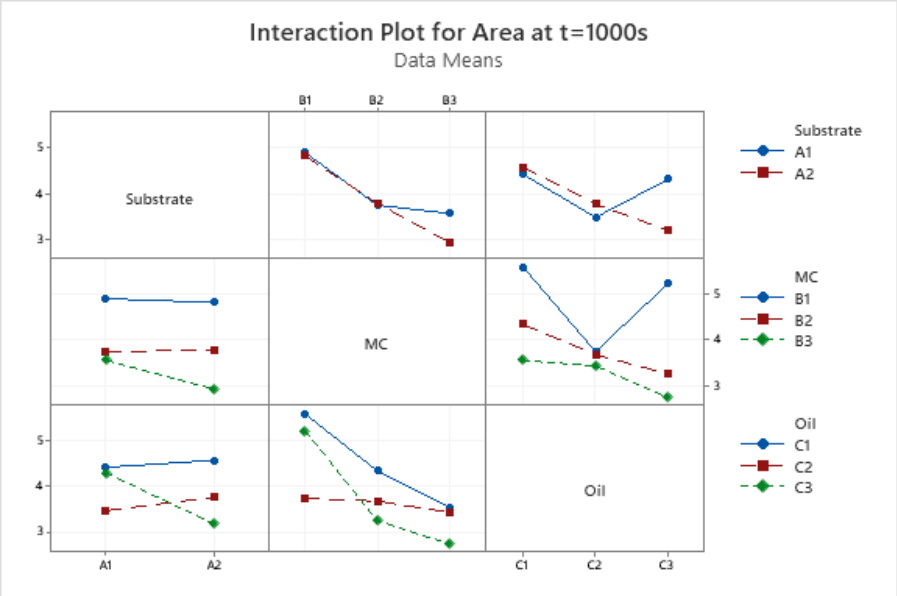

Factor Information

Factor	Type	Levels	Values
Substrate	Fixed	2	A1, A2
MC	Fixed	3	B1, B2, B3
Oil	Fixed	3	C1, C2, C3

Model Summary

S	R-sq	R-sq(adj)
0.501813	94.14%	75.09%

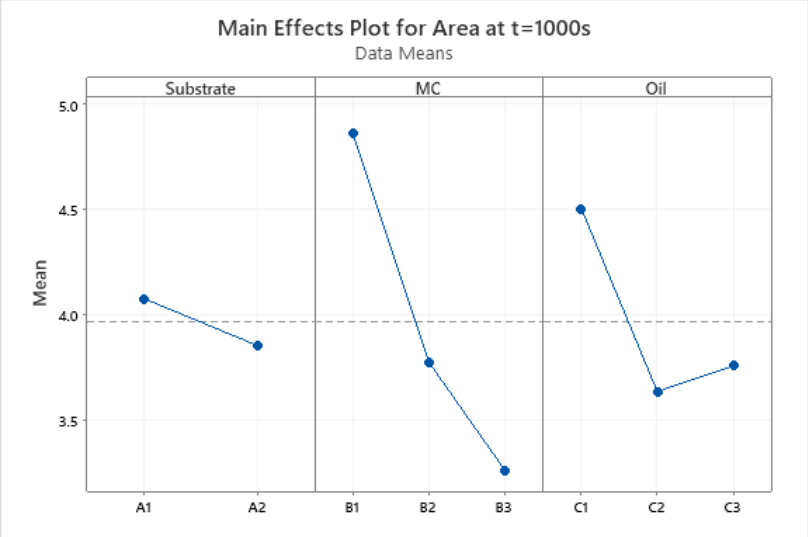

Analysis of Variance for Area at t=1000s

Source	DF	SS	MS	F	P
Substrate	1	0.2244	0.2244	0.89	0.399
MC	2	8.0587	4.0293	16.00	0.012
Oil	2	2.6526	1.3263	5.27	0.076
Substrate*MC	2	0.3829	0.1914	0.76	0.525
Substrate*Oil	2	1.7962	0.8981	3.57	0.129
MC*Oil	4	3.0613	0.7653	3.04	0.154
Error	4	1.0073	0.2518		
Total	17	17.1834			

<u>Conclusions:</u> Only MC was the influential factor to affect the spreading area at 1000s. The F_{calc} value (16.00) > F_{crit} (5.99) and p-value (0.012) < α (0.05) in the case of MC, which confirmed

that the MC was a statistically significant factor to affect the spreading area of oils at 1000s. The S and R^2 values were good for this model. The R^2-adj was reasonable but maybe a little low.

A3 Spreading kinetics data with XG

A3.1 Time of first recorded spread

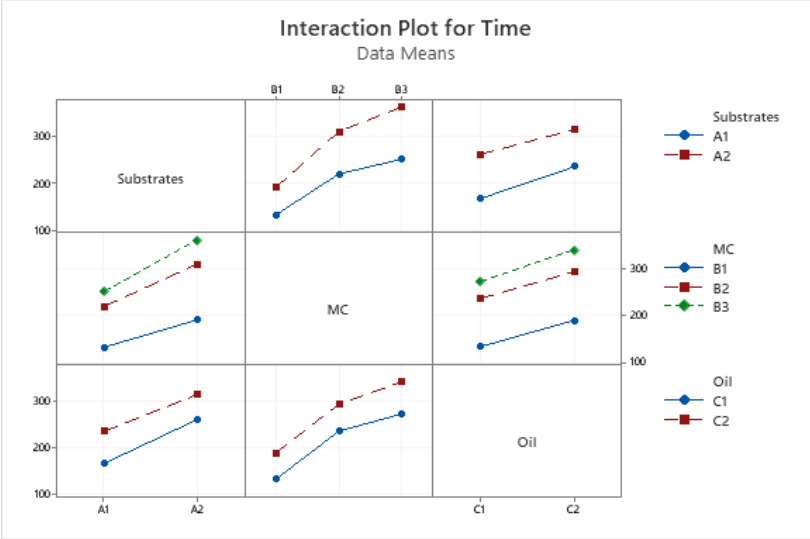

Factor Information

Factor	Type	Levels	Values
Substrates	Fixed	2	A1, A2
MC	Fixed	3	B1, B2, B3
Oil	Fixed	2	C1, C2

Model Summary

S	R-sq	R-sq(adj)
32.4500	97.43%	85.88%

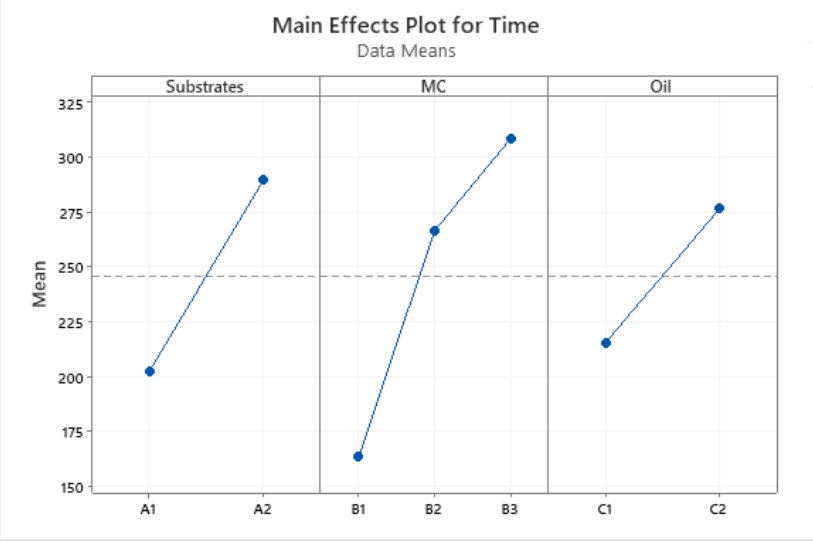

Analysis of Variance for Time

Source	DF	SS	MS	F	P
Substrates	1	22620.1	22620.1	21.48	0.044
MC	2	44530.7	22265.3	21.14	0.045
Oil	1	11102.1	11102.1	10.54	0.083
Substrates*MC	2	1424.7	712.3	0.68	0.596
Substrates*Oil	1	168.8	168.8	0.16	0.728
MC*Oil	2	88.7	44.3	0.04	0.960
Error	2	2106.0	1053.0		
Total	11	82040.9			

Conclusions: The substrate, MC, and oil type individually influenced the time recorded for the first spread. The strongest influence of these was the substrate type with F and p-value: F_{calc}

>F_{crit} (21.48>3.84) and p<α (0.04<0.05), respectively. The typical standard deviation in time was no more than ±30s. The S, R^2, and R^2-adj were good for this model. Refer to Table A1 for the remarks about S, R^2, and R^2-adj.

A3.2 Spreading area at t=1000s

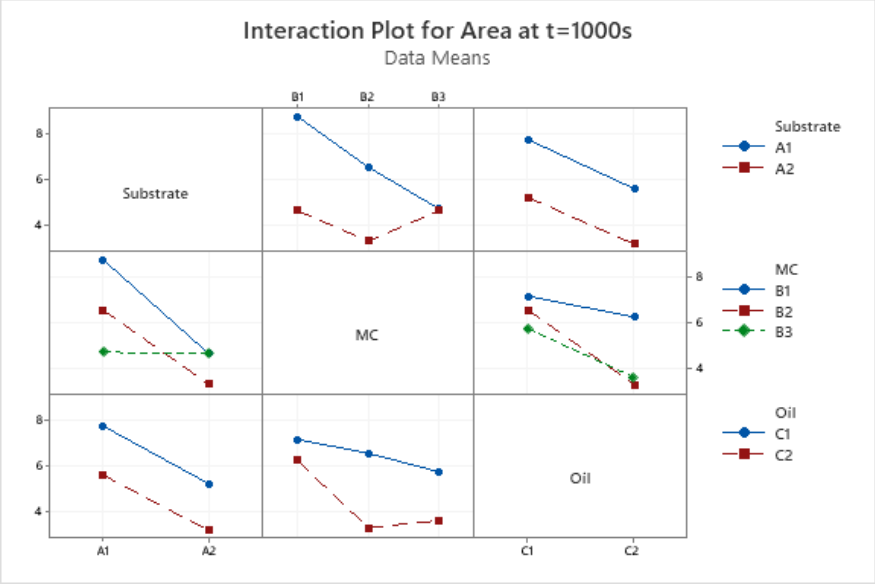

Factor Information

Factor	Type	Levels	Values
Substrate	Fixed	2	A1, A2
MC	Fixed	3	B1, B2, B3
Oil	Fixed	2	C1, C2

Model Summary

S	R-sq	R-sq(adj)
0.992224	96.40%	80.20%

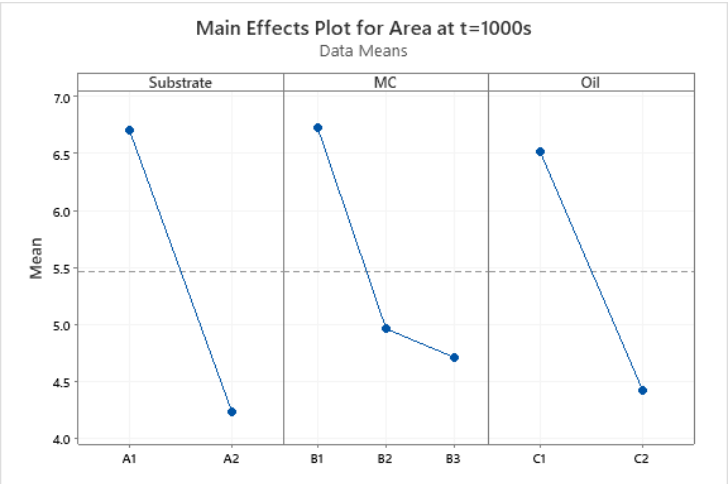

Analysis of Variance for Area at t=1000s

Source	DF	SS	MS	F	P
Substrate	1	18.2533	18.2533	18.54	0.050
MC	2	9.6910	4.8455	4.92	0.169
Oil	1	13.1043	13.1043	13.31	0.068
Substrate*MC	2	8.9542	4.4771	4.55	0.180
Substrate*Oil	1	0.0065	0.0065	0.01	0.942
MC*Oil	2	2.7279	1.3640	1.39	0.419
Error	2	1.9690	0.9845		
Total	11	54.7063			

Conclusions: The substrate and oil type were statistically significant to influence the time

recorded at 1000s to be observed. The strongest influence between substrate and oil type was substrate type (with XG) with F and p-value comparisons: $F_{calc} > F_{crit}$ (18.54>3.84) and $p \leq \alpha$ (0.05≤0.05), respectively. The S and R^2 values are good for this model. R^2-adj was reasonable but it was expected a little bit high.

A4 Statistics analysis of Surface and Interfacial Study over different variables without XG

A4.1 Initial CA

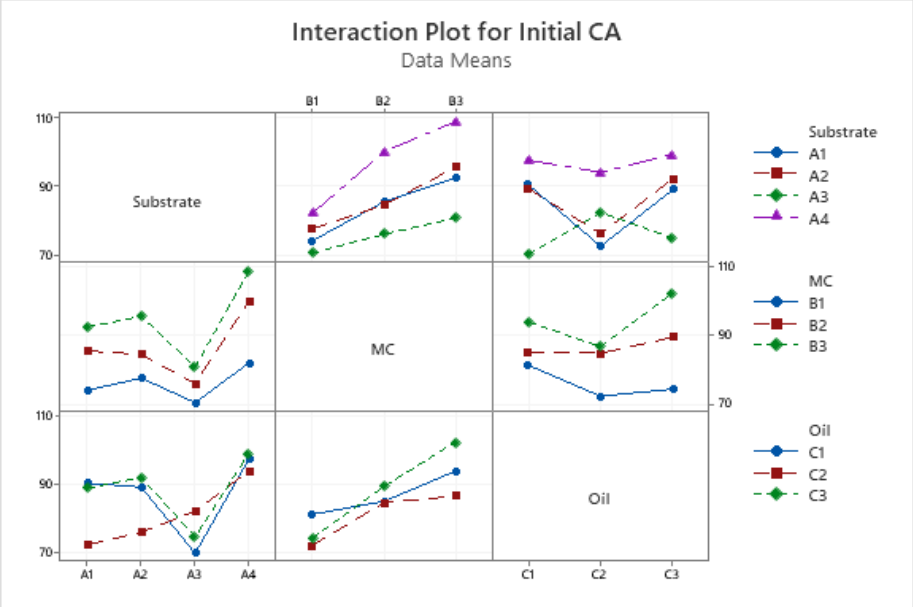

Factor Information

Factor	Levels	Values
Substrate	4	A1, A2, A3, A4
MC	3	B1, B2, B3
Oil	3	C1, C2, C3

Model Summary

S	R-sq	R-sq(adj)	R-sq(pred)
7.05349	91.00%	73.74%	18.97%

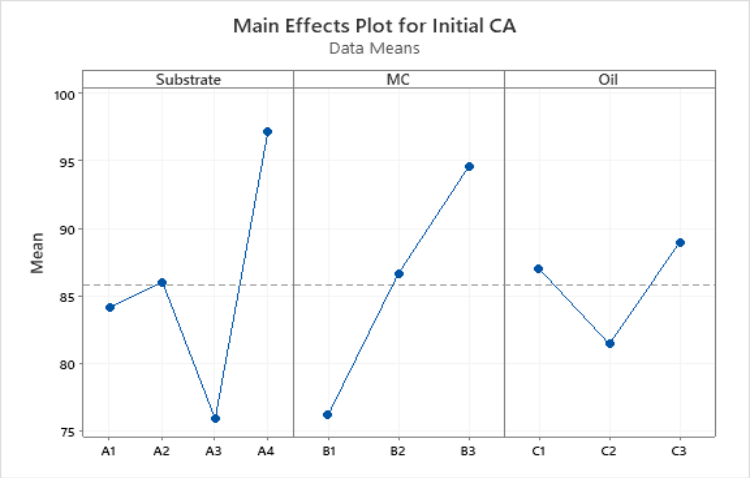

Analysis of Variance

Source	DF	Adj SS	Adj MS	F-Value	P-Value
Model	23	6034.1	262.35	5.27	0.002
Linear	7	4473.4	639.05	12.84	0.000
Substrate	3	2064.2	688.05	13.83	0.000
MC	2	2041.9	1020.94	20.52	0.000
Oil	2	367.4	183.68	3.69	0.056
2-Way Interactions	16	1560.8	97.55	1.96	0.121
Substrate*MC	6	252.0	42.00	0.84	0.560
Substrate*Oil	6	939.9	156.65	3.15	0.043
MC*Oil	4	368.9	92.22	1.85	0.184
Error	12	597.0	49.75		
Total	35	6631.2			

Conclusions: MC and substrate have statistically significant effect on the initial CA with F and p-value comparison: $F_{calc} > F_{crit}$ (20.52>5.99); (13.83>7.81) and $p<\alpha$ (0.00<0.05); (0.00<0.05), respectively. The S was reasonably low, however, R^2 was good. R^2-adj means nearly 74% was explained by the model. Substrate*oil potentially significant when based on the p-value.

A4.2 Time at CA = 20°

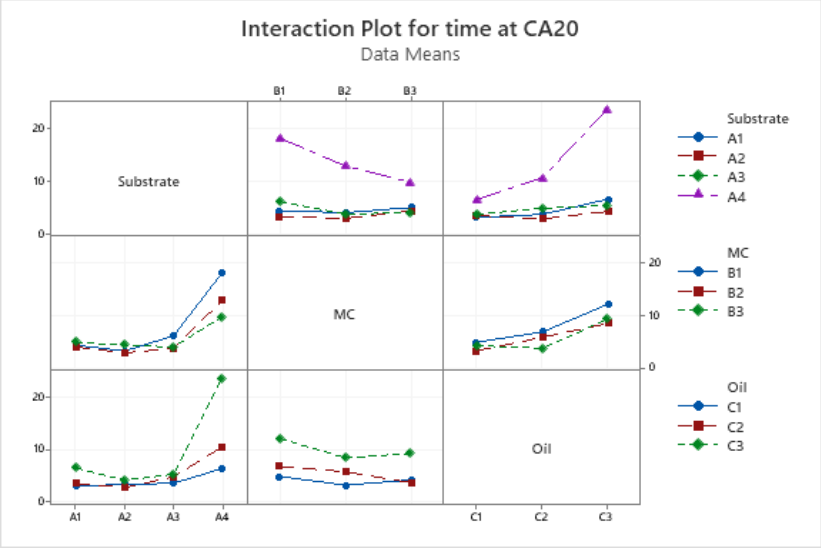

Factor Information

Factor	Type	Levels	Values
Substrate	Fixed	4	A1, A2, A3, A4
MC	Fixed	3	B1, B2, B3
Oil	Fixed	3	C1, C2, C3

Model Summary

S	R-sq	R-sq(adj)
1.29290	98.43%	95.43%

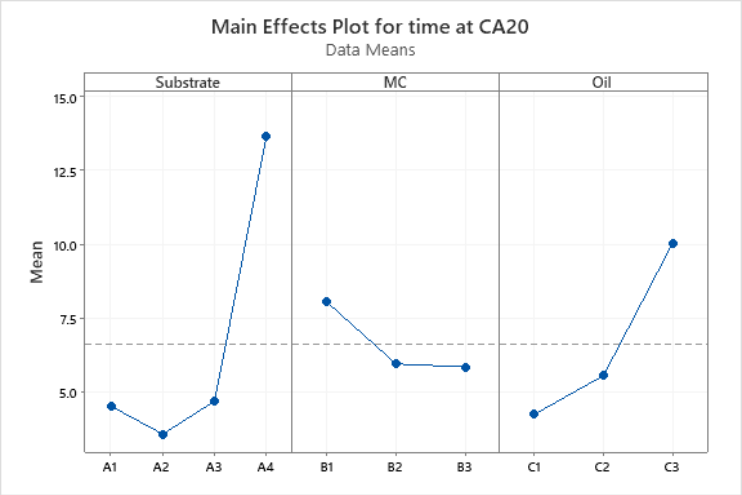

Analysis of Variance for time at CA20

Source	DF	SS	MS	F	P
Substrate	3	603.93	201.311	120.43	0.000
MC	2	36.80	18.401	11.01	0.002
Oil	2	221.83	110.914	66.35	0.000
Substrate*MC	6	85.34	14.224	8.51	0.001
Substrate*Oil	6	294.05	49.008	29.32	0.000
MC*Oil	4	17.59	4.397	2.63	0.087
Error	12	20.06	1.672		
Total	35	1279.60			

Conclusions: The substrate, MC, and oil type individually influenced the time taken to reach a CA of 20°. The strongest influence of these was the substrate with F comparisons: $F_{calc} > F_{crit}$ (120.43>7.81); followed by oil type (66.35> 5.99), and finally MC (11.01>5.99). The overall model summary was good. Substrate*MC potentially significant when based on the p-value.

A4.3 Initial baseline

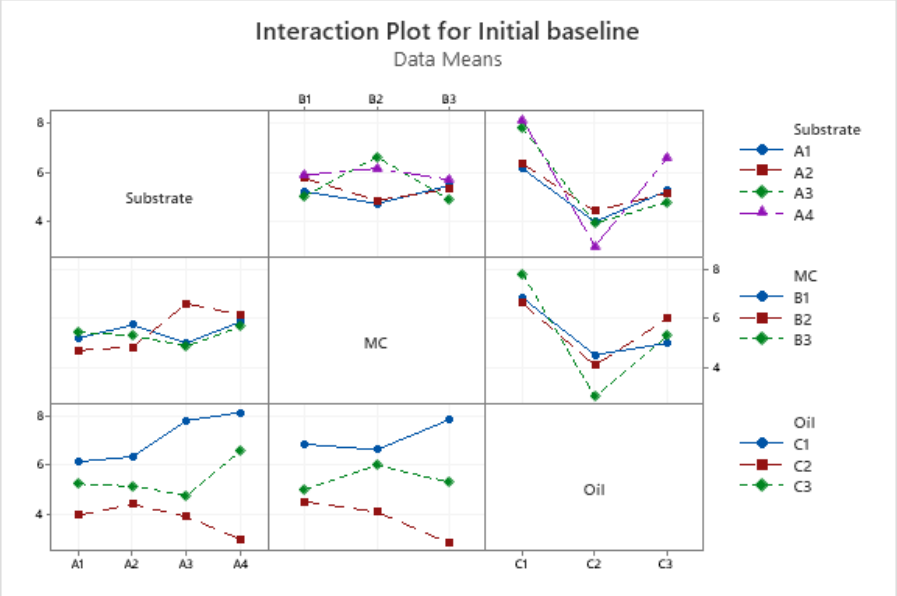

Factor Information

Factor	Type	Levels	Values
Substrate	Fixed	4	A1, A2, A3, A4
MC	Fixed	3	B1, B2, B3
Oil	Fixed	3	C1, C2, C3

Model Summary

S	R-sq	R-sq(adj)
0.918593	91.00%	73.75%

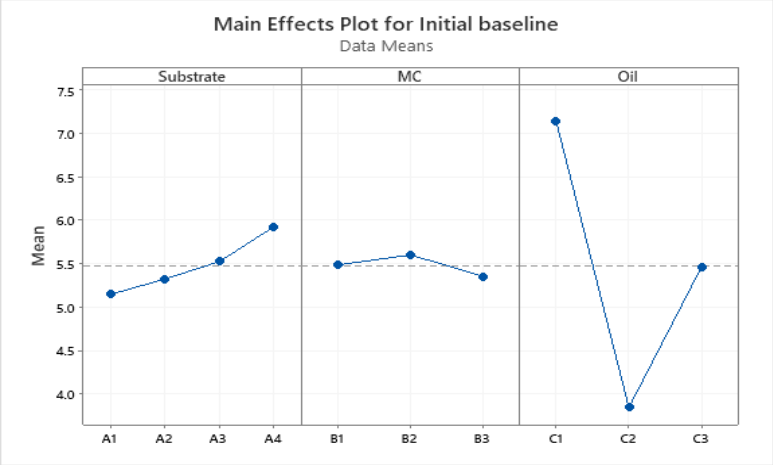

Analysis of Variance for Initial baseline

Source	DF	SS	MS	F	P
Substrate	3	3.022	1.0074	1.19	0.354
MC	2	0.373	0.1865	0.22	0.805
Oil	2	64.985	32.4923	38.51	0.000
Substrate*MC	6	7.591	1.2652	1.50	0.259
Substrate*Oil	6	15.053	2.5088	2.97	0.051
MC*Oil	4	11.377	2.8443	3.37	0.046
Error	12	10.126	0.8438		
Total	35	112.527			

Conclusions: Only the oil type has an impact on the initial baseline. For being statistically significant according to section A1.1, the oil type was satisfied the condition with F value comparison - $F_{calc}>F_{crit}$ (38.51>5.99). The effect of different variables on the initial baseline shows an overall good model summary. MC*Oil potentially significant when based on the p-value.

A4.4 Maximum baseline

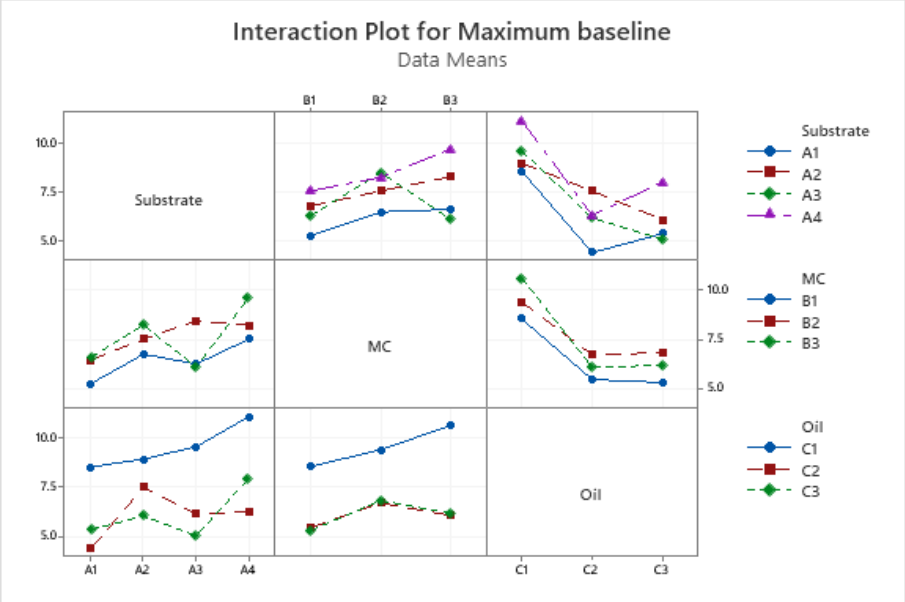

Factor Information

Factor	Type	Levels	Values
Substrate	Fixed	4	A1, A2, A3, A4
MC	Fixed	3	B1, B2, B3
Oil	Fixed	3	C1, C2, C3

Model Summary

S	R-sq	R-sq(adj)
1.38529	87.86%	64.60%

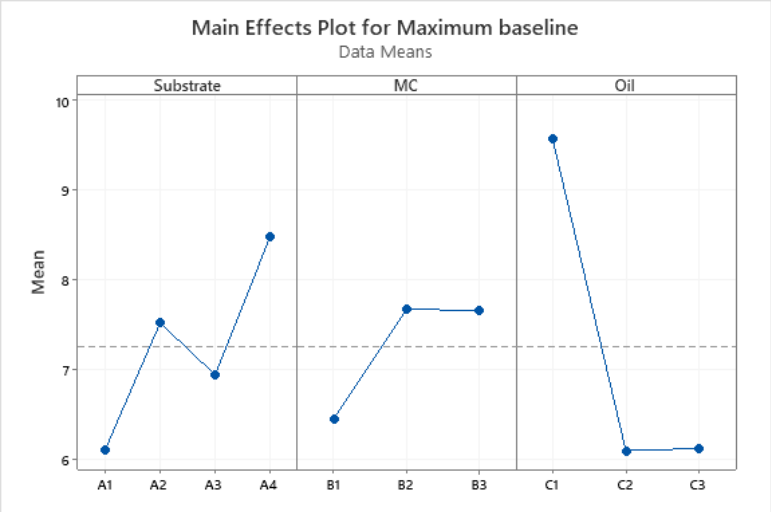

Analysis of Variance for Maximum baseline

Source	DF	SS	MS	F	P
Substrate	3	26.741	8.914	4.64	0.022
MC	2	11.682	5.841	3.04	0.085
Oil	2	95.454	47.727	24.87	0.000
Substrate*MC	6	12.493	2.082	1.09	0.424
Substrate*Oil	6	15.315	2.553	1.33	0.317
MC*Oil	4	5.029	1.257	0.66	0.634
Error	12	23.028	1.919		
Total	35	189.743			

Conclusions: Only the oil type was the influencing factor to affect the size of the maximum baseline with F value $F_{calc} > F_{crit}$ (24.87>5.99). The S was quite good fit for this model. However, R^2 was low which was reducing the model's prediction.

A4.5 time at maximum baseline

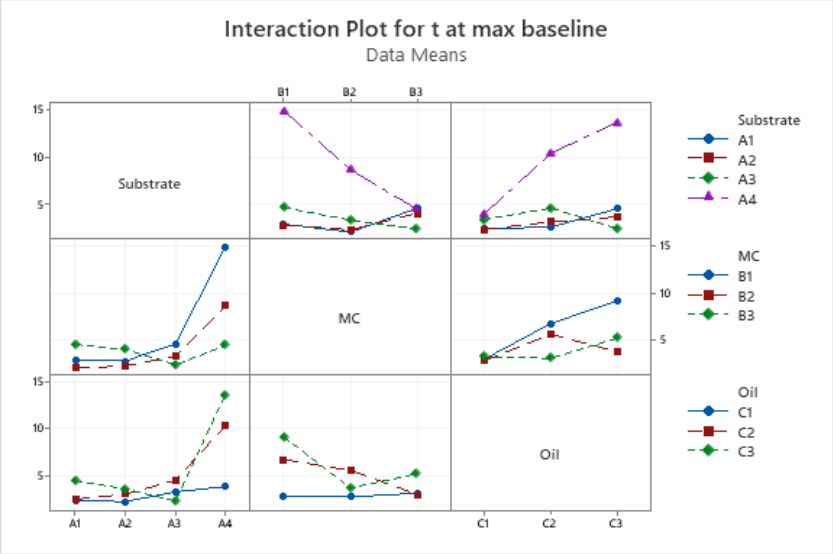

Factor Information

Factor	Type	Levels	Values
Substrate	Fixed	4	A1, A2, A3, A4
MC	Fixed	3	B1, B2, B3
Oil	Fixed	3	C1, C2, C3

Model Summary

S	R-sq	R-sq(adj)
1.75986	94.59%	84.22%

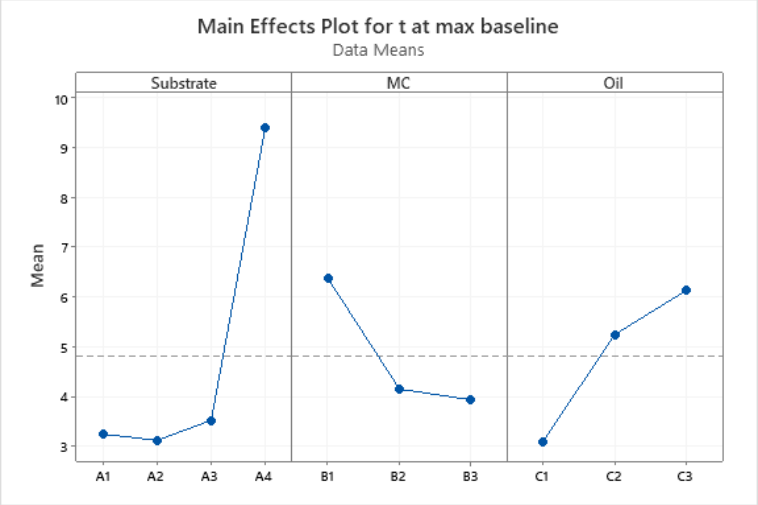

Analysis of Variance for t at max baseline

Source	DF	SS	MS	F	P
Substrate	3	251.42	83.805	27.06	0.000
MC	2	43.74	21.872	7.06	0.009
Oil	2	59.13	29.564	9.55	0.003
Substrate*MC	6	142.65	23.774	7.68	0.001
Substrate*Oil	6	106.12	17.686	5.71	0.005
MC*Oil	4	46.56	11.640	3.76	0.033
Error	12	37.17	3.097		
Total	35	686.77			

Conclusions: The substrate, MC, and oil were statistically significant when considered individually for the 'time at maximum baseline' variable. The strongest influence of these was the substrate type, with F and p-value - $F_{calc} > F_{crit}$ (27.06>7.81), and $p \leq \alpha$ (0.00<0.05), respectively. The overall model summary was good.

A5 Statistics analysis of Surface and Interfacial Study over different variables with XG

A5.1 Initial CA

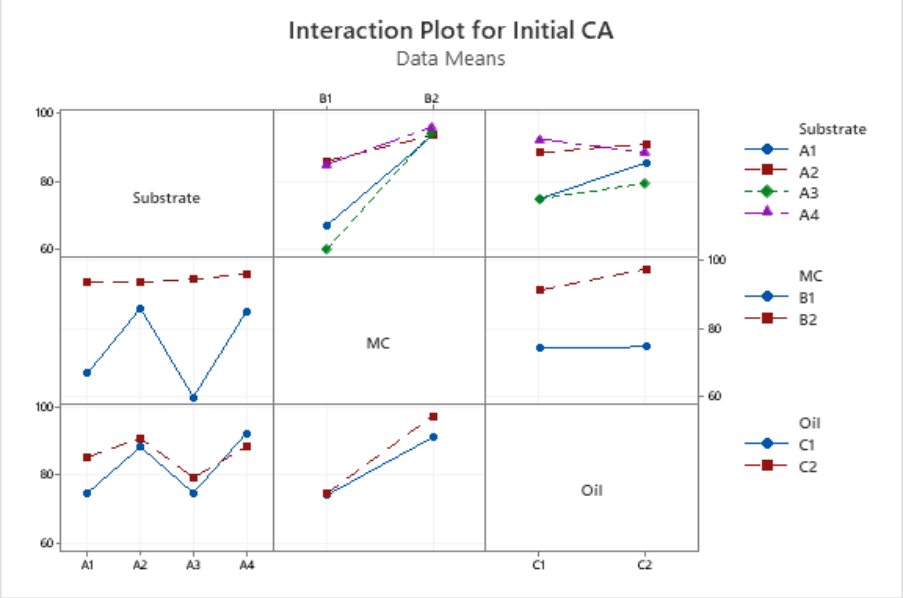

Factor Information

Factor	Type	Levels	Values
Substrate	Fixed	4	A1, A2, A3, A4
MC	Fixed	2	B1, B2
Oil	Fixed	2	C1, C2

Model Summary

S	R-sq	R-sq(adj)
2.92617	99.09%	95.44%

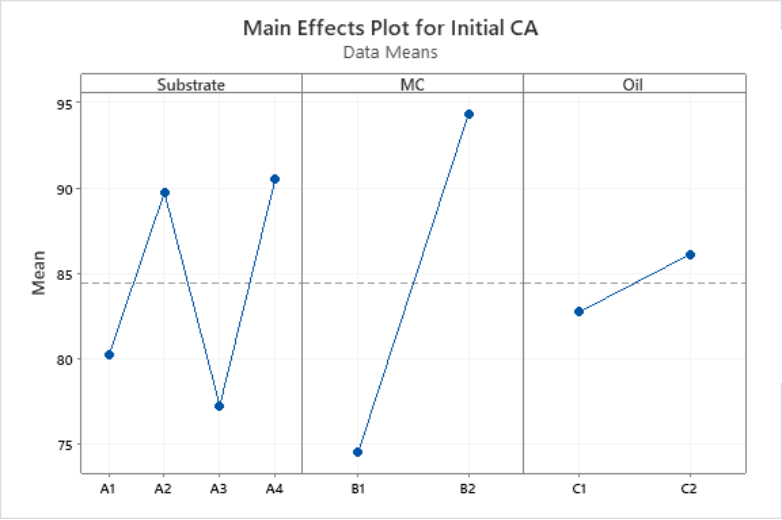

Analysis of Variance for Initial CA

Source	DF	SS	MS	F	P
Substrate	3	536.69	178.90	20.89	0.016
MC	1	1580.06	1580.06	184.53	0.001
Oil	1	45.56	45.56	5.32	0.104
Substrate*MC	3	489.69	163.23	19.06	0.019
Substrate*Oil	3	107.19	35.73	4.17	0.136
MC*Oil	1	33.06	33.06	3.86	0.144
Error	3	25.69	8.56		
Total	15	2817.94			

<u>Conclusions:</u> MC, substrate, and oil type individually influence the initial CA with F comparisons: $F_{calc} > F_{crit}$ (20.89>7.81), followed by substrate (184.53>3.84), and finally oil type (5.32>3.84). The S was reasonably low. However, R^2 was good. R^2-adj means nearly 95% is explained by the model. Overall good model summary.

A5.2 time at CA = 20°

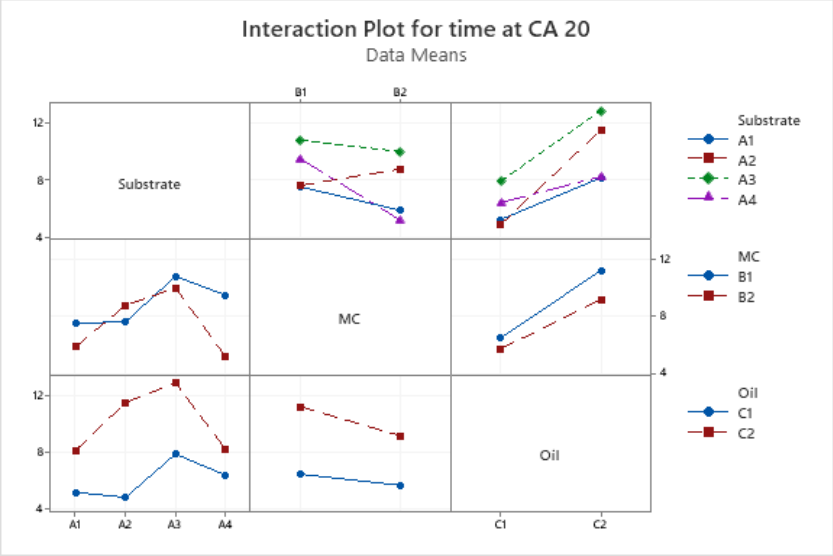

Factor Information

Factor	Type	Levels	Values
Substrate	Fixed	4	A1, A2, A3, A4
MC	Fixed	2	B1, B2
Oil	Fixed	2	C1, C2

Model Summary

S	R-sq	R-sq(adj)
1.43559	95.69%	78.45%

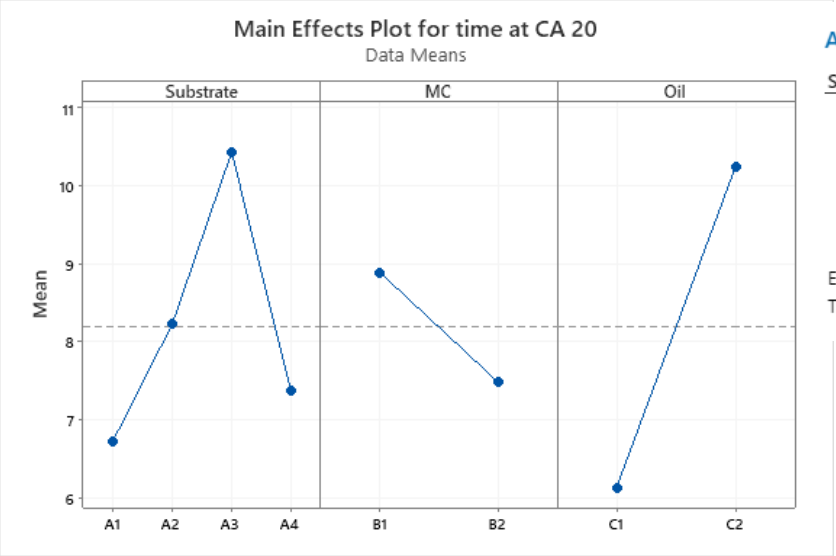

Analysis of Variance for time at CA 20

Source	DF	SS	MS	F	P
Substrate	3	31.338	10.446	5.07	0.108
MC	1	7.882	7.882	3.82	0.145
Oil	1	67.363	67.363	32.69	0.011
Substrate*MC	3	15.317	5.106	2.48	0.238
Substrate*Oil	3	13.761	4.587	2.23	0.264
MC*Oil	1	1.619	1.619	0.79	0.441
Error	3	6.183	2.061		
Total	15	143.463			

Conclusions: Only the oil type ($F_{calc} > F_{crit}$:32.69 > 3.84) has dominant influence on the time taken to reach a CA of 20° which indicates that the oil type was statistically significant. The S was reasonably low and R^2 was good. R^2-adj means nearly 95% was explained by model.

A5.3 Initial baseline

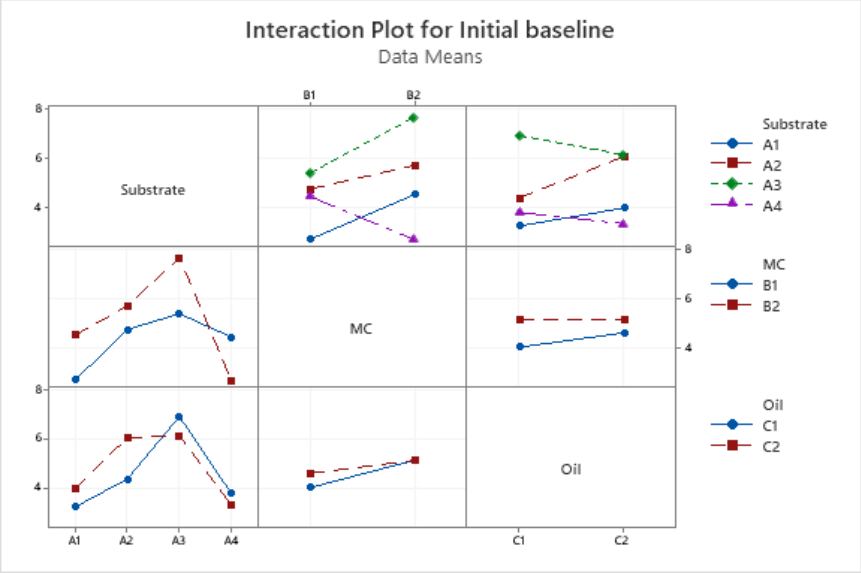

Factor Information

Factor	Type	Levels	Values
Substrate	Fixed	4	A1, A2, A3, A4
MC	Fixed	2	B1, B2
Oil	Fixed	2	C1, C2

Model Summary

S	R-sq	R-sq(adj)
1.05313	92.52%	62.61%

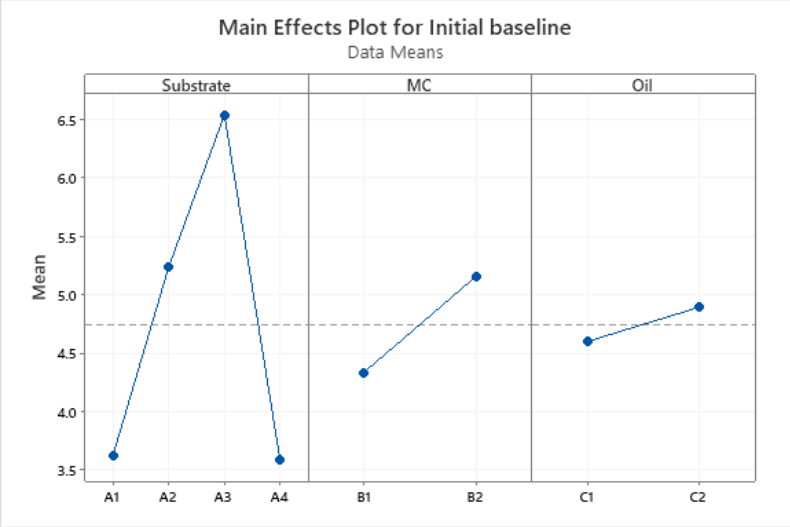

Analysis of Variance for Initial baseline

Source	DF	SS	MS	F	P
Substrate	3	24.2233	8.0744	7.28	0.069
MC	1	2.7060	2.7060	2.44	0.216
Oil	1	0.3422	0.3422	0.31	0.617
Substrate*MC	3	9.7559	3.2520	2.93	0.200
Substrate*Oil	3	3.7967	1.2656	1.14	0.458
MC*Oil	1	0.3422	0.3422	0.31	0.617
Error	3	3.3273	1.1091		
Total	15	44.4936			

<u>Conclusions:</u> The substrate, MC, and Oil type did not have any influence on initial baseline. For all variables $F_{calc} < F_{crit}$ and $p>\alpha$, this result indicates that variables were not statistically significant (section A1.1). The S was very low, however, R^2 was good. R^2-adj means nearly 63% was explained by the model.

A5.4 Maximum baseline

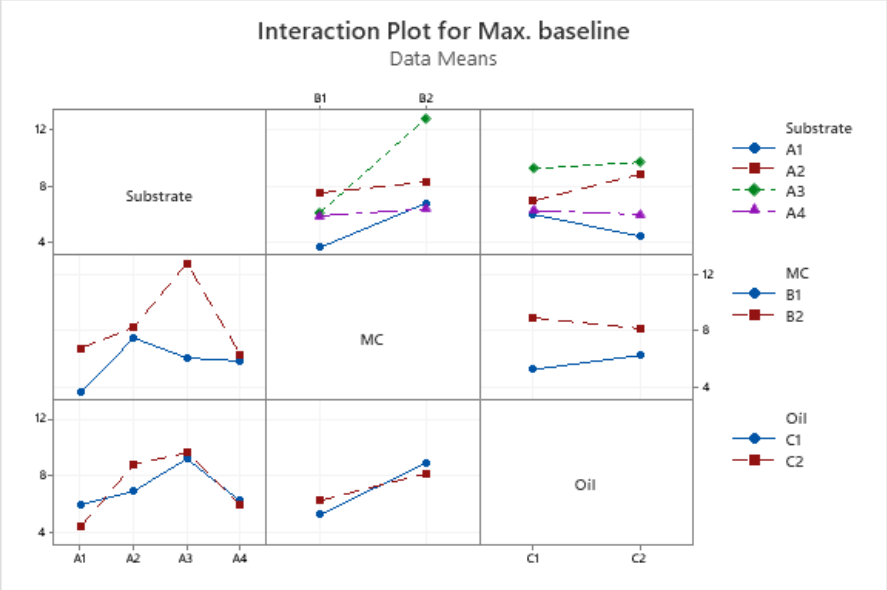

Factor Information

Factor	Type	Levels	Values
Substrate	Fixed	4	A1, A2, A3, A4
MC	Fixed	2	B1, B2
Oil	Fixed	2	C1, C2

Model Summary

S	R-sq	R-sq(adj)
1.13724	96.51%	82.56%

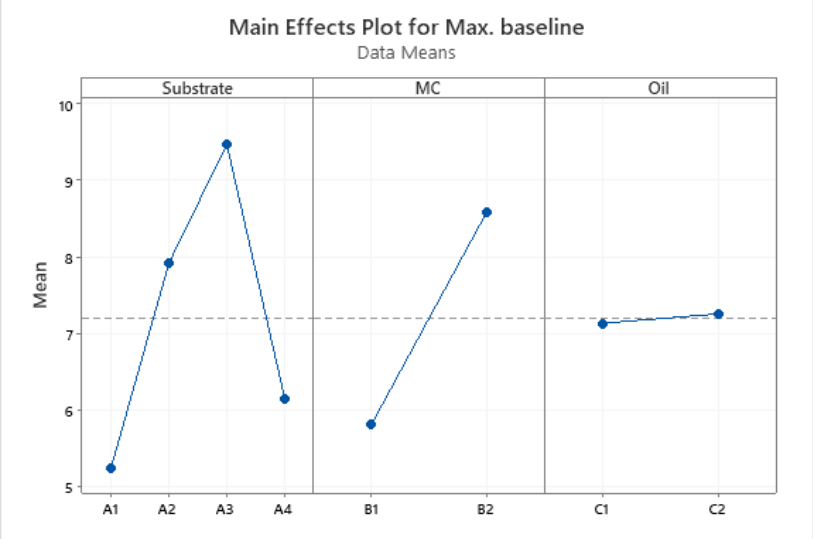

Analysis of Variance for Max. baseline

Source	DF	SS	MS	F	P
Substrate	3	42.451	14.1502	10.94	0.040
MC	1	30.692	30.6916	23.73	0.017
Oil	1	0.060	0.0600	0.05	0.843
Substrate*MC	3	24.878	8.2927	6.41	0.081
Substrate*Oil	3	6.203	2.0677	1.60	0.355
MC*Oil	1	3.062	3.0625	2.37	0.221
Error	3	3.880	1.2933		
Total	15	111.226			

<u>Conclusions:</u> The substrate and MC were statistically significant to affect the size of the maximum baseline. The strongest influence of these was the MC, with F comparisons: $F_{calc} > F_{crit}$ (23.73>3.84); followed by substrate (10.94>7.81). S value was low, and R^2 was good. R^2-adj was moderate.

A5.5 Time at maximum baseline

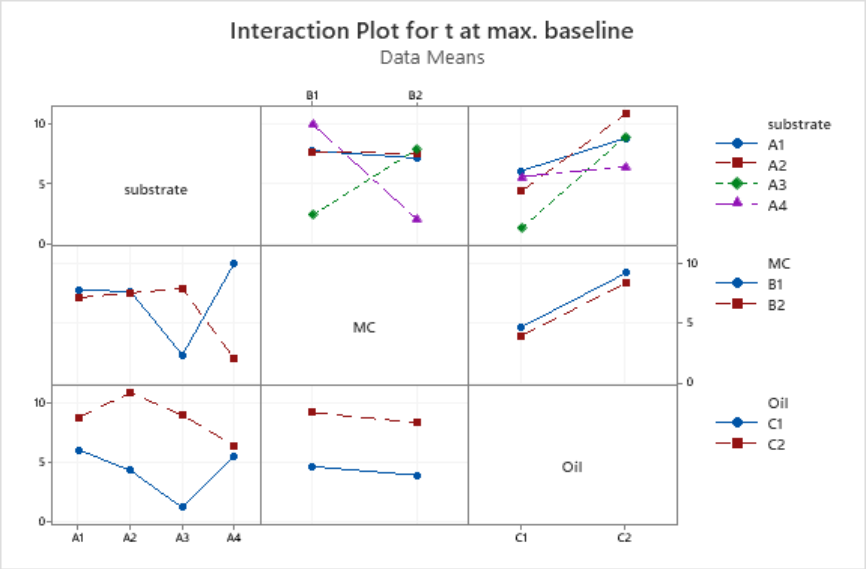

Factor Information

Factor	Type	Levels	Values
substrate	Fixed	4	A1, A2, A3, A4
MC	Fixed	2	B1, B2
Oil	Fixed	2	C1, C2

Model Summary

S	R-sq	R-sq(adj)
3.54177	85.40%	27.00%

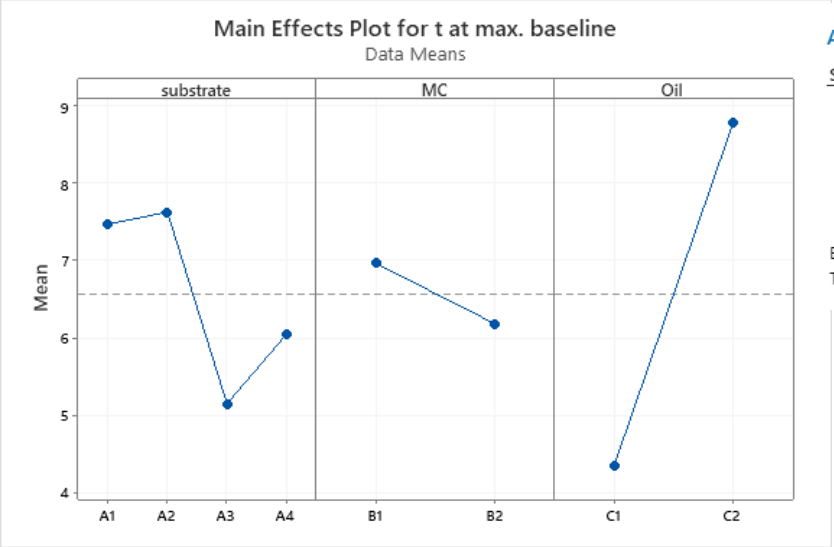

Analysis of Variance for t at max. baseline

Source	DF	SS	MS	F	P
substrate	3	16.899	5.6330	0.45	0.736
MC	1	2.457	2.4571	0.20	0.688
Oil	1	78.810	78.8100	6.28	0.087
substrate*MC	3	91.366	30.4553	2.43	0.243
substrate*Oil	3	30.575	10.1917	0.81	0.566
MC*Oil	1	0.015	0.0150	0.00	0.975
Error	3	37.632	12.5441		
Total	15	257.754			

<u>Conclusions:</u> only the oil type ($F_{calc} > F_{crit}$: 6.28>3.81) has an influence on the time taken to reach maximum baseline. The S value was a little higher than other conditions; R^2 was good. R^2-adj was reasonably low.

VITA

Md Firoz Ahmed

Education

The University of Mississippi Jun 2021

GPA: 3.54

MS- Chemical Engineering

Graduate teaching assistant

Research area – Surface and interfacial phenomena between soil and oil

Shahjalal University of Science and Technology May 2018

GPA: 3.72

MS-Chemical Engineering and Polymer Science

University of Rajshahi

CGPA – 3.77

BSc-Applied Chemistry and Chemical Engineering

Work Experience

Graduate teaching assistant Jan. 2019- present

The University of Mississippi, University, MS.

- Designed the experimental method and figure out the appropriate amount of mixture for performing experimental trial.

- Investigated and studied the spreading kinetics and penetration rate of different oils in various realistic soil-based matrices over different variables.
- Designed, optimized, and operated the apparatus for conducting experiments.
- Identified the most dominating variables on spreading and penetration rates of oils in soil-based matrices.
- Adding XG, a bio-emulsifier to study its effect on oil spreading kinetics and penetration rates into the matrices.

Part-time junior chemist Nov. 2016-May 2018

Omi Food Products, Sylhet, Bangladesh

- Controlled the quality of edible oil as per Bangladesh Standards and Testing Institution (BSTI)
- Monitored the oil quality by checking some vital parameter oil oils such as Vitamin-A, Iodin value, Color, Peroxide value, saponification value.

Major Projects

Project – (MS thesis)

Surface and Interfacial Phenomena between soil and oil Jan. 2019- present

This project involves the study of spreading kinetics and penetration rate of two crude oils (CO-1 & CO-2) and motor oils on realistic soil-based matrices over different variables including surface roughness, porosity and moisture content.

Project -2 (MS project)

Removal of Arsenic by the adsorption process using activated carbon Dec. 2016- May 2018

This project involved to prepare mesoporous activated carbon from agricultural waste and separation of arsenic from wastewater by using the activated carbon as an adsorbent.

Project – 3 (BS project)

Air sampling techniques Jun. 2015-Dec. 2015

This project was involved to the assessment of inorganic and organic pollutants in the indoor and outdoor air by applying different air sampling techniques.

Awards

- 2016- Graduate research fellowship- Shahjalal University of Science and Technology.
- 2016- National Science and Technology (NST) Fellowship- Ministry of Science and Technology, Bangladesh.

Publications

Journal publications

- Firoz Ahmed, Brenda Hutton-Prager, 'Bulk and Surface Interactions from Thick, Porous, Soil-based Substrates on the Spreading Behavior of Different Viscosity Oils'. Environmental Challenges (2021), doi: https://doi.org/10.1016/j.envc.2021.100045.
- R. Hossain, A. Khatun, F. Ahmed, O. Faroque, and A. Sobahan, 'Experimental behavior of bituminous mixes with waste concrete aggregate' Intl J. Edu Researchers, 9(3), 32-50, (2018).

Poster presentation

F. Ahmed 'Biogas production through dry fermentation', Research poster presentation in GREC Research showcase day-Round-1, 2017 Feb 03, Dhaka, Bangladesh.